Luísa Alexandra Graça Neves

Membrane Design and Characterisation by Incorporation of Ionic Liquids

Lisboa

Fevereiro 2010

nº de arquivo

“copyright”

Luísa Alexandra Graça Neves

Membrane Design and Characterisation by Incorporation of Ionic Liquids

Dissertação apresentada para obtenção do Grau de Doutor em
Engenharia Química, especialidade de Operações Unitárias e Fenómenos de
Transferência, pela Universidade Nova de Lisboa,
Faculdade de Ciências e Tecnologia

Lisboa

Fevereiro 2010

Agradecimentos

Em primeiro lugar gostaria de agradecer aos orientadores deste trabalho, João Paulo Crespo e Isabel Coelhoso por me terem proposto o presente trabalho de inegável interesse científico, e por tudo terem feito para que o conseguisse levar a bom termo. O meu agradecimento pelo apoio científico, e também humano, que me deram ao longo destes anos permitindo-me ultrapassar todas as dificuldades. O seu sentido crítico e criativo, disponibilidade, exigência e rigor, bem como a amizade demonstrada foram decisivos para a realização deste trabalho. Agradeço-lhes ainda terem-me proporcionado e incentivado nos contactos e intercâmbio científico com outros grupos de investigação, os quais seguramente foram importantes para a minha formação pessoal e científica.

À Professora Juana Benavente, da Universidade de Málaga, desejo agradecer o ter-me recebido no seu laboratório para realizar os ensaios de espectroscopia de impedância. A atenção e disponibilidade que sempre manifestou, bem como o seu apoio teórico beneficiaram bastante a análise dos resultados de XPS e de impedância aqui propostos.

Ao Professor Pedro Sebastião, do Instituto Superior Técnico, desejo agradecer por me recebido no seu laboratório para realizar os ensaios de NMR. Em particular gostaria de agradecer a sua disponibilidade, simpatia, por me fazer sentir parte integrante do seu grupo de trabalho, paciência, apoio técnico e teórico e pelas longas discussões que fizeram despertar o meu interesse para as "coisas" complicadas do mundo da Física.

Ao Professor Philipe Sistat e ao Professor Patrice Huguet o facto de me terem recebido no Institut Europeén des Membranes, onde tive a oportunidade de trabalhar com espectroscopia de Raman confocal e ampliar o meu conhecimento geral em relação às membranas de Nafion.

Gostaria também de agradecer a um conjunto de pessoas pelo apoio técnico que foi muito importante para a obtenção de alguns dos resultados presentes nesta tese, nomeadamente, à María Martinez de Yuso da Universidade de Malaga pelas medidas de XPS, à

Maria Celeste Azevedo da Universidade de Aveiro pelas medidas de termogravimetria e ao Professor António Lopes do IBET pelas medidas de ângulos de contacto feitos às SILMs.

Agradeço ainda à Maria Jesus e à Patrícia Luís pela amizade e ajuda na realização do trabalho relacionado com este projecto de investigação.

Aos meus colegas do BioEng agradeço a boa disposição, interesse e espírito de entreajuda ao longo destes anos. Em particular gostaria de agradecer ao Vitor Alves todo o apoio, preocupação e amizade demonstrados; à Cristiana Torres, Joana Pais, Graça Albuquerque, Rita Moita e aos restantes membros do "gang da marmita" pela amizade e pelos momentos de risota e descontracção; e em especial, à Ana Rita Ricardo pela amizade, ajuda, "paciência" para me ouvir e me aturar quando estava mais rabugenta, e pelo optimismo sempre presente que me ajudou a olhar para todas as dificuldades de uma maneira mais positiva.

À minha família, aos meus pais, à Célia, Vitor, André e Mariana, queria agradecer todo o apoio, incentivo, interesse e miminhos dados ao longo de todo este tempo.

Por último, um agradecimento muito, muito, muito especial ao Zé Luís pelo apoio incondicional, motivação e incentivo contantes, por toda a ajuda e interesse demonstrados pelo meu trabalho, pela compreensão e carinho presente nos momentos mais complicados, e principalmente por acreditar sempre em mim.

Sumário

Nesta tese de doutoramento foi estudado o desenho e a caracterização de novas membranas preparadas pela incorporação/imobilização de líquidos iónicos. Estas membranas foram desenvolvidas tendo em vista duas aplicações distintas: células de combustível e separação de CO_2 de correntes gasosas.

Na primeira parte do trabalho desenvolvido neste projecto de doutoramento, membranas de Nafion foram modificadas através da incorporação de diferentes tipos de catiões de líquidos iónicos, com diferentes graus de concentração, a fim de avaliar o potencial para utilização em células de combustível. A caracterização das membranas de Nafion modificadas foi efectuada utilizando as seguintes técnicas: XPS (Espectroscopia de fotoelectrões de raios-X), EIS (Espectroscopia de Impedância Electroquímica), NMR (Relaxação Magnética Nuclear de Protão) e termogravimetria. Foram ainda efectuados estudos de transporte de metanol e de gases puros, e todos os resultados obtidos foram comparados com os de uma membrana de Nafion não modificada. Verificou-se que é possível desenhar membranas com propriedades ajustadas, consoante o catião de líquido iónico incorporado e o seu grau de incorporação. Para além disso, verificou-se que a introdução de catiões volumosos de líquidos iónicos altera o teor em água existente na membrana e o seu grau de estruturação. Estas alterações no grau de estruturação da água melhorou a estabilidade das membranas modificadas a altas temperaturas (até 200 °C) e reduziu o transporte de metanol e de gases. No entanto, a abordagem seguida neste trabalho de modificação de membranas de Nafion com catiões de líquidos iónicos reduziu a sua mobilidade protónica quando comparada com a de uma membrana de Nafion não modificada.

Na segunda parte do trabalho desenvolvido nesta tese, diferentes líquidos iónicos foram imobilizados na estrutura porosa de membranas poliméricas, a fim de avaliar o seu potencial para utilização em processos de permeação gasosa. Foram efectuados estudos para avaliar a estabilidade das membranas suportadas com líquidos iónicos, utilizando diferentes suportes de distinta hidrofobicidade. Para além disso, foram determinados valores de permeabilidade para gases puros, gases humificados e misturas gasosas. Verificou-se que as membranas assim desenhadas são estáveis e muito selectivas para o CO_2, quando comparado com o N_2 ou com o CH_4. Verificou-se que a presença de vapor de água na corrente gasosa é um parâmetro que deverá ser tido em conta no estudo do processo, uma vez que afecta a estabilidade das membranas. Neste trabalho, os resultados obtidos relativamente à separação CO_2/CH_4 são bastante promissores, indicando que membranas suportadas com líquidos iónicos podem ser utilizadas para esta separação em particular.

Neste trabalho de doutoramento foi demonstrado que, modificando os dois tipos de membranas com líquidos iónicos – membranas de Nafion e membranas poliméricas porosas – as suas propriedades podem ser ajustadas e melhoradas de acordo com uma aplicação específica, através de uma selecção cuidadosa da estrutura do líquido iónico e/ou da sua concentração.

Abstract

This thesis concerns the design and characterisation of new membranes prepared by incorporation/immobilisation of ionic liquids (ILs). These membranes were developed aiming for two distinct applications: fuel cells and CO_2 separation from gas streams.

In the first part of this PhD thesis, Nafion membranes were modified by incorporating different types of ionic liquids cations, with different degrees of concentration, in order to evaluate their potential use for fuel cells. The characterisation of the modified Nafion/IL cation membranes was performed using the following techniques: XPS (X-ray photoelectron spectroscopy), EIS (Electrochemical Impedance Spectroscopy), proton NMR relaxometry and thermogravimetry analysis. Methanol and gas crossover studies were also performed for these modified Nafion/IL cation membranes. It has been shown that it is possible to obtain membranes with tailored properties, depending on the IL cation incorporated and its degree of incorporation. Moreover, the introduction of the bulky IL cations leads to changes in the membrane water content and in the water degree of structuring. Modifications in the water structuring improved the stability of the modified membranes at high temperatures (up to 200 °C) and reduced both their methanol and gas crossover. However, this modification appears to decrease the proton mobility (at room temperature) when compared to that of an unmodified Nafion membrane.

In the second part of this Thesis, different ionic liquids were immobilised in the porous structure of polymeric porous membranes, in order to evaluate their potential use for gas separation processes. Studies were performed to assess the supported ionic liquid membranes (SILMs) stability, using membrane supports of different

chemical nature. Moreover, permeabilities were measured for pure gases, humidified gases, and gas mixtures. It was concluded that the SILMs are stable (for difference pressures up to 2 bar) and highly selective for CO_2, when compared with N_2 and CH_4. The presence of water vapour in the gas stream is an important factor, since it decreases their selectivity. In this work, the results obtained for the CO_2/CH_4 separation are rather promising suggesting SILMs may be potentially applied for this specific gas separation.

This work shows that by using ionic liquids in both membrane types – Nafion membranes and polymeric porous membranes – the properties of the membranes can be tuned and improved according with the application envisaged, through a careful selection of the IL structure and its concentration.

Résumé

Dans cette thèse étudie la conception et la caractérisation de nouveaux membranes préparées par l'incorporation et l'immobilisation des liquides ioniques. Ces membranes ont été élaborés en vue de deux applications distinctes : la cellule de combustible et de séparation du CO_2 des flux de gaz.

Dans la première partie du travail développé dans ce projet de thèse, membranes Nafion ont été modifiés par l'incorporation différents types de cations des liquides ioniques avec différents degrés de concentration afin d'évaluer le potentiel d'utilisation dans les piles à combustible. La caractérisation des membranes Nafion modification a été effectuée en utilisant les suivantes techniques : XPS (spectroscopie de photoélectrons de rayos X), EIS (impédance électrochimique Spectroscopy), RMN (relaxation magnétique nucléaire des protons) et thermogravimétrie. Ont également été menées des études sur le transport de méthanol et de gaz purs, et tous les résultats ont été comparés avec ceux d'une membrane Nafion non modifié. Il a été constaté qu'il est possible de concevoir des membranes avec des propriétés ajusté, selon le cation liquide ionique constituée et le degré d'intégration. En outre, il a été constaté que l'introduction de cations volumineux de changements liquides ioniques la teneur en eau existant dans la membrane et le degré de structuration. Ces changements dans le degré de structuration de l'eau a amélioré la stabilité de la modification de membranes à haute température (jusqu'à 200 °C) et réduire le transport de méthanol et de gaz. Toutefois, l'approche adoptée dans ce travail de modifier la membrane Nafion avec les cations des liquides ioniques a réduit sa mobilité protons par rapport à une membrane Nafion non modifié.

Dans la deuxième partie de l'œuvre dans cette thèse, différents liquides ioniques

ont été immobilisés sur des membranes de polymère poreux afin d'évaluer leur potentiel d'utilisation dans les processus de perméation gazeuse. Des études ont été effectuées pour évaluer la stabilité des membranes soutenues par des liquides ioniques, en utilisant différents médias pour hydrophobicité différents. En outre, les valeurs de perméabilité ont été déterminées pour les gaz purs, des gaz et mélanges de gaz décomposé. Il est conçu de sorte que les membranes sont stables et hautement sélectif pour le CO_2, par rapport à N_2 ou CH_4. Il a été constaté que la présence de vapeur d'eau dans le gaz est un paramètre qui doit être pris en compte dans l'étude du processus, car il influe sur la stabilité des membranes. Dans cet article, les résultats concernant la séparation du CO_2 et de CH_4 sont très prometteurs, ce qui indique que les membranes avec appuyé liquides ioniques peuvent être utilisés pour cette séparation en particulier.

Dans cette thèse il a été démontré qu'en modifiant les deux types de membranes liquides ioniques - membranes Nafion et membranes poreuses - leurs propriétés peut être adaptée et améliorée en fonction à une application spécifique, à travers une sélection minutieuse de la structure d'un liquide ionique et/ou sa concentration.

Abbreviations

ALIQUAT$^+$DCA$^-$	Methyltricaprylylammonium dicyanamide
ARXPS	Angle resolution XPS
A.C.	Atomic concentration, %
B.E.	Binding energy, eV
BMIM$^+$PF$_6^-$	1-n-Butyl-3-methylimidazolium hexafluorophosphate
BPP	Bloembergen, Purcel and Pound model
C	Capacitance, F
CPE$_i$	Equivalent capacitance, F
CTA$^+$Br$^-$	Hexadecyltrimethylammonium bromide
[C$_4$MIM][PF$_6$]	1-n-Butyl-3- methylimidazolium hexafluorophosphate
[C$_8$MIM][PF$_6$]	1-n-Octyl-3-methylimidazolium hexafluorophosphate
[C$_4$MIM][BF$_4$]	1-n-Butyl-3- methylimidazolium tetrafluoroborate
[C$_{10}$MIM][BF$_4$]	1-n-Decyl-3-methylimidazolium tetrafluoroborate
[C$_4$MIM][Tf$_2$N]	1-n-Butyl-3-methylimidazolium bis(trifluoromethanesulfonyl)imide
DMFC	Direct methanol fuel cell
DTA$^+$Cl$^-$	n-Dodecyltrimethylammonium chloride
EIS	Electrochemical Impedance Spectroscopy
IL	Ionic Liquid
IS	Impedance Spectroscopy
NMR	Nuclear Magnetic Resonance
OMIM$^+$PF$_6^-$	1-n-Octyl-3-methylimidazolium hexafluorophosphate
PEM	Polymer Electrolyte Membranes / Polymer Exchange Membrane
PEMFC	Polymer Electrolyte Membrane Fuel Cell

PTFE	Polytetrafluoroethylene
PVDF	Polyvinylidene fluoride
RMTD	Rotations mediated by translational displacements
RTIL	Room Temperature Ionic Liquid
SLM	Supported Liquid membrane
SILM	Supported Ionic Liquid membrane
TGA	Thermogravimetry Analysis
TMA^+Cl^-	Tetramethylammonium chloride
$TMPA^+Cl^-$	Phenyltrimethylammonium chloride
TSIL	Task Specific Ionic Liquid
XPS	X-ray photoelectron spectroscopy

Variables

A	Cross-sectional area of the membrane, m^2
D	Diffusivity or diffusion coefficient, $m^2\ s^{-1}$
f	Frequency, Hz
F	Faraday constant, 96485.3394(24) $C\ mol^{-1}$
i	Electric current, A
I_m	Maximum current intensity, A
L or l	Membrane thickness, m
l_{max}	Largest displacement distance, m
l_{min}	Smallest displacement distance, m
P	Permeability, $m^2\ s^{-1}$

p_{feed}	Pressure in the feed compartment, Pa
p_{perm}	Pressure in the permeate compartment, Pa
R_i	Membrane resistance, Ω
R_1	Proton spin-lattice relaxation rate, s^{-1}
S	Solubility
t	Time, s
T_1	Proton spin-lattice relaxation time, s
V_{feed}	Volume of the feed compartment, m^3
V_{perm}	Volume of the permeate compartment, m^3
V_m	Maximum voltage intensity, V
$\overline{V_1}$	Gas molar volume, $cm^3\ mol^{-1}$
x_A	Mole fractions of A in the feed compartment
x_B	Mole fractions of B in the feed compartment
y_A	Mole fractions of A in the permeate compartment
y_B	Mole fractions of B in the permeate compartment
$Z(\omega)$	Electrical impedance, Ω
Z_{real}	Real part of the electrical impedance, Ω
Z_{imag}	Imaginary part of the electrical impedance, Ω

Greek Letters

α	Ideal selectivity
β	Geometric parameter related with the geometry of the permeation cell, m^{-1}
μ	Proton mobility, $cm^2\ s^{-1}\ V^{-1}$

μ_2	RTIL viscosity, mPa s
σ	Ionic conductivity, S cm−1
τ_c	Correlation time, s
υ	Voltage applied, V
υ	Larmor frequency, Hz
ϕ	Take-off angle, °
χ	Orientational structure factor
ω	Angular frequency, Hz
$\omega_{RMTD,max}$	High cut-off frequency, Hz
$\omega_{RMTD,min}$	Low cut-off frequency, Hz

Contents

1 Introduction **1**

1.1 Background and motivation 1

1.2 Research strategy 8

1.3 Thesis Outline 15

2 Design and Characterisation of Nafion Membranes with Incorporated Ionic Liquid Cations **17**

2.1 Summary 17

2.2 Introduction 18

2.3 Experimental 22

2.3.1 Materials 22

2.3.2 Incorporation of the ionic liquid (IL) cations in Nafion membranes 23

2.3.2.1 Incorporation method 23

2.3.2.2 Monitoring the incorporation of IL cations in the Nafion membrane 23

2.3.3 Assessment of the Nafion-IL membranes for potential PEM applications 26

2.3.3.1 Electrical impedance spectroscopy (EIS) measurements 26
2.3.3.2 Thermogravimetry Analysis 27
2.4 Results and Discussion 28
2.4.1 Incorporation of IL cations in Nafion membranes 28
2.4.2 X-ray photoelectron spectroscopy (XPS) results 30
2.4.3 Characterisation of modified Nafion membranes using electrochemical impedance spectroscopy (EIS) 35
2.4.4 Potential use of the modified membranes as polymer electrolyte membranes (PEM) 46
2.5 Closure 49

3 Proton NMR Relaxometry Study of Nafion Membranes Modified with Ionic Liquid Cations 51

3.1 Summary 51
3.2 Introduction 52
3.3 Materials and Methods 56
3.3.1 Materials 56
3.3.2 Incorporation of Ionic Liquid (IL) cations in Nafion membranes 58
3.3.3 NMR Relaxometry experiments 58
3.4 Results and Discussion 59
3.4.1 Characterisation of modified Nafion/IL cation membranes using NMR relaxometry 59
3.4.2 Modelling of proton spin-lattice relaxation of modified Nafion/IL cation membranes 67
3.4.3 Temperature effect on the spin-lattice relaxation time 72

3.5 Closure 75

4 Methanol and Gas Crossover Through Modified Nafion Membranes by Incorporation of Ionic Liquid Cations 79

4.1 Summary 79

4.2 Introduction 80

4.3 Experimental 84

4.3.1 Materials 84

4.3.2 Incorporation of Ionic Liquid (IL) cations in Nafion membranes 85

4.3.3 Methanol crossover measurements 87

4.3.4 Gas crossover measurements 88

4.4 Results and Discussion 89

4.4.1 Methanol crossover results 89

4.4.1.1 Effect of the incorporation degree of the IL cation . . . 90

4.4.1.2 Effect of the different IL cations incorporated 92

4.4.1.3 Comparison with the different strategies presented in the literature 95

4.4.2 Gas crossover results 96

4.5 Closure 101

5 Gas Permeation Studies using Supported Ionic Liquid Membranes 103

5.1 Summary 103

5.2 Introduction 104

5.3 Experimental 108

5.3.1 Materials 108

5.3.1.1 Polymeric Porous Membranes 108

5.3.1.2 Room Temperature Ionic Liquids (RTILs) 109
5.3.1.3 Gases 109
5.3.2 Preparation of supported ionic liquid membranes (SILMs) . . . 111
5.3.3 Stability of supported ionic liquid membranes (SILMs) 111
5.3.4 Gas permeation experiments 112
5.3.4.1 Single gas permeability 112
5.3.4.2 Humidified gas permeability 114
5.3.4.3 Gas mixture permeability 115
5.3.5 Calculation methods 115
5.4 Results and Discussion 116
5.4.1 Stability of SILMs 116
5.4.2 Single gas permeation results 119
5.4.2.1 Effect of the RTIL cation 120
5.4.2.2 Effect of the RTIL anion 124
5.4.2.3 Ideal Selectivities 126
5.4.3 Gas streams containing water vapour 127
5.4.4 Gas mixture permeation results 131
5.5 Closure 133

6 Conclusions and Future Work 135

6.1 Study of the incorporation of ionic liquid cations in Nafion membranes and their characterisation 135
6.2 Study of the immobilisation of ionic liquids in porous membranes and gas permeation studies 140
6.3 Suggestions for Future Research 141

Bibliography 143

List of Figures

1.1 Schematic representation of a (a) Hydrogen fuel cell and (b) Direct methanol fuel cell. 2

1.2 Robeson upper bound correlation for CO_2/N_2 and CO_2/CH_4 separations. 6

2.1 Chemical structure of Nafion. 19

2.2 Incorporation degree in the Nafion membrane, for the different cations studied as a function of contact time. 29

2.3 Atomic concentration percentage (A.C. %) of the elements present in Nafion/DTA^+ samples as a function of the contact time (a) carbon and fluorine and (b) nitrogen and sulfur. 32

2.4 Deep-profile XPS analysis of (a) Nafion/$BMIM^+$ and (b) Nafion/$OMIM^+$ membranes. 33

2.5 C *1s* core level normalized spectra and main bonds for the studied membranes (a) Nafion-112/H^+, Nafion/$TMPA^+$, Nafion/DTA^+, and Nafion/CTA^+ and (b) Nafion-112/H^+, Nafion/$BMIM^+$ and Nafion/$OMIM^+$. 36

2.6 Bode plot for Nafion in contact with DTA^+ along time (a) representation of -Z_{imag} as a function of the frequency and (b) representation of Z_{real} as a function of the frequency. 37

2.7 Bode plot for Nafion in contact with CTA^+ along time (a) representation of -Z_{imag} as a function of the frequency and (b) representation of Z_{real} as a function of the frequency. 38

2.8 (a) Bode plot for Nafion in contact with $TMPA^+$ along time (representation of -Z_{imag} as a function of the frequency) and (b) Bode plot for Nafion in contact with $BMIM^+$ along time (representation of -Z_{imag} as a function of the frequency). 39

2.9 Equivalent circuit for Nafion/DTA^+ and Nafion/CTA^+, where R_1 is the membrane resistance, CPE_1 the membrane equivalent capacitance, R_2 the interface resistance and CPE_2 the interface equivalent capacitance. 41

2.10 Equivalent circuit for Nafion/$TMPA^+$, Nafion/$BMIM^+$ and Nafion/$OMIM^+$, where R_1 is the membrane plus IL resistance and CPE_1 the membrane plus IL equivalent capacitance. 41

2.11 (a) Dependence of the membrane resistance for Nafion/CTA^+ and Nafion/DTA^+, as a function of the incorporation degree (%) and (b) Dependence of the membrane plus IL resistance for Nafion/$TMPA^+$, Nafion/$BMIM^+$ and Nafion/$OMIM^+$, as a function of the incorporation degree (%). . . 42

2.12 Variation of the membrane plus electrolyte resistance with the electrolyte ionic conductivity. 45

2.13 (a) Evolvement of the relative amount of water in each membrane with increasing temperature, and (b) Evolvement of each membrane weight with increasing temperature. 48

3.1 Chemical structure of Nafion. 52

3.2 Frequency dependence of the proton spin-lattice relaxation rate R_1 for Nafion/H^+. 61

3.3 Spin-lattice relaxation time (T_1) as a function of the incorporation degree for different values of frequency. 62

3.4 Comparison of the frequency dependence of the proton spin-lattice relaxation rate R_1 for: (a) Nafion/H^+, Nafion/DTA^+ (13 %) and Nafion/DTA^+ (13 %)_D_2O, and (b) Nafion/H^+, Nafion/DTA^+ (68 %) and Nafion/DTA^+ (68 %)_D_2O). 63

3.5 Comparison of the frequency dependence of the proton spin-lattice relaxation rate R_1 for the unmodified and modified Nafion/IL cation membranes. 66

3.6 Calculated relaxation rates obtained through fitting for (a) Nafion/H^+, (b) Nafion/$TMPA^+$, (c) Nafion/$BMIM^+$, and (d) Nafion/DTA^+. The symbols represent the experimental values, the solid lines represent the calculated total relaxation rates, while the dash and dash-dot lines represent respectively the single contribution of the RMTD and BPP equations. 70

3.7 Time evolution of the spin-lattice relaxation time for different temperatures: 23 °C, 80 °C and 120 °C for (a) Nafion/H^+, (b) Nafion/$TMPA^+$, (c) Nafion/$BMIM^+$, (d) Nafion/DTA^+ membrane. 73

4.1 Chemical structure of Nafion. 81

4.2 Scheme of the experimental set-up for measuring pure gas crossover through the modified Nafion/IL membranes. 88

4.3 Methanol crossover as a function of the DTA^+ cation incorporation degree and of the total volume of incorporated cation per final membrane volume ($cm^3_{ILcation}$ / $cm^3_{membrane}$). 91

4.4 Methanol crossover as a function of the volumetric ratio of the incorporated IL cation volume per final membrane volume, in equilibrium ($cm^3_{ILcation}$ / $cm^3_{membrane}$). 93

4.5 Evolvement of each membrane weight with increasing temperature (figure adapted from Chapter 2). 94

4.6 Gas crossover obtained for the Nafion/IL membranes as a function of the Lennard-Jones diameter of each gas, at a temperature of 30 °C. . . . 98

4.7 Gas crossover of the modified Nafion/IL cation membranes as a function of the volume of incorporated IL cation per final membrane volume, for the gases (a) H_2; (b) O_2; (c) N_2; (d) CO_2. 99

5.1 Typical cations and anions present in imidazolium type of RTILs. . . . 105

5.2 Experimental set-up to evaluate the stability of the SILMs. 112

5.3 Experimental set-up for measuring the permeability of the SILMs (a) for a single gas, (b) for mixed gas/water vapour, and (c) for gas mixtures. TC - Temperature Controller; HI - Humidity Indicator; PI - Pressure Indicator; GC-TCD – Gas Chromatograph - Thermal Conductivity Detector. 113

5.4 Relative membrane weight in (a) hydrophilic, and (b) hydrophobic membranes immobilized with different RTILs as a function of time. Applied pressure difference: 1 bar. 117

5.5 Relative membrane weight in (a) hydrophilic, and (b) hydrophobic membranes immobilized with $[C_4MIM][Tf_2N]$ as a function of time, for different applied pressures. 119

5.6 Permeability of the SILMs as a function of the gas Lennard-Jones diameter. 120

5.7 Gas permeability of the SILMs prepared with the hydrophobic support and the RTILs $[C_4MIM][PF_6]$, $[C_8MIM][PF_6]$, $[C_4MIM][BF_4]$, $[C_{10}MIM][BF_4]$, as a function of the number of carbons of the imidazolium cation (a) H_2; (b) O_2; (c) N_2; (d) CH_4; and (e) CO_2. 122

5.8 Permeability of the SILMs prepared with the hydrophobic support and the RTILs $[C_4MIM][Tf_2N]$, $[C_4MIM][BF_4]$, $[C_4MIM][PF_6]$, as a function of the RTIL viscosity. 124

5.9 (a) CO_2/N_2 selectivity as a function of CO_2 permeability, and (b) CO_2/CH_4 selectivity as a function of CO_2 permeability 127

5.10 CO_2, N_2 and CH_4 gas permeability as a function of the gas humidity content for the hydrophobic support immobilized with (a) $[C_4MIM][PF_6]$, (b) $[C_4MIM][Tf_2N]$, and (c) $[C_8MIM][PF_6]$. 128

5.11 (a) CO_2/N_2 selectivity as a function of CO_2 permeability, and (b) CO_2/CH_4 selectivity as a function of CO_2 permeability 133

List of Tables

2.1 Characteristics of the ionic liquid cations studied 24

2.2 Atomic concentration percentages (A.C. %) of the different elements on the surfaces of the Nafion and Nafion/IL modified membranes Membranes 34

2.3 Nafion/DTA^+ and Nafion/CTA^+ membrane resistance, ionic conductivity and proton mobility values 44

3.1 Characteristics of the ionic liquid cations studied 57

3.2 The best fit values of parameters used in calculating the dispersion curves presented in Fig. 3.6 71

3.3 Fitted values of maximum frequency and diffusion coefficient for the modified Nafion/IL cation membranes 72

4.1 Characteristics of the ionic liquid cations studied 86

4.2 Methanol crossover obtained for the different Nafion/IL cation membranes studied 92

4.3 Methanol crossover reduction: comparison with different approaches presented in the literature 97

4.4 Reduction in gas crossover for the modified Nafion/IL cation membranes 100

5.1 Polymeric porous membranes used as support of SILMs 108
5.2 Properties of the RTILs studied 110
5.3 Permeability, diffusivity and solubility ratios for the pairs C_8MIM^+/C_4MIM^+ and $C_{10}MIM^+/C_4MIM^+$ with the respective anions $[PF_6]^-$ and $[BF_4]^-$. 123
5.4 Permeability, diffusivity and solubility ratios for the pair $[Tf_2N]^-/[BF_4]^-$ 125
5.5 Ideal Selectivities (CO_2/N_2 and CO_2/CH_4) obtained for the tested SILMs 126
5.6 Ratio (P_H/P_0) between the humidified gas permeability, P_H, and the pure gas permeability, P_0, for the different SILMs 130
5.7 CO_2/N_2 and CO_2/CH_4 ideal selectivities obtained with dry and humidified gases 130
5.8 CO_2/N_2 and CO_2/CH_4 ideal and mixed-gas selectivities obtained for the tested SILMs 132

Chapter 1

Introduction

1.1 Background and motivation

The design and modification of existing membranes is nowadays commonly applied for the fine tuning of membrane properties for specific applications. There are several membrane applications where their design and modification proved to be particularly important, especially when the separation and transport capabilities of the existing membranes are not satisfactory. Within these various applications, amongst the most studied nowadays are fuel cells and gas separations processes, where the membrane plays a major role and may be considered as the limiting step of the processes under study [1–3].

Fuel cells may be nowadays regarded as one of the solutions for environmental friendly and cost effective alternatives to traditional power sources. In recent years their demand in industry has significantly grown, and scientific publications have increased exponentially [4]. Basically, a fuel cell is an electrochemical device which converts chemical energy of a fuel into electricity. The fuels most commonly stud-

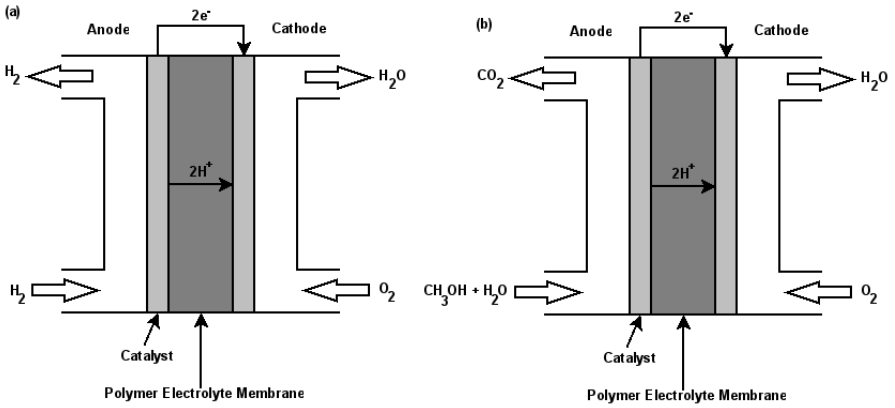

Figure 1.1: Schematic representation of a (a) Hydrogen fuel cell and (b) Direct methanol fuel cell.

ied are hydrogen and liquid methanol, being designated as hydrogen fuel cells and direct methanol fuel cells, respectively. Representations of these fuel cells are shown in Fig. 1.1.

Energy is produced in a hydrogen fuel cell (Fig. 1.1a) by the catalytic reaction which occurs in the anode compartment, thereby dissociating hydrogen into protons and electrons. The protons produced are then transported by diffusion to the cathode compartment through a polymer exchange membrane (PEM), while electrons are transported along an external circuit from the anode to the cathode side, producing electrical energy. In the cathode side, the protons react with oxygen (from the air), producing water. The methanol fuel cell operation is very similar to the one described before, with the difference that at the anode side, carbon dioxide is produced in the dissociation reaction of liquid methanol at the anode (Fig. 1.1b) [1, 5]. Among the innumerous parameters that may influence the performance and durability of a fuel cell, the polymer exchange membrane performance has been regarded as the most relevant aspect to investigate. Nafion membranes

are the most common material used in fuel cells, due to the fact that this material presents unique characteristics such as a high ionic conductivity and, consequently a high proton mobility which is essential for the conduction of protons from the anode to the cathode. Moreover, these materials present high mechanical, chemical and thermal stabilities at temperatures up to 80 °C. Although Nafion membranes are considered as the reference material to be used in fuel cells, there are some limitations that need to be overcome in order to further improve their performance. One example of such limitations is the membrane water content decrease at temperatures higher than 80 °C, which results in a decrease of the ionic conductivity and consequently, in the decrease of its efficiency for conducting protons from the anode to the cathode side. Therefore, Nafion membranes are not adequate for operation at high temperatures (above 100 °C) although it would be favorable for fuel cell operation. Additionally, Nafion presents a high methanol and gas crossover, and both could lead to fuel inefficiency [1, 5–7]. It is therefore challenging to consider modifications of Nafion membrane in order to try to obtain solutions for the mentioned drawbacks.

During the last years another area that has attracted considerable industrial interest, is focused on gas separation processes, especially those where CO_2 is present. CO_2 emissions are considered to be among the main contributors to the global climate change. Membrane processes have been widely studied in the literature and are already used in industry for different gas separation processes, namely for the production of oxygen enriched air, separation of CO_2 from natural gas, and purification of H_2 [3]. Amongst the diverse membrane gas separations, there are two main applications that have been receiving the highest interest from the scientific community and industry: 1) the improvement of membranes for the capture of carbon

dioxide from flue gas (CO_2/N_2) [3], and 2) the purification of natural gas (CO_2/CH_4) [8]. A typical flue gas composition in post-combustion processes contains approximately 70 % of N_2 and 3–15 % of CO_2 at a temperature of 200 °Cand at 1 atm [9]. Polymeric membranes have been widely studied for the separation of CO_2 from N_2 in flue gas streams [3]. Regarding natural gas, its original composition varies, depending on the source. Methane is always the major component, typically between 70 %–90 % of the total, but natural gas also contains significant amounts of ethane, propane and butane (0 %–20 %), carbon dioxide (0 %–8 %) and water, oxygen, nitrogen and hydrogen sulfide, in small quantities. Although the composition of natural gas varies from source to source, it is always necessary to proceed to the purification of natural gas before its distribution to consumers [10]. Nowadays, the purification of natural gas using membranes occurs at high pressures of 30–60 bar, using hollow fibber membranes or flat sheets packaged in spiral wound modules [8].

Even though there a large number of different membrane materials and operating conditions used for the separation of CO_2 either from flue gas or natural gas, the performance of existing processes to effectively separate CO_2 are not yet satisfactory. The applications developed so far have been compromised mainly by the membrane selectivity [11]. It is therefore mandatory to develop membranes that have a high CO_2 permeability, a high CO_2/N_2 or CO_2/CH_4 selectivity, depending on the application, to be thermally and chemical resistant to be used at high temperatures and/or high pressures if necessary, and also to present resistance to plasticization effects which normally occur due to absorption of CO_2 and may have negative implications on the process selectivity.

When using nonporous membranes in gas separations processes, the transport occurs according to a solution-diffusion mechanism, where some of the compon-

ents solubilizes in the membrane, followed by their diffusion across it and partition to the permeate phase. Therefore, when choosing the best membrane to be used in a specific gas separation process it is necessary to take into consideration not only the diffusivity of the species within the membrane, but also the affinity/solubility of each compound in the membrane [11]. Robeson et al. [12] estimated different correlations regarding important gas separations with all the data available in the literature. Examples of these gas separations are the CO_2/N_2 and CO_2/CH_4 separations. The ideal selectivity as a function of the CO_2 permeability as well as the upper bound correlations for CO_2/N_2 (solid line) and CO_2/CH_4 (dashed line) separations are represented in Fig. 1.2 [12]. The analysis of this figure indicates that more efficient membranes for these specific separations (CO_2/N_2 and CO_2/CH_4) should preferentially have values located above these upper bound correlations, in order to have higher CO_2 selectivity values when compared with N_2 or CH_4. Additionally, for a membrane to be useful for the capture of carbon dioxide it should have a high CO_2 permeability, and therefore values located to the right of each one of these upper bound correlations would be favourable [3].

One approach for enhancing flux through a solution-diffusion mechanism is to use liquid membranes, due to the high diffusivity of gases when compared with solid membranes, which in principle will lead to higher permeability values. In particular, supported liquid membranes (SLMs) have been considered one of the most attractive membranes to be used in gas separation applications [13]. However, operating conditions such as high temperature and high pressure, as well as lack of differentiated selectivity towards specific gases is still limiting its application. In a SLM configuration, a solvent is immobilised inside the porous support of the supporting membrane by capillary forces. However, high temperatures may lead to the

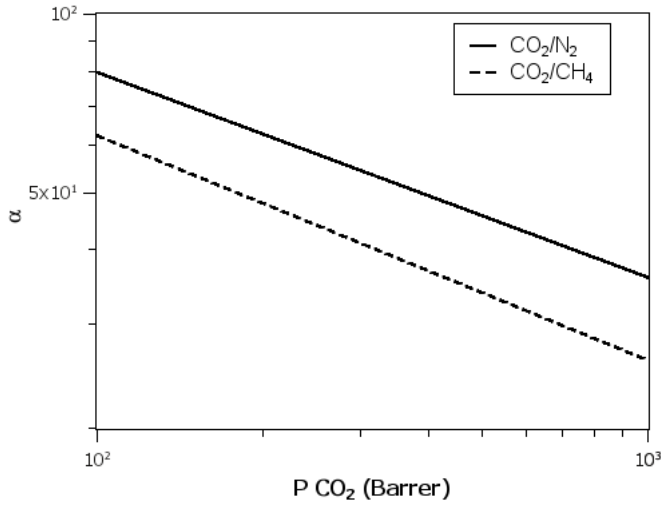

Figure 1.2: Robeson upper bound correlation for CO_2/N_2 and CO_2/CH_4 separations.

evaporation of the solvent contained within the membrane pores, and high pressures may lead to the displacement of the liquid from the membrane pores [14]. One of the main challenges regarding supported liquid membranes is the designing of a liquid membrane in which the solvent contained inside the membrane pores is not lost through evaporation. Additionally, its mechanical and long-term stability should not be affected at high operating pressures. Finally, the liquid solvent within the membrane pores should present high selectivity values towards the specific target gas of interest.

Ionic Liquids (ILs) are regarded nowadays as valuable solvents that may in the short to mid-term replace conventional solvents in specific applications. Ionic Liquids are compounds consisting entirely of ionic species, with an organic cation and an inorganic or organic anion. The physical and chemical properties of ILs may be tuned according to the cation and anion present in their structure, and one of their most important properties is that they present a negligible vapour pressure.

Moreover, due to their excellent chemical and thermal stabilities, as well as good electrical conductivity and high ionic conductivity, ILs are becoming very attractive in a number of applications [15, 16]. Also in the case of membrane processes, ILs are being used in the design and modification of advanced materials that enable performance levels not typical of conventional materials [17].

The approach followed in the work developed in this thesis was to modify both Nafion and porous polymeric membranes with ILs. Nafion membranes are cation-exchange membranes which means that, in the presence of an electrolyte, an exchange between cations occurs. In the case of modifying Nafion membranes with ILs, it is expected that the Nafion membranes will acquire the physical and chemical properties associated with the incorporation of the IL cations [18]. Generally, it is expected that the introduction of bulky IL cations will modify the way water is structured and involved in solvation processes, which can improve the stability of the membrane at high temperatures, and the reduction of species transport (e.g. methanol and gases). On the other hand, it is expected that this modification will reduce the proton mobility of the membrane as protons are replaced by the less mobile IL cations.

In supported liquid membranes, the use of an IL as the immobilised liquid phase within the membrane pores may bring significant advantages. In this case, the properties of the resulting membrane after modification are associated with the ionic liquid and not with the IL cation, as is the case of the Nafion membranes. It is expected that with such modification the loss of ionic liquid from the pores of a supported membrane by evaporation will be less than with conventional solvents due to the negligible vapour pressure of the ILs. Moreover, ILs have shown high solubility for CO_2 when compared to other gases, which encourages the use of supported

membranes with ionic liquids in gas separations, especially when CO_2 is present [19, 20].

The main objectives of this thesis are the design and characterisation of new membranes prepared by incorporation / immobilisation of ionic liquids and their evaluation in two distinct applications: 1) Nafion membranes for potential use in fuel cells; 2) supported ionic liquid membranes (SILMs) for CO_2 separation from gas streams. The first application will be focused on the incorporation of ionic liquids cations in proton carrier membranes - Nafion - while the second will be focused on the study of the immobilisation of ionic liquids within the porous structure of ultrafiltration membranes. The aim is to develop membranes with chemical, mechanical and thermal stability, and unique features that will be conferred by incorporation/immobilisation of ionic liquids with different properties. It is expected that ionic liquids with a large variety of properties and affinity for different types of molecules, will enable the designing of tailor-made membranes with a defined selectivity for specific applications.

1.2 Research strategy

Taking into consideration the objectives identified above, the work carried out was divided in two major parts. In the first part, it was given emphasis to the development of modified Nafion membranes in the protonated form, by replacing the H^+ protons for an IL cation. Since the use of thinner membranes in polymer exchange membrane fuel cells (PEMFCs) will improve the power efficiency of a fuel cell due to the reduction on the ionic resistance, a Nafion-112 membrane with a thickness of 51 μm in the protonated form was chosen as the unmodified membrane (start-

ing material) [21]. This membrane is thinner than Nafion 117 and Nafion 115, with thicknesses of 175 μm and 125 μm, respectively, but with a thickness larger than 25 μm (Nafion membrane NR211), due to the fact that the risk of membrane failure increases with a decrease in membrane thickness. Then, different IL cations were selected in order to cover a wide range of molecular sizes and structures.

After studying the incorporation method and quantifying the number of IL cations incorporated in the membrane, a number of characterisation techniques were selected for the characterisation of ion exchange membranes, helping answering questions such as: how is distributed the IL cation within the membrane after its modification, with different degrees of incorporation or with a maximum incorporation degree; which were the resulting electrical properties; what happens to proton mobility and to the degree of water structuring present after the modification; and finally, if the stability and proton mobility of these membranes could be affected at high temperatures.

To start answering these questions, the first characterisation technique used in this work was X-ray photoelectron spectroscopy (XPS). X-ray photoelectron spectroscopy [22] is a technique that consists of irradiating a sample with X-rays under vacuum and measuring the kinetic energy of the photoelectrons ejected from the surface of the sample. The emitted electrons binding energy can be calculated as: $E_{binding} = E_{photon} - E_{kinetic}$, where $E_{kinetic}$ is the measured kinetic energy and E_{photon} is the energy of the X-ray incident radiation. Since the binding energies of the electrons are characteristic of each chemical element, it is possible to identify which elements are present in a thin layer of the membrane's surface and calculate their relative percentages [22]. Additionally, by changing the irradiation angle (designed as take-off angle), it is possible to obtain this chemical characterisation

at different depths inside the membrane, in the range between 2.5 nm and 9.3 nm deep. In this thesis this characterisation technique was used to evaluate wether the IL cations were incorporated in the Nafion membrane and to evaluate their distribution in the membrane surface layer.

After verifying that the IL cation was indeed incorporated in the membrane, the electrical properties of these membranes were determined using Electrochemical Impedance Spectroscopy (EIS). Impedance Spectroscopy (IS) [23] is a powerful method for characterising many of the electrical properties of materials and their interfaces with electronically conducting electrodes. Since impedance is frequency-dependent, in general IS measurements consist in applying an alternating voltage, over a wide frequency range, to an electrochemical cell and by measuring the resulting electric current. The applied voltage (υ) is a sine wave input, varying with time (t) and defined by:

$$\upsilon(t) = V_m \sin(\omega\, t) \tag{1.1}$$

where V_m is the maximum voltage intensity and $\omega = 2\,\tau\, f$ is the angular frequency. The resulting electric current (i) is also a sin wave and is defined by:

$$i(t) = I_m \sin(\omega\, t + \theta) \tag{1.2}$$

where I_m is the maximum current intensity, ω the angular frequency, and θ the phase difference between the voltage and the current. The electrical impedance is defined as the ratio between the applied voltage and the resulting electric current, $Z(\omega) = \upsilon(t)/i(t)$, and may be expressed as

$$Z(\omega) = Z_{real} + j\, Z_{imag} \tag{1.3}$$

where Z_{real} is the real part of the electrical impedance and Z_{imag} is its imaginary part. In order to interpret the results, the experimental data can be represented in a Nyquist plot, where the impedance imaginary part (-Z_{imag}) is represented as a function of the impedance real part (Z_{real}); or in a Bode plot, where the real (Z_{real}) or the imaginary part (-Z_{imag}) of the impedance is represented against the frequency (f). By analysing the shape of the curves of both representations it is possible to conclude qualitatively if the system behaves like a parallel resistance-capacitor (RC) circuit (semicircle representation in the Nyquist plot) or if the system under study is complex and involves two or more subsystems with different dielectric properties. In this case two or more relaxation processes may appear in the Nyquist and Bode plots, and the equivalent circuit for the entire system is a series association of two or more RC elements, one for each sub-system [23]. Quantitatively, it is also possible to analyse the experimental data using a specific software, in order to quantify the electrical parameters, such as resistances (R) and capacitances (C) present in the system under study. In this thesis, impedance spectroscopy was used as a monitoring tool to follow the incorporation of the different IL cations into Nafion until reaching equilibrium. For each incorporation degree, it was possible to determine the electrical properties of modified Nafion membranes and consequently to understand the influence of different degrees of incorporation of IL cations on the electrical properties of these membranes.

Following the characterisation of the modified Nafion/IL cation membranes, thermogravimetric analysis seemed the best technique to further investigate if the

modified Nafion/IL cation membranes retained their water content at increasing temperatures, when compared with an unmodified Nafion membrane. Thermogravimetric Analysis [24] is a technique that allows for determining changes in samples weight with changes in temperature. This analysis relies on a high degree of precision of three parameters: the weight, the temperature, and temperature changes. For that purpose this technique usually requires a high-precision balance with a pan (generally platinum) loaded with the sample. The pan is placed in a small electrically heated oven with a thermocouple to measure the temperature with high accuracy. An inert gas is used for purging the atmosphere for preventing oxidation or other undesired reactions. The analysis is carried out by increasing the temperature gradually and plotting the weight against temperature [24]. This technique was used in this work to evaluate the degree of water loss of the modified membranes with increasing temperature (up to 210 °C). The results obtained were compared with those obtained for an unmodified Nafion membrane, to assess their stability and potential use as PEM for fuel cells.

After concluding that the modification of Nafion membranes using this procedure has potentially interesting properties for its application in fuel cells, the question that arose was: what will happen to the proton mobility and to the molecular mobility of these membranes at room temperature and, especially, at high temperatures? To answer this question Proton Nuclear Magnetic Resonance (NMR) Relaxometry studies were performed in a wide frequency range. The proton NMR relaxation technique describes the energy exchange between the proton spins of the hydrogen nuclei and the energy exchange between this spin system and the surrounding lattice. These energy exchanges are characterised by two relaxation rates: the spin-spin relaxation rate, $R_2=1/T_2$, and the spin-lattice relaxation rate, $R_1=1/T_1$,

where T_2 is defined as the spin-spin relaxation time and T_1 as the spin-lattice relaxation time. Generally, the molecules are orientated in a defined way when they are in the presence of a magnetic field. In these experiments, the magnetic field is disturbed, for example by reversing its direction in 180 degrees, and the time that takes for the molecules to be reoriented with the magnetic field is measured (T_1 and T_2). When both relaxation times are determined for a large range of Larmor frequencies (υ) it is possible to obtain information regarding the molecular dynamics of the system. The Larmor frequency is defined as $\upsilon = \frac{\gamma B}{2\pi}$, where B is the magnetic field and γ is the proton gyromagnetic ratio [25]. The strategy followed when using this technique was to select three different IL cations that in the previous studies have shown to be potentially the most interesting ones. By using NMR relaxometry an effort was made in understanding on the one hand the proton mobility and on the other hand to identify different levels of confinement within the modified membranes. This study was carried out at three different temperatures, 23 °C, 80 °C and 120 °C.

To conclude the first part of this thesis, methanol and gas crossover studies of the modified Nafion/IL cation membranes were performed. Methanol crossover studies were performed to understand if these modified Nafion/IL cation membranes are less permeable to methanol and whether they could be used in direct methanol fuel cells applications (Fig. 1.1b). The effect of using different degrees of incorporated IL cations, as well as the type of IL cation incorporated, was studied in detail in the transport of methanol. Moreover, gas crossover studies were performed, specifically for the gases that may be present as reagents or reaction products in both fuel cells configurations (Fig. 1.1), since a high crossover may have a negative effect on the fuel cell performance. The H_2, O_2, N_2 and CO_2 permeabilities were determ-

ined for the equilibrium degree of concentration for each IL cation incorporated in Nafion.

The second part of this thesis was dedicated to the development of stable supported ionic liquid membranes (SILMs) for potential applications in CO_2/N_2 and CO_2/CH_4 separations. Different ILs were immobilised in two different polymeric membranes with different nature. All the selected ionic liquids were based on the imidazolium cation due to the fact that they present a higher selectivity for CO_2, while the different nature of the membranes supports in terms of hidrophilicity and hidrophobicity was studied in order to understand their effect on the SILMs stability. To evaluate if the SILMs have potential to be used in gas separations, pure gas permeation studies were firstly carried out and ideal selectivities were calculated. After verifying that the SILMs are very selective for CO_2 when compared to other gases, especially CH_4, focus was then given to study the effect of the presence of water vapour in the gas streams on the stability of a SILM. Water vapour, even in small quantities, is present in many gas streams. Therefore, this is an important parameter which is necessary to take into account when using SILMs in gas separation processes. Indeed, recent studies have suggested that these membranes have the ability to form water clusters in the presence of water, which are expected to significantly influence both the membrane gas selectivity and permeability. Finally, gas mixture experiments were also carried out by preparing binary mixtures of CO_2/N_2 and CO_2/CH_4 to assess the effect of using gas mixtures on the permeability and selectivity when compared with pure gases. The results obtained were compared with the data available in the literature and strategies for designing better SILMs for these specific applications are proposed.

1.3 Thesis Outline

This Thesis is divided into six chapters, following the work performed during this PhD project. Each chapter includes a short review of the state of the art, describes the materials and methods used in that chapter and discuses the results and main conclusions obtained in that part of the work. The methodology used in each individual chapter is detailed in the context of the respective subject and, when applicable, is related to that used in previous chapters. Chapter 2, 3 and 4, are dedicated to the study of the incorporation of ionic liquids cations in Nafion membranes and their characterisation. Chapter 5 is dedicated to the study of immobilisation of ionic liquids in porous membranes and gas permeation studies. The work performed during this PhD has resulted in three scientific articles, presented in Chapters 2, 4 and 5, respectively. The article related to Chapter 2 is already published, and the articles related to Chapters 4 and 5 were recently submitted for publication.

Chapter 1 introduces this Thesis, by presenting the context and motivation for this PhD project, and the research strategy followed.

Chapter 2 presents the approach used for the incorporation of cations of ionic liquids in Nafion membranes. The quantification of the concentration of the cations of ionic liquid incorporated in the Nafion membranes was made through measurements of pH and conductivity, and also by studies of XPS (X-ray photoelectron spectroscopy). The electric properties of the modified Nafion membranes were characterised by EIS (Electrochemical Impedance Spectroscopy). Finally, information obtained with thermogravimetry analysis was included to establish a possible relationship between the modified Nafion membrane stability at high temperatures with the water content and its degree of structuring.

Following the characterisation studies of Nafion membranes modified with ionic liquid cations, in Chapter 3, these modified membranes were characterized by Proton Nuclear Magnetic Resonance (NMR) Relaxometry. The aim of this study was to characterise these modified membranes in terms of their proton mobility and to distinguish different molecular motions that are related with degrees of structuring within the membrane polymeric matrix. The effect of the stability of these membranes at high temperatures in terms of proton mobility was also assessed using this characterisation technique.

In Chapter 4, studies of methanol and gas crossover were performed in Nafion membranes modified with ionic liquid cations, in order to evaluate their potential for direct methanol fuel cells applications. The effect of using different degrees of incorporated IL cations, as well as the type of IL cation incorporated, in the transport of methanol and gases were studied. These results were compared with those obtained with an unmodified Nafion membrane.

Chapter 5 is dedicated to the study of immobilisation of ionic liquids within the porous structure of polymeric membranes, in order to study the potential of using supported ionic liquid membranes (SILMs) for CO_2/N_2 and CO_2/CH_4 gas separations. Different aspects were investigated in this chapter, namely: the evaluation of the SILMs stability using two different supports, one more hydrophilic and other more hydrophobic; and the effect of using RTILs with different alkyl chain length of the cation and different anions, on the permeability and selectivity of pure and humidified gases as well as for gas mixtures.

In Chapter 6, the main results obtained in this PhD project are summarised, and the main conclusions are discussed in an integrated way. Some possible challenges and suggestions for future research are also presented.

Chapter 2

Design and Characterisation of Nafion Membranes with Incorporated Ionic Liquid Cations

Published as: Luísa A. Neves, Juana Benavente, Isabel M. Coelhoso, João G. Crespo, Design and Characterisation of Nafion Membranes with Incorporated Ionic Liquid Cations, Journal of Membrane Science, 347 (2010) 42-52

2.1 Summary

Nafion membranes were modified by incorporation of ionic liquid (IL) cations, at controllable degrees. These modified membranes were then characterised with the use of different techniques. X-ray photoelectron spectroscopy (XPS) demonstrated that the IL cations are incorporated in the membrane material and allowed to evaluate the distribution of the cation in the membrane surface layer. Electrochemical

impedance spectroscopy (EIS) was used to monitoring membrane modification by incorporation of IL cations, and to study the electrical properties of the modified membranes, with different degrees of cation incorporation. These results were adjusted to mathematical models of equivalent electrical circuits to extract data of membrane ionic conductivity. Finally, thermogravimetry studies allowed assessing the stability of the modified membranes with increasing temperature in terms of their water content, and these results were used to establish a possible relation between the membrane stability at high temperatures with their water content and degree of structuring. It was concluded that it is possible to obtain membranes with tailored properties depending on the type of cation and the degree of incorporation.

2.2 Introduction

Nafion membranes are widely used as a reference material in polymer electrolyte membrane fuel cells (PEMFCs) studies and other electrochemical applications such as actuators and transducers, due to their good mechanical, chemical and thermal stability up to temperatures of 80 °C[1, 6, 26, 27]. In addition, these membranes combine the extremely high hydrophobicity of the polytetrafluoroethylene backbone with the high hydrophilicity of the sulfonic acid side-groups arranged in intervals along the chain [28]. These acid groups, which are known to aggregate into clusters, allow for the transport of ions and thus serve as a polymer electrolyte. The chemical structure of Nafion is shown in Fig. 2.1.

The mechanism of ion transport in Nafion membranes has been widely studied in the literature and it is believed that the presence and the state of water within the membrane structure play an important role in the transport of protons through

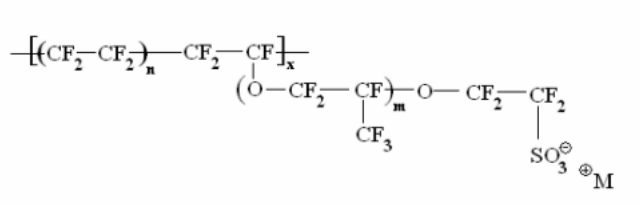

Figure 2.1: Chemical structure of Nafion.

these membranes [6, 29–31]. Indeed, one of the problems observed for Nafion when used as a PEMFC is that, at high temperatures, particularly above 80 °C, a decrease in water content is observed lowering the ionic conductivity of Nafion.

In order to overcome the problem of water loss with increasing temperature, one of the solutions proposed in a number of works available in the literature is the modification of Nafion membranes with ionic liquids (ILs) [32–34]. Ionic liquids (ILs) are compounds consisting entirely of ionic species comprising an organic cation and an inorganic or organic anion [35]. One of the most interesting properties of ILs is their negligible vapour pressure, which allows the use of these compounds in a wide range of applications, namely as solvents for organic and catalytic reactions, production of new materials, solvents for separation and extraction processes, novel electrolytes for electrochemical devices and processes, and enzymatic catalysis/multiphase bioprocess operations [16, 36–42]. Additionally, they present a good electrical conductivity, a high ionic mobility and good thermal and chemical stability [43, 44].

According to the literature, the use of ILs in Nafion membranes can lead to low solvent evaporation rates due to their negligible vapour pressure. Due to the decrease in the conductivity of Nafion membranes at temperatures above 80 °C, Doyle et al. [32] studied the incorporation of different ionic liquids in Nafion. It was shown

that these membranes have the ability to swell in contact with ionic liquids, which resulted in membranes with an excellent stability and proton conductivity in the range of 100–200 °C, while retaining the low volatility of the ionic liquid. Tigelaar et al. [33] studied the incorporation of protic ionic liquids into different polymers, including Nafion, evaluating the resulting mechanical and thermal properties, and the uptake of water. It was observed that the conductivity of the modified membranes was mainly dependent on the relative amount of the ionic liquid inside the membrane, while the acidity of the sulfonic groups of the polymer backbone was shown to be of lower importance. Schmidt et al. [34] studied the effect of impregnating different ionic liquids in Nafion-117 on the mechanical properties, thermal stability, ion-exchange capacity, swelling and conductivity of the resulting membranes.

In all the aforementioned works, ionic liquids have been assumed to behave as solvents when incorporated in Nafion. However, in a recent study [18], it was demonstrated by confocal Raman spectroscopy that, when ILs are incorporated inside a cation-exchange membrane (such as Nafion), a cation-exchange process occurs between the counter cation of the membrane and the ionic liquid cation, which is incorporated permanently unless a reverse cation-exchange process takes place. This indicates that the ionic liquid, in this kind of ion-exchange process, should be regarded as an electrolyte rather than a solvent. In this way, by using an ion-exchange process, “tailor-made” membranes may be designed for target applications, by controlling the degree of incorporation of the selected IL cation.

The effect of the different degrees of incorporation of ILs, on the chemical and electrical properties of the modified Nafion membranes, has not been taken into account in the literature. The works referred above were mainly focused on the effect of temperature on the membrane conductivity, where Nafion was modified with a

maximum degree of incorporation of ILs.

The approach followed in this work was the design of modified membranes by partially replacing the Nafion protons with IL cations. This procedure is expected to lead to a decrease in proton conductivity of the resulting modified membranes. This decrease in proton conductivity may be associated to a decrease in the number of protons, and additionally it may be a result of a more confined environment which could hinder proton mobility. On the other hand, the incorporated cations may improve the thermal stability of the modified membranes by an expected increase in water retention at high temperatures, made possible by additional involvement of water molecules in the solvation of the incorporated cations. The expected higher water retention would open the possibility of using the modified membranes in high temperature applications.

This work investigates two different aspects: (1) the incorporation of selected IL cations in Nafion membranes at different degrees, and the evaluation of the distribution of the incorporated cations in the membrane surface layer; (2) the influence of the incorporated cations on the ionic conductivity, proton mobility and thermal stability of the modified membranes, for potential application as polymer electrolyte membranes (PEM) at high temperature. The modified membranes were characterised by the following techniques: X-ray photoelectron spectroscopy (XPS), electrochemical impedance spectroscopy (EIS) and thermogravimetry. XPS measurements were performed in order to evaluate the distribution of the IL cation in the membrane surface layer for different degrees of incorporation. EIS was used as a dynamic monitoring technique to determine the electrical properties of the modified Nafion membranes with the degree of incorporation of the IL cation. Finally, thermogravimetric analyses were performed in order to understand the water retention

ability of the modified membranes at high temperature.

2.3 Experimental

2.3.1 Materials

The membrane used in this work was Nafion-112 in the protonated form, with an equivalent molecular weight of 1100 g mol^{-1} and a thickness of 51 μm. This membrane is available from Dupont (USA).

The compounds used as source materials for typical Ionic Liquid (IL) cations are listed below:

- phenyltrimethylammonium chloride, $TMPA^+Cl^-$ from Fluka (Germany);
- n-dodecyltrimethylammonium chloride, DTA^+Cl^- from TCI Instruments (England);
- hexadecyltrimethylammonium bromide, CTA^+Br^- from Sigma (USA);
- 1-n-butyl-3-methylimidazolium hexafluorophosphate, $BMIM^+PF_6^-$ from Solchemar (Portugal);
- 1-n-octyl-3-methylimidazolium hexafluorophosphate, $OMIM^+PF_6^-$ from Solchemar (Portugal).

It should be noted that the first three compounds are not ionic liquids, but contain cations that are typical of common ILs. The chemical formula, geometric structure, molecular weight and molar volume of the corresponding IL cations studied are listed in Table 2.1. These IL cations may be categorised in two distinct groups,

regarding the physical state of the corresponding ionic liquid at room temperature. The compounds that are solid at room temperature (with cations $TMPA^+$, DTA^+ and CTA^+) are all quaternary amines and were selected due to their different alkyl chain length, and also to assess the effect of the presence of an aromatic ring in the structure of the cation ($TMPA^+$).

Two imidazolium-based ILs were selected, comprising the $BMIM^+$ and $OMIM^+$ cations, which differ in the length of the alkyl chain. The corresponding ionic liquids $BMIM^+PF_6^-$ and $OMIM^+PF_6^-$ are liquid at room temperature.

2.3.2 Incorporation of the ionic liquid (IL) cations in Nafion membranes

2.3.2.1 Incorporation method

Each protonated Nafion membrane was immersed in 20 mL of the solution of the IL for a specific period of time, in order to exchange the protons from the Nafion membrane with the cations from the IL. When incorporating the cations from the ILs that are solid at room temperature ($TMPA^+$, DTA^+ and CTA^+), it was necessary to prepare a 40 % (w/w) IL aqueous solution with deionised water.

2.3.2.2 Monitoring the incorporation of IL cations in the Nafion membrane

- **pH and conductivity measurements in the liquid phase**

In order to determine the concentration of cations incorporated inside the Nafion membrane for each contact time, both the pH and the conductivity of the IL solutions were measured at different time intervals. The pH and conductivity of the

Table 2.1: Characteristics of the ionic liquid cations studied

Ionic liquid cation	Molecular formula	Molecular structure	Molecular weight, g mol^{-1}	Molar volume, cm^{3}mol^{-1} [a]
Phenyltrimethylammonium, TMPA$^+$	$(CH_3)_3NC_6H_5^+$		136	189
n-Dodecyltrimethylammonium, DTA$^+$	$C_{12}H_{25}N(CH_3)_3^+$	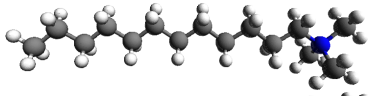	228	350
Hexadecyltrimethylammonium, CTA$^+$	$C_{19}H_{42}N^+$	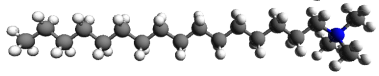	284	434
1-n-Butyl-3-methylimidazolium, BMIM$^+$	$C_8H_{15}N_2^+$	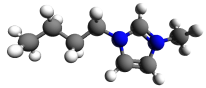	139	182
1-n-Octyl-3-methylimidazolium, OMIM$^+$	$C_{12}H_{23}N_2^+$	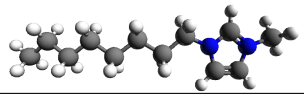	195	266

[a] Estimated parameter by Shroeder's method [45].

liquid phase were measured with a pH conductivity meter (model 720 A, Orion) and with a laboratory conductivity meter (model 960, Schott Instruments), respectively.

- **X-ray photoelectron spectroscopy (XPS) measurements**

In order to characterise the chemistry of the surface of the modified Nafion membranes, X-ray photoelectron spectroscopy (XPS) measurements were performed. XPS spectra were recorded with a Physical Electronics PHI 5700 spectrometer with a multi-channel hemispherical electroanalyzer. Non-monochromatic MgKa X-ray (300 W, 15 kV, 1253.6 eV) was used as excitation source. The binding energy (B.E.) of photoelectron peaks was referenced to C *1s* core level for aliphatic and adventitious carbon at 285.0 eV. High-resolution spectra were recorded by a concentric hemispherical analyzer operating in the constant pass energy mode at 29.35 eV and using a 720 μm diameter aperture. The residual pressure in the analysis chamber was maintained below 1.33×10^{-7} Pa during the spectra acquisition. Membranes were irradiated less than 20 minutes to minimize X-ray induced sample damage. The PHI ACCESS ESCA-V6.0F software package was used for acquisition and data analysis [22]. Atomic concentration percentages (A.C. %) of the characteristic membrane elements were determined from high-resolution spectra after subtraction of a Shirley-type background, and taking into account the corresponding area sensitivity factor for every photoelectron line [46].

Most of the XPS measurements with the Nafion/IL cation modified membranes were performed at a take-off angle $\phi = 45\,°$, after contact during 24 h with the corresponding IL solutions. However, in order to evaluate chemical changes related to time evolution of membrane modification, XPS measurements with Nafion/DTA^+ samples with different degrees of DTA^+ incorporation (resulting from different con-

tact times) were also carried out. Moreover, angle resolution XPS (ARXPS) or deep-profile analysis for Nafion-modified membranes after cation incorporation was also performed by using different take-off angles (ϕ = 15 °, 30 °, 45 °, 60 °and 75 °), which allows for obtaining chemical information for depths ranging, correspondingly, between 2.5 nm and 9.3 nm deep [47].

2.3.3 Assessment of the Nafion-IL membranes for potential PEM applications

2.3.3.1 Electrical impedance spectroscopy (EIS) measurements

Impedance spectroscopy (IS) was used as a dynamic characterisation technique in order to evaluate the electrical properties of the modified Nafion-ILs membranes and to obtain information about the electrical changes associated with the IL cation incorporation in Nafion membranes.

Electrochemical impedance spectroscopy (EIS) measurements were performed using an Impedance Analyzer (Solartron 1260) controlled by a computer and connected to the electrochemical cell by fixed silver/silver chloride electrodes. The electrochemical cell consisted of two glass half-cells [48] filled with the electrolyte solution, separated by the Nafion membrane in the protonated form. In these experiments the electrolyte solution was the IL solution. Since impedance measurements were carried out at different time intervals, this experimental set-up allows for obtaining information of the resulting electric properties of the modified membranes due to the different degrees of concentration/incorporation of IL inside the membrane. The EIS measurements were performed for 100 different frequencies, ranging from 10 Hz to 10^7 Hz, and a maximum voltage of 0.01 V was applied. All

measurements were performed at room temperature. The experimental data were corrected and analysed by the software Equivalent Circuit [49], in order to obtain the electrical parameters, resistances (R) and capacitances (C), of the modified Nafion-IL membranes.

A similar device was used for the electrical characterisation of the IL solutions. In this case no membrane was placed between both glass half-cells, which were filled with the IL solutions.

Another set of experiments were performed using the same experimental set-up, where glass half-cells were filled with a HCL solution, and separated by the Nafion membrane in the protonated form. Different concentrations of HCl were prepared and EIS measurements were carried out.

The electrical impedance is defined as the ratio between the applied voltage and the resulting electric current, $Z(\omega) = v(t)/i(t)$, and may be expressed as

$$Z(\omega) = Z_{real} + j\, Z_{imag} \tag{2.1}$$

where Z_{real} is the real part of the electrical impedance and Z_{imag} is its imaginary part. The experimental data can be represented in a Bode plot, where the real (Z_{real}) or the imaginary part (-Z_{imag}) of the impedance is represented against the frequency (f).

2.3.3.2 Thermogravimetry Analysis

In order to determine the effect of increasing temperature on the relative amount of water in Nafion and Nafion/IL modified membranes, thermogravimetry analysis (TGA) was performed for a temperature range between 25 °C and 210 °C. The experiments were carried out in nitrogen (flow rate 20 mL/min) with a Shimadzu TGA-50

system at a heating rate of 5 °C/min.

2.4 Results and Discussion

2.4.1 Incorporation of IL cations in Nafion membranes

During the incorporation of IL cations in Nafion membranes an exchange between the H^+ protons of the membrane and the IL cation is expected to occur. The degree of concentration of cations incorporated inside the membrane was determined by two independent measurements, the pH and the conductivity of the aqueous solutions with $TMPA^+$, DTA^+ and CTA^+, which corresponding source of these IL cations are solid at room temperature. By measuring the pH of the IL aqueous solution before and after incorporation, it is possible to quantify the protons that exchanged with the IL cations. Additionally, by also measuring the conductivity of the IL aqueous solution, before and after incorporation, and knowing the molar conductivity of each species, it is possible to quantify by mass balance the amount of protons exchanged. Both measurements gave similar results, with a maximum deviation of 3 %. Regarding the cations $BMIM^+$ and $OMIM^+$, which corresponding IL is liquid at room temperature, the concentration of cations inside the membrane and the remaining concentration of protons was only determined by conductivity measurements in the liquid phase.

Fig. 2.2 represents the evolvement of the incorporation degree along time, when a Nafion membrane was in contact with the cations phenyltrimethylammonium ($TMPA^+$), n-dodecyltrimethylammonium (DTA^+), hexadecyltrimethylammonium (CTA^+), 1-butyl-3-methylimidazolium ($BMIM^+$) and 1-octyl-3-methylimidazolium

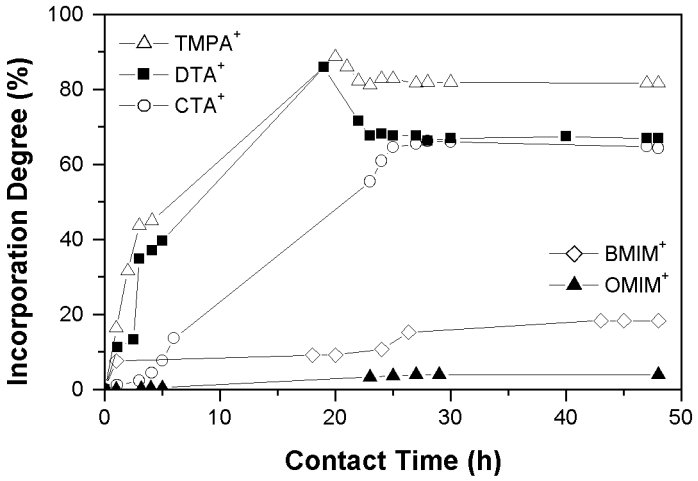

Figure 2.2: Incorporation degree in the Nafion membrane, for the different cations studied as a function of contact time.

($OMIM^+$). The incorporation degree was calculated assuming a maximum incorporation degree of 0.92 meq g^{-1} for Nafion-112 (data provided by Dupont (USA)).

For all the IL cations studied it is observed an increase in the incorporation degree (in percentage) with increasing contact time. Regarding the Nafion/$TMPA^+$ and Nafion/DTA^+ membranes, the incorporation degree shows a sharp increase until a contact time up to 20 h and 19 h, respectively, followed by a slight decrease until reaching a constant value. This slight decrease in the incorporation degree may be due to a possible accommodation process that the IL cation suffers as it is incorporated inside the membrane. It is also shown for all the ILs cations studied that, after a contact time of 24 hours, the incorporation degree reaches a constant value which is assumed to correspond to equilibrium.

The results shown in Fig. 2.2 suggest that the cations under study may be grouped

according to the physical state of the corresponding IL at room temperature. The first group refers to the cations, $TMPA^+$, DTA^+ and CTA^+, which show an incorporation degree higher than 60 % at equilibrium. In this case, for a contact time of 24 hours, it may be observed that the amount of IL cation incorporated decreases with an increase in the size of the cation. The CTA^+ cation has the lowest value of incorporation degree (maximum 65 %) and this may be due to its alkyl chain length, larger than in the DTA^+ and $TMPA^+$ cations, which showed maximum values of incorporation degree of 68 % and 82 %, respectively. The second group refers to the ionic liquid cations $BMIM^+$ and $OMIM^+$, which present much lower incorporation degree values. The $BMIM^+$ cation achieved a maximum incorporation degree value of 18 % while for the $OMIM^+$ cation the maximum value achieved was 4 %, which indicates that the amount of incorporated IL decreases with an increase in the size of the cation incorporated. It is also observed that these incorporation degrees are much lower when compared with the ones obtained for the ILs in aqueous solution. This behaviour may be due to the fact that cation incorporation is possibly facilitated by the presence of water, used for preparing the solutions with the solid compounds. Since Nafion membranes contain water clusters, it is expected that cations dissolved in an aqueous solution partition more easily to those hydrophilic membrane environments, when compared with the case of pure ionic liquids which are comparatively more hydrophobic.

2.4.2 X-ray photoelectron spectroscopy (XPS) results

The XPS analysis allows for determining the atomic concentration percentage (A.C. %) of the elements present on the surfaces of Nafion-112/H^+ and Nafion/IL modified

membranes (after 24 h of IL cation incorporation), obtained from high-resolution spectra of the main photoelectron peaks (C *1s*, O *1s*, F *1s*, S *2p* and N *1s*). Carbon (C *1s*) was chosen as the element to report both the behaviour of the membrane and the IL cation, because it is an element common to both chemical structures, as shown in Fig. 2.1 and Table 2.1. The element fluorine (F *1s*) is characteristic of the polytetrafluoroethylene backbone of the membrane, and the element sulfur (S *2p*) corresponds to the sulfonic groups (SO_3^-) of Nafion. Finally, the element nitrogen (N *1s*) is characteristic of the IL cations.

The first experiments performed were for Nafion-112 incorporated with DTA^+ cation. In these experiments, the protonated membrane was immersed for different time periods in the aqueous solution of this IL, as explained in section 2.3.2.1. Fig. 2.3 represents the A.C. (%) of these elements on the surface of Nafion/DTA^+ samples at different membrane-IL cation contact times, where a 30 % reduction in the fluorine percentage (Nafion characteristic element) as a function of time can be observed, while carbon percentage increases due to DTA^+ incorporation. The decrease in the atomic concentration of the element F *1s* may be attributed to the fact that the IL cation is being incorporated in the membrane with time. The fact that the DTA^+ cation is incorporated in the structure of Nafion is more evident if the time evolution of nitrogen A.C. (%) is also considered, since this element is only related to the presence of the DTA^+ cation. An average value of 1.51 ± 0.07 % can be observed for N *1s* in Fig. 2.3b, for the interval between 8 h and 40 h. It is also detected the presence of the sulfur element (1.28 ± 0.05 %), which is characteristic of the membrane. These XPS results indicate that 24 h of Nafion/IL cation contact time is enough to ascertain the H^+/IL cation exchange, in agreement with the "dynamic" experiments previously discussed in section 2.4.1. Therefore, the following

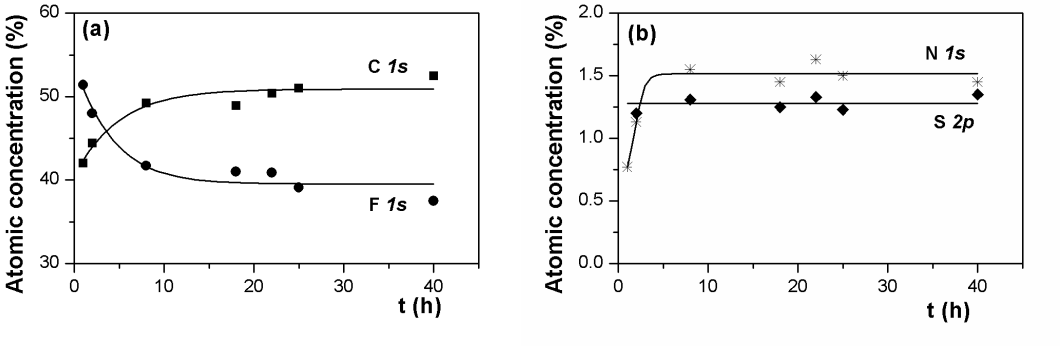

Figure 2.3: Atomic concentration percentage (A.C. %) of the elements present in Nafion/DTA$^+$ samples as a function of the contact time (a) carbon and fluorine and (b) nitrogen and sulfur.

XPS results correspond to samples equilibrated for 24 h.

Although XPS is mainly used as a surface analysis technique, cation incorporation within a thin superficial layer of the Nafion structure may also be analysed by angle resolved XPS (ARXPS), where the measurements at different take-off angles are performed. This non-destructive method was used for a deep-profile analysis between 2.5 nm and 9.3 nm in membrane depth. Fig. 2.4a and Fig. 2.4b shows the variation of nitrogen (N *1s*) and sulfur (S *2p*) atomic concentration percentages as a function of the take-off angle for Nafion/BMIM$^+$ and Nafion/OMIM$^+$ membranes, respectively. The analysis of these figures shows that both IL cations are incorporated inside the membrane, as may be observed by the nitrogen A.C. (%) at the different analysis angles studied. Fig. 2.4 also shows that the nitrogen A.C. (%) slightly increases with an increase in the membrane surface depth, until reaching a constant value at higher take-off angles which suggests a uniform cation distribution deeper inside the membrane. As stated before, XPS allows for the characterisation

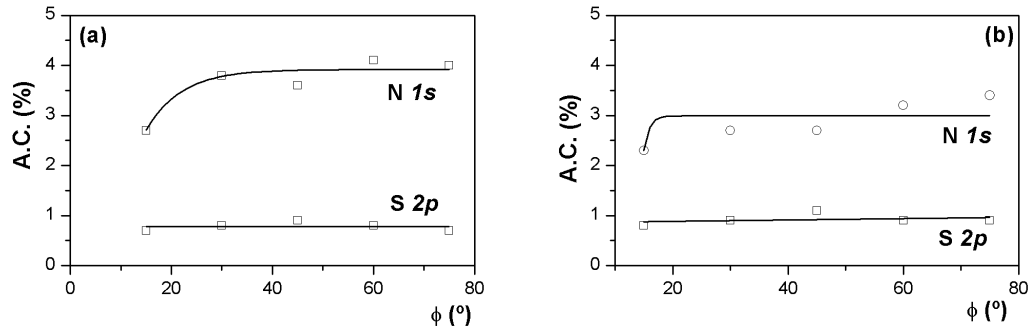

Figure 2.4: Deep-profile XPS analysis of (a) Nafion/BMIM$^+$ and (b) Nafion/OMIM$^+$ membranes.

of the cation distribution in the superficial layer of the membrane until a depth of 9.3 nm. A full characterisation of the cation distribution over the membrane thickness was also performed by Confocal Raman Spectroscopy (data not shown), and it was observed that the IL cation was uniformly distributed inside the 51 μm thick Nafion membranes.

Additionally in Fig. 2.4, when comparing the nitrogen A.C. (%) for Nafion/BMIM$^+$ and Nafion/OMIM$^+$, a higher value is observed for the first case. This was an expected result due to a combination of two distinct effects. Firstly, the N/C molecular ratio is higher for BMIM$^+$ than OMIM$^+$ (please see Table 2.1). Secondly, BMIM$^+$ is smaller than OMIM$^+$ and therefore its incorporation in the membrane is expected to be easier, as previously shown in section 2.4.1. In both cases, the sulfur percentage is constant (0.8 % and 0.9 %, respectively) and similar to that obtained for the Nafion-112/H$^+$ membrane as will be discussed later (Table 2.2).

Table 2.2 shows the A.C. (%) obtained for the Nafion-112/H$^+$ membrane and the different Nafion/IL cations studied, as well as the theoretical Nafion A.C. (%) val-

Table 2.2: Atomic concentration percentages (A.C. %) of the different elements on the surfaces of the Nafion and Nafion/IL modified membranes Membranes

Elements	Membranes						
	Nafion (theor.)	Nafion (exp.)	Nafion/TMPA$^+$	Nafion/DTA$^+$	Nafion/CTA$^+$	Nafion/BMIM$^+$	Nafion/OMIM$^+$
C *1s* (%)	30.8	39.0	45.6	51.0	60.4	45.0	45.8
O *1s* (%)	7.7	6.6	7.0	6.4	6.9	5.5	6.0
F *1s* (%)	60.0	53.4	44.2	39.1	29.0	43.9	44.0
S *2p* (%)	1.5	1.0	1.0	1.2	1.2	1.1	1.1
N *1s* (%)	–	–	1.3	1.5	2.0	3.6	2.8

ues considering its chemical structure with n=6.5, x=1 and m=1 (see Fig. 2.1) [50]. It is important to mention that small concentrations of other elements such as silicon (A.C. between 1 % and 2 %), phosphorous and chlorine (A.C. $\leq$ 0.5 %) were also found in some samples, although they are not included in Table 2.2. Slight differences between experimental and theoretical values for the Nafion membrane can be observed, which are attributed to the higher percentage of carbon obtained from sample analysis and associated to adventitious contamination (aliphatic carbon) [51, 52]. The A.C. percentage of fluorine in all the Nafion-modified membranes is lower than in Nafion as a result of cation incorporation, and the sequence of carbon A.C. (%) for the different modified membranes (Nafion/CTA$^+$> Nafion/DTA$^+$> Nafion/OMIM$^+$$\approx$ Nafion/TMPA$^+$ $\approx$ Nafion/BMIM$^+$) and the higher nitrogen concentration for Nafion/OMIM$^+$ and Nafion/BMIM$^+$ samples, are consistent with their molecular formula (Table 2.1) and incorporation degree of the IL cations.

The incorporation of IL cations can also be confirmed by analyzing the C *1s* core level normalized spectra for Nafion and Nafion/IL cations modified membranes,

which is shown in Fig. 2.5. The Nafion-112/H^+ sample shows three different photoemissions at binding energies (B.E.) of 291.8–292.0 eV (associated to CF_2 and CF-O) and at 284.8–285.0 eV (C-H bond), plus a small shoulder at 294.0 eV (CF_3). C *1s* spectra for all the Nafion/IL cations modified membranes also present those peaks and shoulder, but another shoulder at 286.4 eV, which is associated to C-N, can also be observed [52, 53]. Particularly, this latter peak shows a significant contribution in the case of the Nafion/$BMIM^+$ sample, while a small shoulder at 285.0 eV indicates the contribution of the aliphatic carbon (C-H). Similar cations with aliphatic chains of different lengths, such as DTA^+ and CTA^+, show similar C *1s* core level spectra, but in the case of the cation with a longer aliphatic chain (CTA^+) the shoulder at 286.4 eV shows a lower intensity than that observed for DTA^+ (Fig. 2.5a). On the other hand, the intensity of the peak at 292.0 eV, assigned to the presence of the Nafion membrane, decreases due to the higher covering effect produced by the longer aliphatic chain of CTA^+. The same fact is observed in the case of samples modified with $OMIM^+$ and $BMIM^+$, which are similar molecules but have aliphatic chains of different lengths (see Fig. 2.5b).

2.4.3 Characterisation of modified Nafion membranes using electrochemical impedance spectroscopy (EIS)

The evaluation of the electric properties of the resulting Nafion/IL cation modified membranes becomes of relevance importance for a potential application of these membranes as polymer exchange membranes (PEM).

The study of the electric properties of the membranes was performed using electrochemical impedance spectroscopy (EIS). The Nafion-112/H^+ membrane was placed

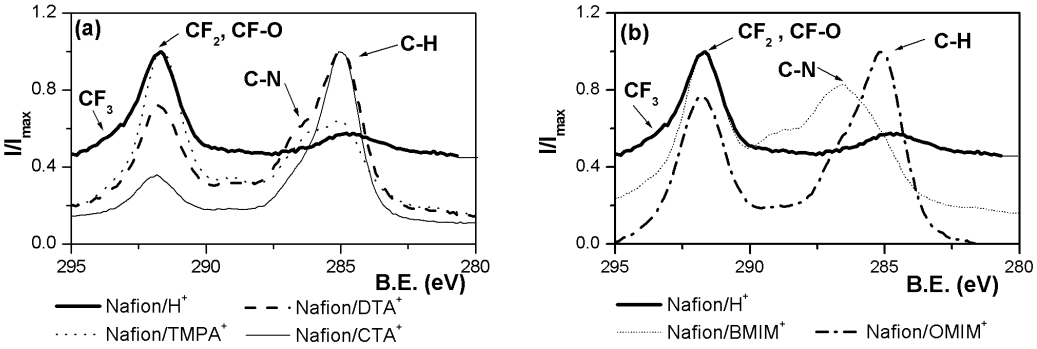

Figure 2.5: C *1s* core level normalized spectra and main bonds for the studied membranes (a) Nafion-112/H^+, Nafion/$TMPA^+$, Nafion/DTA^+, and Nafion/CTA^+ and (b) Nafion-112/H^+, Nafion/$BMIM^+$ and Nafion/$OMIM^+$.

in contact with the different IL solutions and, after a specific period of contact time, impedance spectroscopy measurements were carried out. Using this procedure it was possible to obtain information about the evolvement of the electric properties of the modified membranes with the incorporation degree of each cation.

The EIS results obtained for Nafion-112/H^+ in contact with two different cations, n-dodecyltrimethylammonium (DTA^+) and hexadecyltrimethylammonium (CTA^+), at different contact times are represented in Bode plots, which are shown in Fig. 2.6 and Fig. 2.7, respectively. In the same figures it is also represented the Bode plot for the aqueous IL solution. Both Bode diagrams representation (-Z_{imag} and Z_{real} as a function of the frequency) were considered for all the cases investigated.

In a first analysis, Fig. 2.6 and Fig. 2.7 show that, using impedance spectroscopy as a dynamic characterisation technique, it is possible to observe modifications in impedance diagrams that are expected to be associated with the incorporation of IL cations in Nafion membranes along time. It may be also noticed that the incorpora-

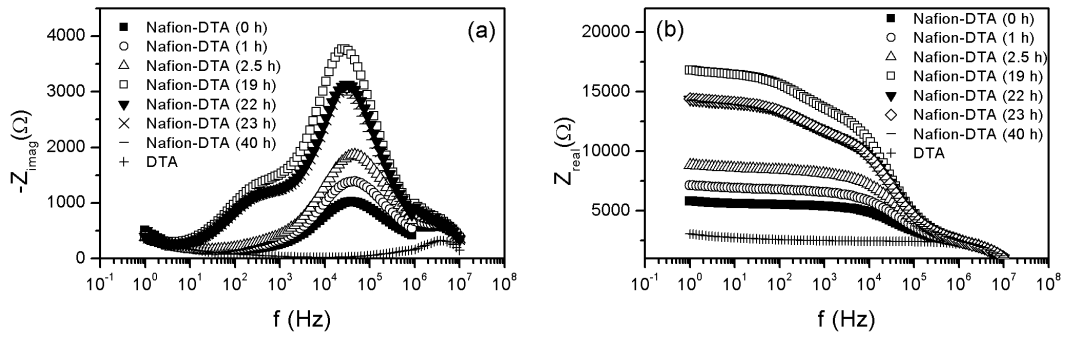

Figure 2.6: Bode plot for Nafion in contact with DTA^+ along time (a) representation of -Z_{imag} as a function of the frequency and (b) representation of Z_{real} as a function of the frequency.

tion of these DTA^+ and CTA^+ bulky cations strongly modifies the electrical behaviour of these membranes.

In Fig. 2.6, the curve that corresponds only to the aqueous solution of the IL (shown as DTA) presents one relaxation at high frequencies ($f_{max} \approx 4$ MHz). In the case of the membrane/IL system, three different relaxations are observed: one at high frequencies, associated with the IL; one at intermediate frequencies, which corresponds to the membrane; and one at low frequencies, with a maximum around 200 Hz associated with the interface. With increasing contact time up to 19 h of contact, the magnitude of these two last relaxations increases. Afterwards, the relaxations of the membrane/IL system seem to reach a constant value which indicates an equilibrium situation. The behaviour of these curves is in agreement with the results obtained in section 2.4.1. It should be mentioned that, although not clearly visible in Fig. 2.6 for contact times lower than 19 h, interfacial effects at the low frequency range are present.

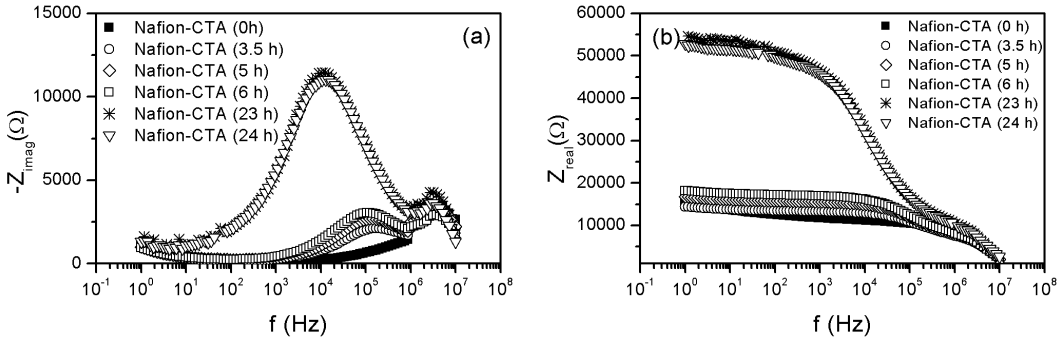

Figure 2.7: Bode plot for Nafion in contact with CTA^+ along time (a) representation of -Z_{imag} as a function of the frequency and (b) representation of Z_{real} as a function of the frequency.

Bode plots for the Nafion/CTA^+ system are represented in Fig. 2.7a and Fig. 2.7b. The analysis of these figures is similar to that of Nafion/DTA^+ shown in Fig. 2.6. However, the equilibrium relaxations of the IL and membrane are observed at frequencies of 3 MHz and 12 kHz, respectively. These values are different from those obtained for Nafion/DTA^+, indicating that the type of incorporated cation influences the electrical behaviour of the membranes. The interface effect, although present, is in this case more difficult to visually detect in Fig. 2.7 mainly due to the large membrane and cation contribution value. This effect may be quantified using mathematical models which will be discussed later in this work.

Bode plots for Nafion modified with the cations phenyltrimethylammonium ($TMPA^+$) and 1-butyl-3-methylimidazolium ($BMIM^+$), are shown in Fig. 2.8. Unlike the systems previously analysed, only one relaxation at high frequencies is clearly visible, which does not allow for identifying separately the electrical contribution associated with the membrane and with the IL placed between the membrane and

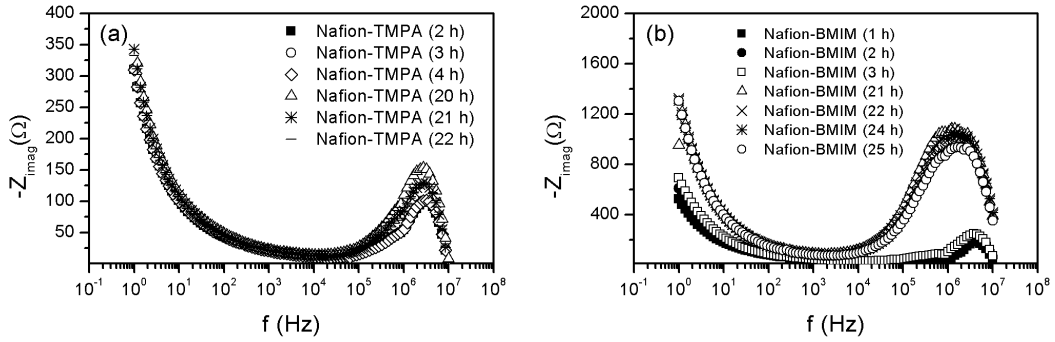

Figure 2.8: (a) Bode plot for Nafion in contact with $TMPA^+$ along time (representation of -Z_{imag} as a function of the frequency) and (b) Bode plot for Nafion in contact with $BMIM^+$ along time (representation of -Z_{imag} as a function of the frequency).

the electrodes. This behaviour is common for membranes with high charge content (fixed or adsorbed charge) [54–56]. Moreover, in the case of Nafion/$TMPA^+$, the curves represented in the Bode plots shown in Fig. 2.8a do not present a significant evolution with time. The same phenomenon was observed for the Nafion/$OMIM^+$ membrane (results not shown). The absence of a time evolvement behaviour observed for Nafion/$TMPA^+$ and Nafion/$OMIM^+$, may be explained differently for both systems. Regarding the Nafion/$TMPA^+$ system, a possible explanation is that being this IL cation the smallest when compared with others, it may be incorporated more easily in the membrane at a larger extent and in a short period of time (45 % in the first 4 h according to the results shown in Fig. 2.2). In the case of the Nafion/$OMIM^+$ system, the incorporation degree is very low (less than 5 %) as mentioned in section 2.4.1, which results in a negligible evolution along time.

In the case of the Nafion/$BMIM^+$ system (results shown in 2.8b) it is possible to distinguish both the IL relaxation at high frequencies ($f_{max} \approx 3$ MHz) and the re-

laxation of the membrane until a contact time of 3 hours. After that time period, a unique relaxation for the membrane plus IL system is observed. The observation of a unique relaxation may result from the incorporation of the $BMIM^+$ cation, which leads to an overlap of the two individual relaxations (membrane and IL), as previously observed for Nafion/$TMPA^+$ and Nafion/$OMIM^+$.

- **Evaluation of the electrical parameters of the modified Nafion/ILs membranes along time**

In order to obtain the best equivalent circuit that represents each modified Nafion-IL membrane, the data obtained by electrochemical impedance spectroscopy was analysed using a non-linear regression software, Equivalent Circuit Program [49], and the membrane and interface circuit parameters were determined taking into account the system under study: Electrode//IL/Membrane/IL//Electrode.

The equivalent circuit obtained for Nafion incorporated with n-dodecyltrimethyl ammonium (DTA^+) and hexadecyltrimethylammonium (CTA^+) cations can be observed in Fig. 2.9, where the resistance R_1 and the equivalent capacitance CPE_1 correspond to the membrane and the resistance R_2 and the equivalent capacitance CPE_2 correspond to the interface. As previously mentioned for Nafion/DTA^+, interface effects are clearly observed for all the incorporation times studied (Fig. 2.6). Although, in the case of Nafion/CTA^+, the interface is not so clearly detected, by analysing the data with the Equivalent Circuit Program it was possible to identify two different contributions, one from the membrane and another from the interface.

In the equivalent circuit represented in Fig. 2.9, the equivalent capacitance CPE_1 is a capacitance Q, which is related with the non-homogenous membrane matrix, while the element CPE_2 is a Warburg element, which is present due to the diffusion

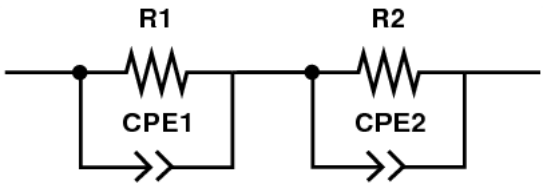

Figure 2.9: Equivalent circuit for Nafion/DTA$^+$ and Nafion/CTA$^+$, where R_1 is the membrane resistance, CPE_1 the membrane equivalent capacitance, R_2 the interface resistance and CPE_2 the interface equivalent capacitance.

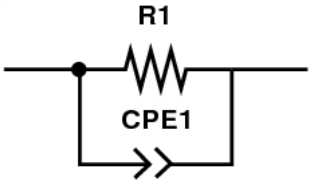

Figure 2.10: Equivalent circuit for Nafion/TMPA$^+$, Nafion/BMIM$^+$ and Nafion/OMIM$^+$, where R_1 is the membrane plus IL resistance and CPE_1 the membrane plus IL equivalent capacitance.

of ions in the interface that results from an ion concentration gradient.

The equivalent circuit for Nafion/TMPA$^+$, Nafion/BMIM$^+$ and Nafion/OMIM$^+$ can be observed in Fig. 2.10. In this case, one unique relaxation process was observed for the whole membrane system, which is comprised by the membrane and the IL. In this circuit, R_1 and the equivalent capacitance CPE_1 correspond to the membrane and IL resistance and to the capacitance Q, which is related with the non-homogenous membrane matrix, respectively. The quantification of the electrical parameters obtained with the equivalent Circuit Program [49] is discussed in the next paragraphs. The dependence of the membrane resistance with the incorporation degree is shown in Fig. 2.11.

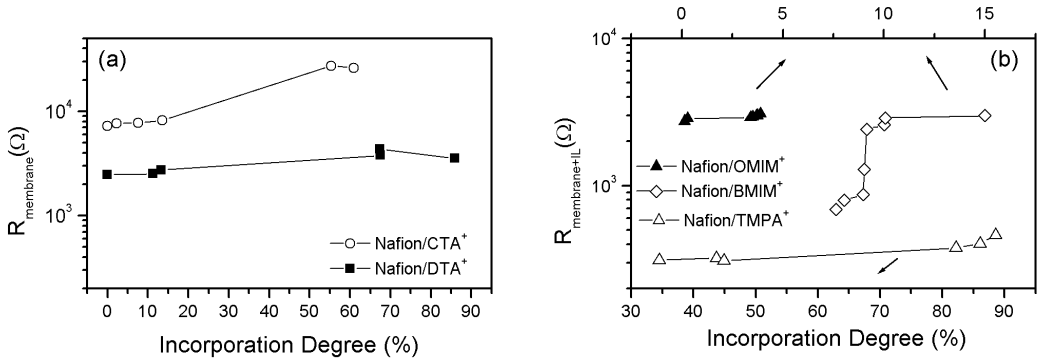

Figure 2.11: (a) Dependence of the membrane resistance for Nafion/CTA$^+$ and Nafion/DTA$^+$, as a function of the incorporation degree (%) and (b) Dependence of the membrane plus IL resistance for Nafion/TMPA$^+$, Nafion/BMIM$^+$ and Nafion/OMIM$^+$, as a function of the incorporation degree (%).

It was concluded in section 2.4.1 that the concentration of the IL cation inside the membrane increases with an increase in the contact time between the cation and the membrane. Fig. 2.11a shows the dependence of the membrane resistance as a function of the incorporation degree, and Fig. 2.11b represents the total resistance (membrane plus IL) also as a function of the incorporation degree. It is shown that both resistances increase with an increase in the incorporation degree of Nafion/IL for all the cases studied. The incorporation of a cation, much larger than the proton present initially in the membrane, seems to be the reason for the increase of the membrane resistance with contact time. In a situation of equilibrium it is also shown that, in general, the membrane resistance and the membrane plus IL resistance increases with an increase in the size of the IL cation incorporated.

- **Ionic conductivity of the modified Nafion/ILs cation membranes**

It is possible to determine the ionic conductivity of these modified membranes

from the membrane electrical resistance values of Nafion membranes incorporated with different IL cations. The membrane electrical resistance was considered to be the one obtained by the equivalent circuit program, when the membrane is in equilibrium. The ionic conductivity of these modified Nafion/IL membranes was calculated assuming a uniform current distribution in the conductivity cell and using Eq. 2.2, where L is the membrane thickness between the two measuring electrodes, A is the cross-sectional area of the membrane and R is the membrane resistance, in ohm [32].

$$\sigma(\mathrm{S\,cm^{-1}}) = \frac{L(\mathrm{cm})}{R(\Omega)\,A(\mathrm{cm^2})} \tag{2.2}$$

Eq. 2.2 will only be applied for the membranes Nafion/DTA^+ and Nafion/CTA^+ due to the fact that only for these two membranes was possible to isolate the electrical membrane resistance value, using the equivalent circuit program. For the other modified Nafion/IL membranes, one unique relaxation process was observed for the whole membrane system, which is comprised by the membrane and the IL placed between the electrodes. In this case it is not possible to use Eq. 2.2, since a part of the electrical membrane resistance, obtained by the equivalent circuit program, corresponds to the IL.

For the membranes Nafion/DTA^+ and Nafion/CTA^+ the proton mobility (μ) of these membranes may also be estimated considering Eq. 2.3, where σ is the ionic conductivity, F is the Faraday constant and $[H^+]$ is the concentration of protons inside the membrane, taking into account the incorporation degree mentioned in Table 2.3 [30].

Table 2.3: Nafion/DTA^+ and Nafion/CTA^+ membrane resistance, ionic conductivity and proton mobility values

Membrane	Incorporation degree, %	Membrane resistance, Ω	Ionic conductivity, S cm−1	Proton mobility, $cm^2\ s^{-1}\ V^{-1}$
Nafion/DTA^+	68	4 300	4×10^{-6}	3.12×10^{-5}
Nafion/CTA^+	65	26 000	7×10^{-7}	4.92×10^{-6}

$$\mu = \frac{\sigma}{F\,[H^+]} \tag{2.3}$$

The membrane resistance, the ionic conductivity and the proton mobility values for Nafion/DTA^+ and Nafion/CTA^+, for the incorporation degree obtained when the membrane is in equilibrium, are presented in Table 2.3.

The modification of Nafion membranes by incorporation of large IL cations leads to an increase in the membrane resistance which consequently results in a decrease of the ionic conductivity as well as of the proton mobility. Also, it is expected that the ionic conductivity and the proton mobility of the modified membranes decreases with an increase in the size of the IL cation incorporated. Accordingly, it is shown in Table 2.3 that the ionic conductivity and the proton mobility of the modified membrane incorporated with DTA^+ cation is higher.

As stated before, since it is not possible to isolate a value for the membrane resistance for Nafion/$TMPA^+$, Nafion/$BMIM^+$ and Nafion/$OMIM^+$ from the EIS data, excluding the resistance of the IL, a comparison between these membrane systems and a system where a Nafion-112/H^+ membrane is in contact with different concentrations of an electrolyte (HCl aqueous solutions) was performed in the same cell. Fig. 2.12 represents the variation of the membrane/electrolyte system resistance

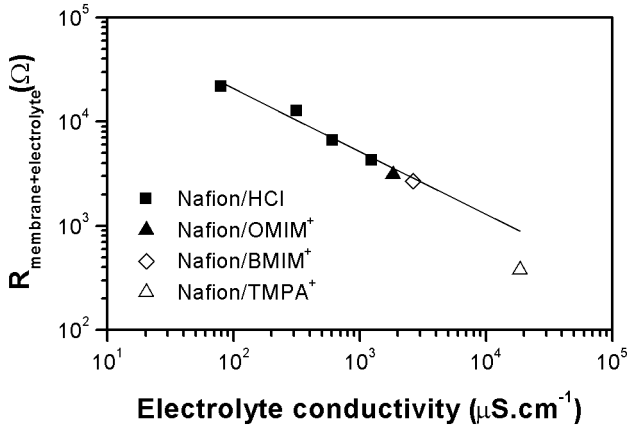

Figure 2.12: Variation of the membrane plus electrolyte resistance with the electrolyte ionic conductivity.

as a function of the electrolyte solution (with HCl or IL) conductivity. The results shown in Fig. 2.12 clearly show that the electric resistance obtained for the three modified membranes (Nafion/$OMIM^+$, Nafion/$BMIM^+$ and Nafion/$TMPA^+$) in contact with the IL aqueous solution is very similar to that expected for the Nafion/H^+ in contact with the aqueous HCl solution under similar conditions (cell and solution conductivity). Moreover, for the Nafion/$TMPA^+$ system the overall electric resistance is lower than could be anticipated, meaning that the ionic conductivity of this membrane should be relatively higher when comparing with the Nafion-112/H^+/HCl system and the other modified membranes.

2.4.4 Potential use of the modified membranes as polymer electrolyte membranes (PEM)

The results obtained and discussed in the previous section show that the modified membranes may exhibit an ionic conductivity comparable with the Nafion membrane, even though an adjustable fraction of the protons are replaced by larger ILs cations. The ionic conductivity of these membranes is undoubtedly related with their water content and the way water is involved in solvation processes, such as the solvation of the sulfonic acid side-groups of Nafion and the newly incorporated cations.

When calculating the relative amount of water in each membrane under study, expressed as the mass of water per mass of dry membrane, it can be concluded (see Fig. 2.13a) that all modified membranes, with exception of the membrane that incorporated $TMPA^+$, have a higher water content when compared with Nafion. This feature results from the interlinked process of cation exchange and water uptake/release that takes place when the membranes are equilibrated with the ILs media and solutions. However, the fact that most modified membranes have a higher water content does not attribute them unequivocally a higher ionic conductivity or lower resistance to the transport of ions (see Table 2.3 and Fig. 2.12). Most probably, this behaviour results from the fact that water inside these membranes is not as free as in Nafion, probably because it is involved in the additional solvation of the larger ILs cations incorporated. This explanation is supported by the analysis of the results presented in Fig. 2.13a, obtained by thermogravimetry, where it can be observed that the rate of water loss for all modified membranes, when heat is supplied in a controlled rate, is lower than the corresponding rate for Nafion. Actually,

it can be observed that Nafion looses water readily even at relatively low temperatures, being completely dried at a temperature of ~ 210 °C [57–59]. This explains its poor behaviour as a polymer electrolyte membrane for temperatures above 80 °C, as referred in the literature.

Fig. 2.13b emphasises, even in a more clear way, the relative loss of water for the Nafion membrane when compared with the modified membranes. As it can be seen, the modified membrane with $TMPA^+$ is extremely stable in the all range of temperatures studied confirming that, although its water content is low, the water present is probably highly structured and deeply involved in solvation processes making its release extremely energy demanding. The reason why this membrane exhibits a low electrical resistance cannot be easily derived from the information gathered about its water content and structuring. The chemical character of this cation, the only one incorporating an aromatic ring, has to be considered when explaining its behaviour. All other modified membranes, although with a higher water content than Nafion, show a higher ability to retain water when compared with the Nafion membrane, probably due to the fact that these water molecules participate in the solvation of the large ILs cations incorporated.

Although it was not possible to perform electrical impedance spectroscopy studies above room temperature, these results strongly suggest that the use of these modified membranes for applications at temperatures above 80 °C may be potentially interesting due to their ability to retain their water content.

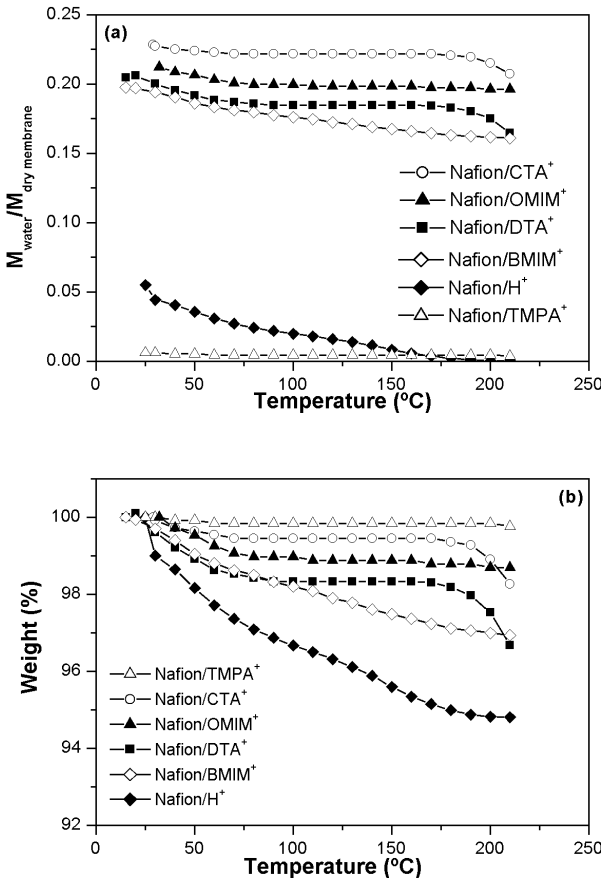

Figure 2.13: (a) Evolvement of the relative amount of water in each membrane with increasing temperature, and (b) Evolvement of each membrane weight with increasing temperature.

2.5 Closure

It was shown that the methodology developed in this work for incorporating different IL cations in Nafion membranes at a controllable degree allows for obtaining tailor-made membranes, and enabled for understanding the dependence of their physicochemical properties with the degree of cation incorporated.

The results obtained by XPS showed that the IL cation was indeed incorporated in the membrane and it was possible to measure its distribution in the membrane surface layer. With EIS measurements the electrical properties of the modified membranes were determined as a function of the degree of cation incorporation. The resistance and equivalent capacitance parameters of the membranes were obtained using a set of mathematical models of equivalent electrical circuits. It was found that these electrical parameters were strongly dependent from the size of the IL cation incorporated, which opens the possibility to design membranes with either higher or lower ionic conductivity depending on the cation incorporated.

Thermogravimetry was used to determine the relative amount of water in each membrane for a wide range of temperatures. It was clearly understood that the presence of water inside the membranes and the way water is structured and involved in solvation processes (the Nafion sulfonic acid side-groups and the incorporated cations) determine the electrical properties of the corresponding membranes and their behaviour at high temperatures. Extended research is needed in order to deepen understanding of the phenomena taking place, in order to direct efforts for effective membrane design. Further work using methodologies for measurement of membrane properties at high temperatures is necessary aiming the assessment of their potential application as polymer electrolyte membranes.

Chapter 3

Proton NMR Relaxometry Study of Nafion Membranes Modified with Ionic Liquid Cations

3.1 Summary

Proton nuclear magnetic resonance (NMR) relaxometry was used as a characterisation technique to study the proton mobility and levels of confinement within Nafion membranes modified by incorporation of selected ionic liquid (ILs) cations. Since different levels of confinement will have an important effect on the degree of water structuring and consequently, on the proton transport of these membranes, studies were performed aiming at understanding the effect of using different types of ionic liquid cations, and their degree of incorporation, in the values of the spin-lattice relaxation times (T_1) obtained at different values of frequency. The frequency dependence of the proton spin-lattice relaxation rates, $R_1=1/T_1$, for the modified

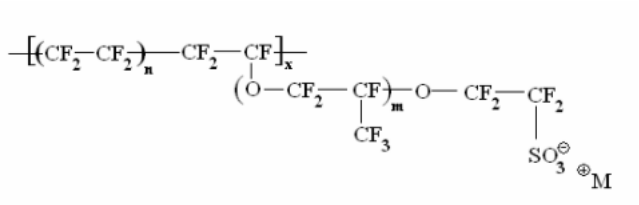

Figure 3.1: Chemical structure of Nafion.

Nafion/IL cation membranes was compared with that obtained for an unmodified Nafion membrane, allowing for distinguishing different contributions of the motions of the molecules depending on the frequency tested. These results were adjusted to physical relaxation models in order to estimate a diffusion coefficient for the protons present in the modified membranes. Finally, the stability of these membranes at high temperatures in terms of proton mobility was also assessed using this characterisation technique.

3.2 Introduction

Nafion is a polymer that combines the extremely high hydrophobicity of the polytetrafluoroethylene backbone with the high hydrophilicity of the sulfonic acid sidegroups arranged in intervals along the chain [28]. These acid groups, which are known to aggregate into clusters, allow for the transport of ions and thus serve as a polymer electrolyte. The chemical structure of Nafion is shown in Fig. 3.1, where M^+ can be either a proton in the acid form or a metal cation in the neutralized form.

Nafion membranes have been widely used as a reference material in polymer electrolyte membrane fuel cells (PEMFCs), due to their high ionic conductivity, mechanical, thermal and chemical stability at temperatures up to 80 °C. Additionally, due

to the fact that these materials present unique properties, several attempts aiming at describing their molecular structure and organization have been published in the literature, during the last 30 years [6]. Although several models have been proposed in the literature, they all agree that the ionic groups are aggregated in the perfluorinated polymer matrix to form a network of clusters which allow for the transport of ions and swelling by polar solvents. However, there is still no agreement regarding the geometry and the spatial distribution of these clusters [6]. These ionic clusters may be connected to each other by narrow channels, leading to the formation of membrane environments with different levels of confinement. These different levels of confinement of the ionic clusters will have an important effect on the degree of water structuring within the membrane matrix, which is expected to directly influence the mechanisms of proton transport through these membranes.

While seeking to understand the structure of Nafion, there are still some problems in the performance of these materials that need to be investigated when used in fuel cells. One of the main problems observed is the decrease in ionic conductivity at temperatures above 80 °C, that may be attributed to the loss of water contained inside the membrane, which impacts negatively in the proton mobility. In order to overcome the water loss observed at high temperatures, a possible solution has been proposed in the previous chapter (chapter 2) which consists on the modification of Nafion membranes by incorporation of Ionic Liquids (ILs) cations. Ionic Liquids (ILs) are compounds consisting entirely of ionic species comprising an organic cation and an inorganic or organic anion [35]. They present a good electrical conductivity, a high ionic mobility and good thermal and chemical stability [43, 44]. In Chapter 2, Nafion membranes were modified by partially replacing the H^+ of the membrane by the IL cation, which leads to different degrees of IL cation

incorporated inside the membrane. It has been observed that the ionic conductivity of the modified Nafion/IL cation membranes may be tuned according to the type of IL cation incorporated as well as their incorporation degree inside the membrane. The most important result obtained with these modified membranes was the higher stability observed at temperatures up to 200 °C. The modified membranes were characterised in terms of distribution of the IL cation within the superficial layer of the membrane using X-ray photoelectron spectroscopy (XPS); their electric properties were also determined by Electrochemical Impedance Spectroscopy (EIS); and, finally, the stability at high temperatures was evaluated by thermogravimetric analysis. However, the effect of incorporating IL cations into Nafion on the proton mobility and its impact in the resulting levels of confinement within the membrane are not yet fully understood.

In this work, in order to better understand the proton mobility and levels of confinement inside the modified Nafion/IL cation membranes, Nuclear Magnetic Resonance (NMR) relaxometry studies were performed, in a wide range of frequencies, at low and at high temperatures. This characterisation technique seems to be adequate to study the molecular dynamics on these modified membranes as it has already been used for studying systems with high molecular complexity, such as liquid crystals in confined environments [25, 60–62] and also for characterisation of proton mobility in Nafion membranes with different degrees of water content [63–65]. Basically, the proton NMR relaxation technique describes the energy exchange between the proton spins of the hydrogen nuclei and the energy exchange between this spin system and the surrounding lattice. These energy exchanges are characterised by two relaxation rates: the spin-spin relaxation rate, $R_2=1/T_2$, and the spin-lattice relaxation rate, $R_1=1/T_1$, where T_2 is defined as the spin-spin relax-

ation time and T_1 as the spin-lattice relaxation time. When both relaxation times are determined for a large range of Larmor frequencies (υ) it is possible to obtain detailed information regarding the molecular dynamics of the system [25]. The Larmor frequency is defined as $\upsilon = \frac{\gamma B}{2\pi}$, where B is the magnetic field and γ is the proton gyromagnetic ratio.

The approach followed in this work involves the use of proton NMR relaxometry, in a wide range of frequencies, to characterise the modified Nafion/IL cation membranes in terms of their proton mobility and levels of confinement, and compare them with an unmodified Nafion membrane. The effect of using different degrees of incorporation of IL cations into Nafion, on the spin-lattice relaxation times (T_1) obtained at different frequencies was studied. Additionally, the diffusion coefficient of protons was estimated by fitting physical relaxation models to the R_1 dispersion obtained for the Nafion membranes. The models used have already been successfully applied for the interpretation of the proton spin-lattice relaxation dispersion, obtained for nano-confined low molecular mass liquid crystals in controlled porous glasses [62]. Finally, the effect of increasing temperature on the stability of the modified Nafion/IL cation membranes was also assessed through NMR relaxometry, making possible a qualitative correlation of the transient behaviour of the relaxation rate with water content.

3.3 Materials and Methods

3.3.1 Materials

Different Ionic Liquid (IL) cations were incorporated in a Nafion-112 membrane, which initially is in the protonated form (obtained from Dupont (USA)). The compounds used as source materials for the IL cations are listed bellow:

- phenyltrimethylammonium chloride, $TMPA^+Cl^-$ from Fluka (Germany);
- 1-n-butyl-3-methylimidazolium bis(trifluoromethanesulfonimide), $BMIM^+BF_4^-$ from Solchemar (Portugal);
- n-dodecyltrimethylammonium chloride, DTA^+Cl^- from TCI Instruments (England).

The molecular formula, molecular structure, molecular weight and molecular length of the corresponding IL cations studied are listed in Table 3.1. These IL cations were studied in Chapter 2, and were selected in this work in order to study the effect caused by cation incorporation into the membranes. Three cation systems were considered: one cation dissolved in an aqueous solution (DTA^+), one cation which is comprised in a room temperature ionic liquid (RTIL) whose water content is very low ($BMIM^+$), and finally a cation that contains an aromatic ring in its structure ($TMPA^+$). It should be mentioned that, in a Chaper 2, this last cation ($TMPA^+$) was considered one of the most interesting due to the resulting high ionic conductivity of the modified membranes, as well as their enhanced thermal stability at high temperatures (up to 200 °C), when compared with an unmodified Nafion membrane.

Table 3.1: Characteristics of the ionic liquid cations studied

Ionic liquid cation	Molecular formula	Molecular structure	Molecular weight, g mol^{-1}	Molecular Length, Å [a]
Phenyltrimethylammonium, $TMPA^+$	$(CH_3)_3NC_6H_5^+$		136	7.2
1-n-Butyl-3-methylimidazolium, $BMIM^+$	$C_8H_{15}N_2^+$	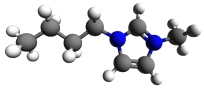	139	10.2
n-Dodecyltrimethylammonium, DTA^+	$C_{12}H_{25}N(CH_3)_3^+$	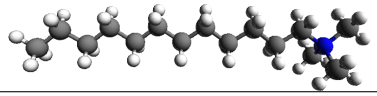	228	18.2

[a] Estimated by using the Avogadro software (http://avogadro.openmolecules.net)

3.3.2 Incorporation of Ionic Liquid (IL) cations in Nafion membranes

Nafion membranes were incorporated with the ionic liquid cations, by immersing the membrane in a solution that contains the IL cation, during different time periods. Different periods of contact between the membranes and the ILs solutions make possible to obtain different degrees of concentration of cations inside the Nafion membrane due to an exchange that occurs between the membrane protons and the ILs cations. As previously described in Chaper 2, the concentration of cations incorporated in the membrane was determined by measuring the pH and the conductivity of the liquid phase, with a pH conductivity meter (model 720 A, Orion) and with a laboratory conductivity meter (model 960, Schott Instruments), respectively, before and after the incorporation procedure.

In order to incorporate the n-dodecyltrimethylammonium (DTA^+) and phenyltrimethylammonium ($TMPA^+$) cations into Nafion, it was necessary to prepare a 40 % (w/w) IL aqueous solution, since the source of both cations (DTA^+Cl^- and $TMPA^+Cl^-$) is solid at room temperature. The solution of DTA^+Cl^- was prepared either with deionised water or with deuterated water.

3.3.3 NMR Relaxometry experiments

The proton spin-lattice relaxation times (T_1) of the unmodified Nafion membrane as well as for the modified Nafion/IL cation membranes were measured as a function of the Larmor frequency and at different temperatures. In order to cover the frequency range from 400 kHz to 68 MHz, two different spectrometers were used. T_1 measurements at Larmor frequencies between 400 kHz and 8 MHz were performed in a homebuilt fast field-cycling spectrometer [66–68], with a polarization and de-

tection field of 0.21 T (corresponding to the proton Larmor frequency of 8.9 MHz), and switching times of 2–3 ms. The T_1 data between 8 MHz and 68 MHz were obtained in a conventional pulsed NMR Bruker spectrometer with a 0–2.1 T electromagnet and an Avance II 300 console, using the inversion-recovery radio-frequency pulse-sequence with phase cycling $((\pi)_x - (\pi/2)_{x,-x})$ for suppression of the dc bias. It is important to mention that at 8 MHz, the common frequency value of the two techniques, a good agreement between the T_1 values measured by the conventional and by the fast field-cycling spectrometer was achieved. The experimental error in the spin-lattice relaxation time measurements is estimated to be lower than ±10 %.

3.4 Results and Discussion

3.4.1 Characterisation of modified Nafion/IL cation membranes using NMR relaxometry

NMR relaxometry results are typically represented as spin-lattice relaxation rate (R_1=1/T_1, being T_1 the spin-lattice relaxation time) for a range of Larmor frequencies. This representation can provide useful information regarding the molecular dynamics of the system. Fig. 3.2 shows this representation for Larmor frequency values between 200 kHz and 8 MHz, for a Nafion membrane in the protonated form at room temperature. For lower frequencies values, bellow 200 kHz, there was much dispersion and “noise” in the values obtained are therefore these results were not taken into account. It is important to mention that the magnetization decay behaviour for this membrane, at frequencies up to 8 MHz, is well described by a mono-exponential behaviour characterised by a single T_1. For higher frequencies values,

above 43MHz (data not shown), this behaviour was not so clear. Above this frequency, evidence was found of a two exponential decay of the longitudinal magnetization. This behaviour could be possibly associated with a decoupling of the spin-lattice relaxation between two proton spin subsystems. Further work needs to be performed in order to investigate this point. In this work, only those systems characterised by a monoexponential were considered.

The relaxation rates observed in Fig. 3.2 are associated to all the hydrogen nuclei present in the membrane. For Nafion in the protonated form, the relaxation rates correspond both to protons associated with the sulphonic groups (Fig. 3.1) and those of water enclosed in the membrane. The range and evolution of R_1 values obtained in this work are consistent with those of Perrin et. al [63]. A qualitatively analysis of the results shows that for frequency values up to 3 MHz, there is practically not much variation in R_1 values with an increase in the frequency. Above the frequency of 3 MHz, a slight decrease in R_1 is observed. Generally, NMR experiments enable the detection of the slow motions of molecules at low frequencies, while at high frequencies it is possible to detect the rapid motions of molecules. Therefore, the independent frequency behaviour of the relaxation rate observed for Nafion in the protonated form at low frequencies may be attributed to the fact that there are no slow motions of the protons present in this membrane.

Finally, the relaxation rate values obtained for this membrane, in the range between 10 s^{-1} and 35 s^{-1}, are comparatively much higher than the characteristic relaxation rate of bulk water, 0.3 s^{-1} [65]. Such higher relaxation rates suggest that the protons are enclosed in a confined micro environment.

It was already observed in Chapter 2 the possibility of designing Nafion membranes with different degrees of concentration of incorporated cation by varying

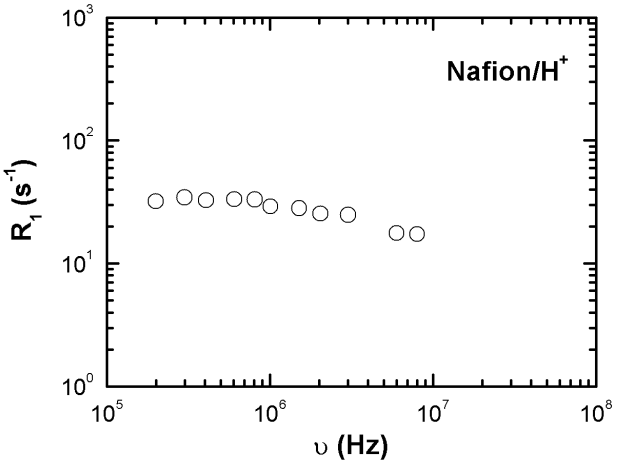

Figure 3.2: Frequency dependence of the proton spin-lattice relaxation rate R_1 for Nafion/H^+.

the contact time between the membrane and the IL cation solution. NMR relaxation experiments were also carried out for a Nafion membrane incorporated with the n-dodecyltrimethylammonium (DTA^+) cation, with different degrees of incorporation. The evolution of the measured spin-lattice relaxation time (T_1) with the incorporation degree for a Nafion membrane with DTA^+, for different values of frequency, is shown in Fig. 3.3.

The magnetization decay behaviour for this membrane, at frequencies up to 67 MHz, is also described by a monoexponential behaviour characterised by a single T_1. For all the frequencies tested, it was observed an increase in the value of T_1 with an increase in the incorporation degree, followed by an apparent stabilization of the T_1 values. It is also observed that for any value of the incorporation degree, the magnitude of T_1 is dependent on the frequency tested, which is a different behaviour than that observed previously for an unmodified Nafion membrane, where

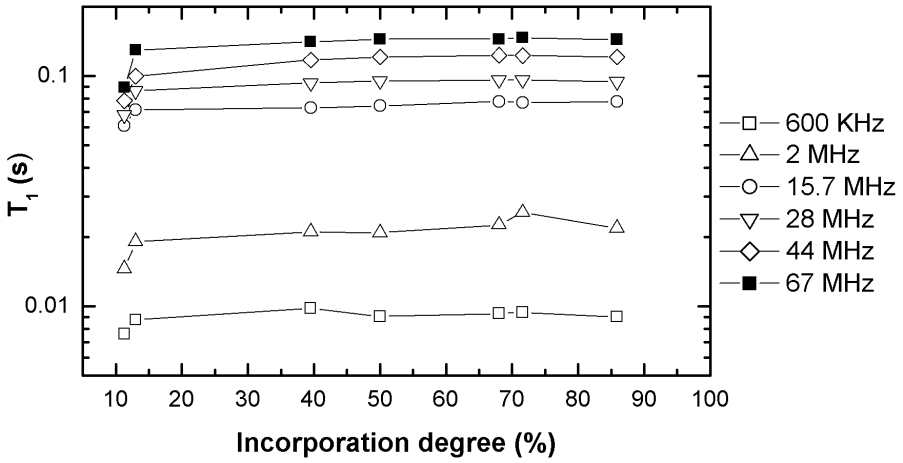

Figure 3.3: Spin-lattice relaxation time (T_1) as a function of the incorporation degree for different values of frequency.

constant values of T_1 were observed at low frequencies.

To better understand the results obtained for the modified Nafion/IL cation membranes, two different Nafion/DTA^+ membranes were prepared, one with a low incorporation degree (13 %), obtained after a contact time of 2 h, and another with the incorporation degree obtained after reaching the equilibrium (68 %), which was obtained after a contact time of 40 h. The evolvement of the incorporation degree obtained for each contact time was determined in Chapter 2. The proton spin-lattice relaxation time was then measured for a wide range of frequencies, between 400 kHz and 68 MHz. The frequency dependence of the proton spin-lattice relaxation rate R_1 for both Nafion/DTA^+ (13 %) and Nafion/DTA^+ (68 %) is represented in Fig. 3.4a and 3.4b, respectively. Additionally, in the same figures there are also represented the results obtained for Nafion/DTA^+ membranes prepared with deuterated water solutions for the same incorporation degree of 13 % and 68 %. The

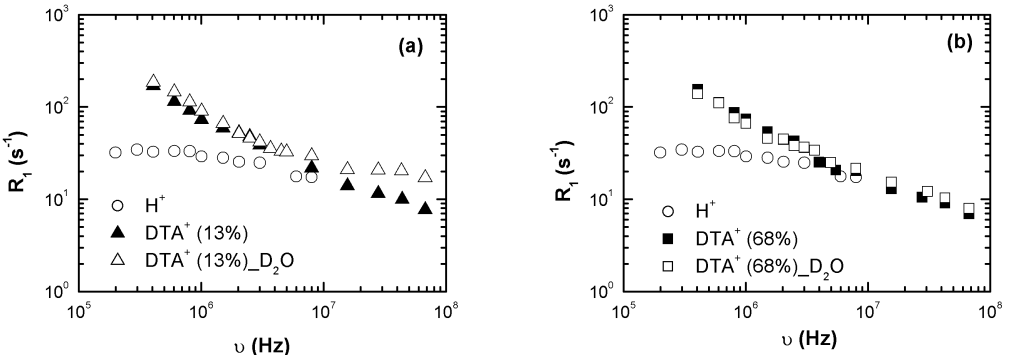

Figure 3.4: Comparison of the frequency dependence of the proton spin-lattice relaxation rate R_1 for: (a) Nafion/H^+, Nafion/DTA^+ (13 %) and Nafion/DTA^+ (13 %)_D_2O, and (b) Nafion/H^+, Nafion/DTA^+ (68 %) and Nafion/DTA^+ (68 %)_D_2O).

use of deuterated water in the NMR experiments assures that the contribution of the protons from water used in the preparation of the aqueous solution of cation is no longer detected. The resulting membranes will be referred to as Nafion/DTA^+ (13 %)_D_2O and Nafion/DTA^+ (68 %)_D_2O).

The relaxation rates observed in Fig. 3.4 are associated to all the hydrogen nuclei present in the membranes. In the case of the modified Nafion/DTA^+ membranes, in addition to the contribution of the protons that a unmodified membrane possess, it is also necessary to take into account possible contributions of the hydrogens present in the structure of the incorporated cation (see Table 3.1 for the molecular structure of this cation). In both subfigures, distinct profiles may be observed for the frequency dependence of the spin-lattice relaxation rate for an unmodified Nafion membrane (Nafion/H^+), and for that of modified Nafion/DTA^+ membranes, prepared either with deionised water or with deuterated water, especially at low frequencies (up to 3 MHz). In contrast with the Nafion/H^+ membrane, both modified

Nafion/DTA^+ membranes show a frequency dependence of the spin-lattice relaxation rate in the all the range of the frequencies tested. As previously mentioned, at low frequencies the slow motions of the molecules are detected, which suggests that the frequency-dependent behaviour observed for Nafion/DTA^+ membranes, in contrast with the flat profile that was observed for a Nafion membrane in the protonated form, may be attributed to the existence of slow motions of the protons of the IL cation.

In the case of the modified membranes prepared with deuterated water, a distinct behaviour was observed, dependent from the degree of IL cation incorporated. In Fig. 3.4a, when Nafion has a DTA^+ cation incorporation degree of 13 %, similar values of T_1 were obtained at low frequencies up to 8 MHz for Nafion/DTA^+ (13 %) and for Nafion/DTA^+ (13 %)_D_2O. However, at high frequencies the same was no longer observed. The difference between these two membranes is that the H-NMR will not detect the orientations and motions of the deuterium proton. Since high frequencies are considered to be more sensitive to detect the rapid movements of the molecules, this result may indicate that with a low DTA^+ cation incorporation degree it is still possible to detect the rapid movements of water molecules present in Nafion/DTA^+ (13 %). In the case of a Nafion membrane incorporated with the degree of cation incorporated at equilibrium (68 %) (Fig. 3.4b) no significant differences on the spin-lattice relaxation rates are observed for the membranes Nafion/DTA^+ (68 %) and Nafion/DTA^+ (68 %)_D_2O in the whole range of frequencies tested. This result could lead to the wrong interpretation that with the maximum incorporation degree, no water molecules remained in the membrane. Actually, in Chapter 2, it is observed that a Nafion membrane with the maximum incorporation degree of the DTA^+ cation, has still a large amount of water molecules inside

its structure, which are deeply involved in the solvation of the incorporated DTA^+ cations. Due to the fact that these water molecules are strongly involved in solvation processes, it is reasonable to consider that they assume a more structured organisation. Therefore, a possible explanation for the results obtained could be that, the increase in the incorporation degree of the DTA^+ cation could lead to a more confined environment and a higher degree of structuring of water within the membrane and, consequently, it was no longer possible to detect rapid motions of water molecules at high frequencies because they are in a more confined environment. In this situation, the only rapid movements that are detected at high frequencies in both membranes are the local fast motions associated with the IL cation.

The modification of Nafion membranes with the IL cations phenyltrimethylammonium chloride ($TMPA^+$) and 1-n-butyl-3-methylimidazolium ($BMIM^+$) was also performed and studied using NMR relaxometry. In both cases, Nafion membranes were prepared with the maximum degree of incorporation, respectively 95 % for Nafion/$TMPA^+$ and 18 % for Nafion/$BMIM^+$. The maximum value of the incorporation degree obtained for each IL cation was determined in Chapter 2. A comparison of the frequency dependence of the proton spin-lattice relaxation rate R_1 is shown in Fig. 3.5 for the unmodified Nafion membrane and for the modified Nafion membranes tested with all different cations, for the situation of maximum incorporation degree.

A monoexponential magnetization decay, characterised by a single T_1, was observed for Nafion incorporated with the $TMPA^+$ and $BMIM^+$ cations, in the whole frequency range analysed. For all of the modified Nafion/IL cation membranes a similar frequency dependence of R_1 may be observed in Fig. 3.5. In the case where Nafion is modified with IL cations, this experimental technique detects slow mo-

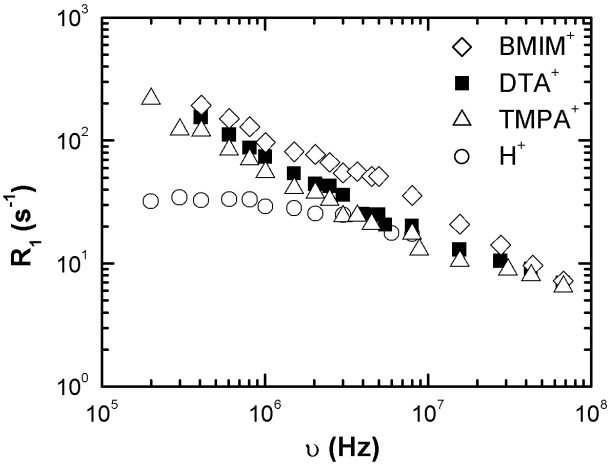

Figure 3.5: Comparison of the frequency dependence of the proton spin-lattice relaxation rate R_1 for the unmodified and modified Nafion/IL cation membranes.

tions of the molecules at low frequencies, that are not detectable or that do not exist in a Nafion membrane in the protonated form. At high frequency values, similar values of R_1 are obtained for all of the modified Nafion/IL membranes, which are associated to fast motions of the molecules. It is clear from Fig. 3.5 that the relaxation rate curves for all of the modified membranes converge to the same value at high frequencies. A possible explanation of this behaviour is that at high frequencies only the fast movements of individual molecules are detected, which are not typically affected by the confinement conditions in their microenvironment at that frequency range. Therefore, these results suggest that the fast and individual motions of the cations are similar, irrespective of their molecular structure.

3.4.2 Modelling of proton spin-lattice relaxation of modified Nafion/IL cation membranes

The proton spin-lattice relaxation rate may be typically analysed in terms of a relaxation model that considers a sum of two contributing relaxation mechanisms. One mechanism is associated with the individual rotations and reorientations of small molecules and is described by the Bloembergen, Purcel and Pound (BPP) model:

$$\left(\frac{1}{T_1}\right)_{BPP} = (R_1)_{BPP} = A\left[\frac{\tau_c}{1+\omega^2\tau_c} + \frac{4\tau_c}{1+4\omega^2\tau_c}\right] \tag{3.1}$$

where A is a fitting parameter which depends of the characteristic angles and distances between proton spins of the hydrogen nuclei and τ_c is a correlation time [25]. Since this equation takes into consideration the free rotation of the molecules, generally it can also describe the bulk free self-diffusion of the molecules which are not affect by confining conditions. The second relaxation mechanism considered is associated with the self-diffusion close to the confining walls and the corresponding reorientations, which depends from the surface structure (RMTD – rotations mediated by translational displacements). In this case, the spin-lattice relaxation rate can be given by Eq. 3.2:

$$\left(\frac{1}{T_1}\right)_{RMTD} = (R_1)_{RMTD} = A_{RMTD}\left\{\frac{1}{\omega^p}\int_{z_{min}}^{z_{max}}\frac{z^{3-2p}}{1+z^4}\,dz + \frac{1}{(2\omega)^p}\int_{\frac{z_{min}}{\sqrt{2}}}^{\frac{z_{max}}{\sqrt{2}}}\frac{z^{3-2p}}{1+z^4}\,dz\right\} \tag{3.2}$$

where $p = (1+\chi)/2$, being χ the orientational structure factor, z_{max}= $(\omega_{RMTD\,max}/\omega)^{1/2}$, $z_{min} = (\omega_{RMTD\,min}/\omega)^{1/2}$. A_{RMTD} is a parameter which depends on the residual dipole-dipole proton spin interaction, on the microstructural features of the confined environment, and on the diffusion coefficient. The high and

low cut-off frequencies, $\omega_{RMTD\,max}$ and $\omega_{RMTD\,min}$, respectively, are related with the self-diffusion constant (D) through the following relations: $(\omega_{RMTD\,max})^{-1} = l_{min}^2/4D$ and $(\omega_{RMTD\,min})^{-1} = l_{max}^2/4D$, where l_{max} and l_{min} are respectively the largest and smallest displacement distances [62]. The RMTD relaxation mechanism was previously referred by Perrin et al. [65] when analysing the diffusion of water molecules inside a Nafion membrane.

As previously mentioned, modified Nafion/IL cation membranes appear to present nano-sized cavities interconnected by narrow channels where the small molecules (e.g. IL cations and hydrogen protons) move. Therefore, the different dimensions of cavities and channels inside the membrane may influence the proton mobility of the membrane, since there are regions that may be more confined than others. Additionally, the presence of water molecules and their degree of structuring, which results from the incorporation of IL cations, may also influence the proton mobility inside the membrane. The motion of the molecules inside Nafion can therefore be considered similar to that observed with confined liquid crystal molecules in nano-porous glasses [62]. The approach followed in this work involved the fitting of a model equation, given by a linear combination of BPP and RMTD models, to the experimental spin-lattice relaxation rate values, in order to verify its potential in describing the frequency dependence of relaxation rates of modified Nafion-IL cation membranes. A similar model was used to analyse the proton spin-lattice relaxation dispersion obtained for confined liquid crystals in nano-porous glasses [61, 62], where analogous frequency dependence of spin-lattice relaxation rates were obtained when compared to those observed in this work (Fig. 3.4 and 3.5).

The fitting model equation is thus given by:

$$(R_1)_{Total} = (R_1)_{BPP} + (R_1)_{RMTD} \tag{3.3}$$

The calculated relaxation rate for an unmodified Nafion membrane, obtained by fitting Eq. 3.1, is shown in Fig. 3.6a, while the calculated relaxation rates for the modified Nafion/IL cation membranes, obtained through fitting of Eq. 3.3, are shown in Fig. 3.6b to 3.6d [69]. The symbols represent the experimental values, the solid lines represent the calculated total relaxation rates, while the dash and dash-dot lines represent respectively, the individual contributions of the RMTD and the BPP relaxation mechanisms.

For a Nafion membrane in the protonated form (Fig. 3.6a), only the BPP equation was taken into consideration in the fitting of the experimental results, since this membrane shows a constant relaxation rate at low frequencies, followed by a frequency dependent relaxation rate behaviour at high frequencies. This indicates that only the individual and fast movements were detected. Excellent fitting of the experimental results was obtained in all cases. Therefore, it may be assumed that the spin-lattice relaxation mechanisms for the modified Nafion/IL cation membranes are well described by the proposed model. The fitted values of the free parameters used in the calculation of the curves shown in Fig. 3.6 are presented in Table 3.2.

Since the fitted cut-off frequency (ω_{max}) parameter can be related with the proton translational self-diffusion in the less confined regions by $(\omega_{RMTD\,max})^{-1}$= $(2\pi f_{c\,max})^{-1} = l_{min}^2/4D$ as mentioned before, the diffusion coefficient, considered as a global diffusion coefficient, including the contribution of every proton present within the membrane, defined in its less confined region, can be estimated assuming physically reasonable values for the l_{min} (e.g. molecular length of the IL cations).

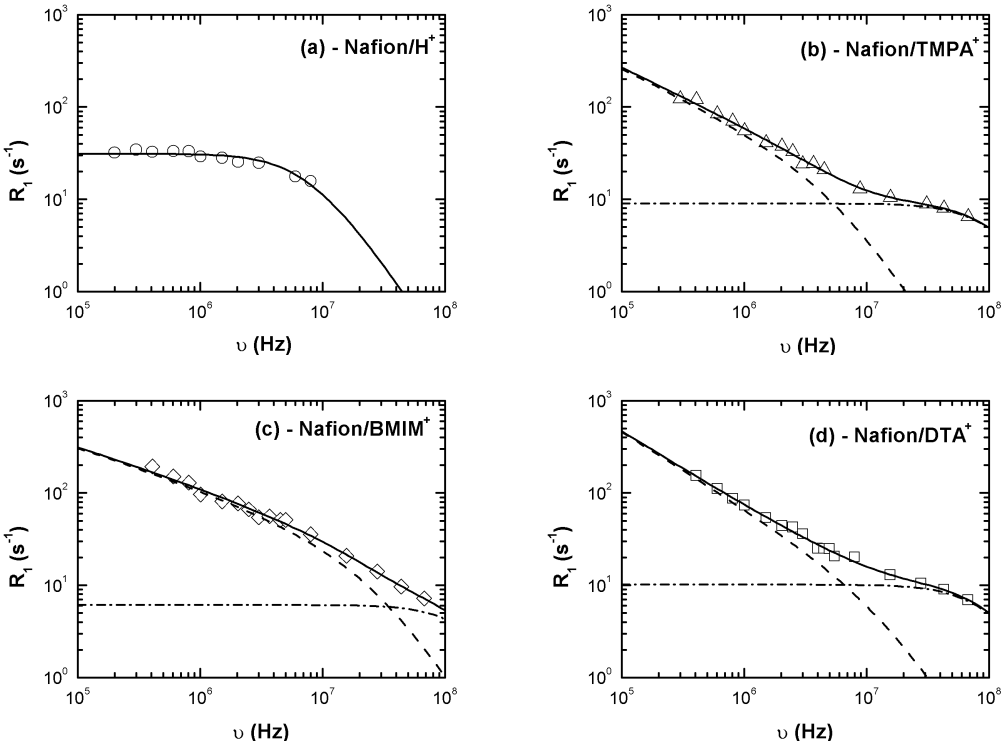

Figure 3.6: Calculated relaxation rates obtained through fitting for (a) Nafion/H^+, (b) Nafion/$TMPA^+$, (c) Nafion/$BMIM^+$, and (d) Nafion/DTA^+. The symbols represent the experimental values, the solid lines represent the calculated total relaxation rates, while the dash and dash-dot lines represent respectively the single contribution of the RMTD and BPP equations.

Table 3.2: The best fit values of parameters used in calculating the dispersion curves presented in Fig. 3.6

	Nafion/H^+	Nafion/$TMPA^+$	Nafion/$BMIM^+$	Nafion/DTA^+
τ_c, s	1.23×10^{-8}	8.23×10^{-10}	5.71×10^{-10}	9.4×10^{-10}
A_{ROT}, s^{-2}	5.06×10^{8}	2.16×10^{9}	2.15×10^{9}	2.16×10^{9}
A_{RMTD}, $s^{-(1+p)}$	–	1.11×10^{5}	6.84×10^{3}	2.2×10^{6}
f_{cmin}, Hz	–	2.3×10^{3}	1.5	1.1
f_{cmax}, Hz	–	1.3×10^{7}	6.19×10^{7}	2.81×10^{7}
p	–	0.63	0.41	0.82

Table 3.3 summarizes the fitted maximum frequency and the estimated diffusion coefficient for the modified Nafion/IL cation membranes with a maximum degree of incorporation. It is not possible to estimate a diffusion coefficient for the Nafion membrane in the protonated form, since only the BPP model (Eq. 3.1) can be fitted to experimental results, which does not include the maximum frequency parameter required for the estimation of diffusion coefficients. The analysis of these results is not straightforward, since the estimated diffusion coefficient takes into account the contribution of all protons. The discrimination of the individual diffusion coefficient of each type of proton, either from the original sulphonic groups (remaining protons after the exchange process) or from the IL cation or from water, is therefore not possible with the applied methodology. Even so, the magnitude of the results obtained suggest that membranes incorporated with the $TMPA^+$ cation are characterized by a slower diffusional transport than those of Nafion/$BMIM^+$ and Nafion/DTA^+, which is indicative of a more confined and structured environment within the membrane.

Table 3.3: Fitted values of maximum frequency and diffusion coefficient for the modified Nafion/IL cation membranes

Membrane	f_{cmax}, Hz	D, $m^2\ s^{-1}$
Nafion/$TMPA^+$	1.30×10^7	1.69×10^{-10}
Nafion/$BMIM^+$	6.19×10^7	1.62×10^{-9}
Nafion/DTA^+	2.81×10^{-7}	2.34×10^{-9}

3.4.3 Temperature effect on the spin-lattice relaxation time

In order to study the stability of the modified membranes at high temperatures, spin-lattice relaxation time measurements were performed for an unmodified Nafion membrane as well as for three different modified membranes with the maximum degree of incorporation, at two different temperatures (80 °C and 120 °C), and at a constant Larmor frequency value of 1500 kHz. Fig. 3.7 illustrates the time evolvement of the spin-lattice relaxation time for the distinct temperatures studied, and for the four membranes tested.

In a first analysis it can be seen that, at room temperature, all the membranes maintain a constant T_1 value throughout the experiment: this result may be taken as an indication of membrane stability in terms of their water content. Moreover, an increase in the initial T_1 value measured is observed with an increase in the temperature for all of the modified Nafion/IL cation membranes. This was an expected result, since T_1 typically increases with an increase in temperature. This behaviour is reasonable since at high frequencies the spin-lattice relaxation rates correspond to the bulk translational self-diffusion and to the fast molecular rotations/reorientations mechanisms which are proportional to the correlation times of these motions. Since these motions are usually thermally activated, their correl-

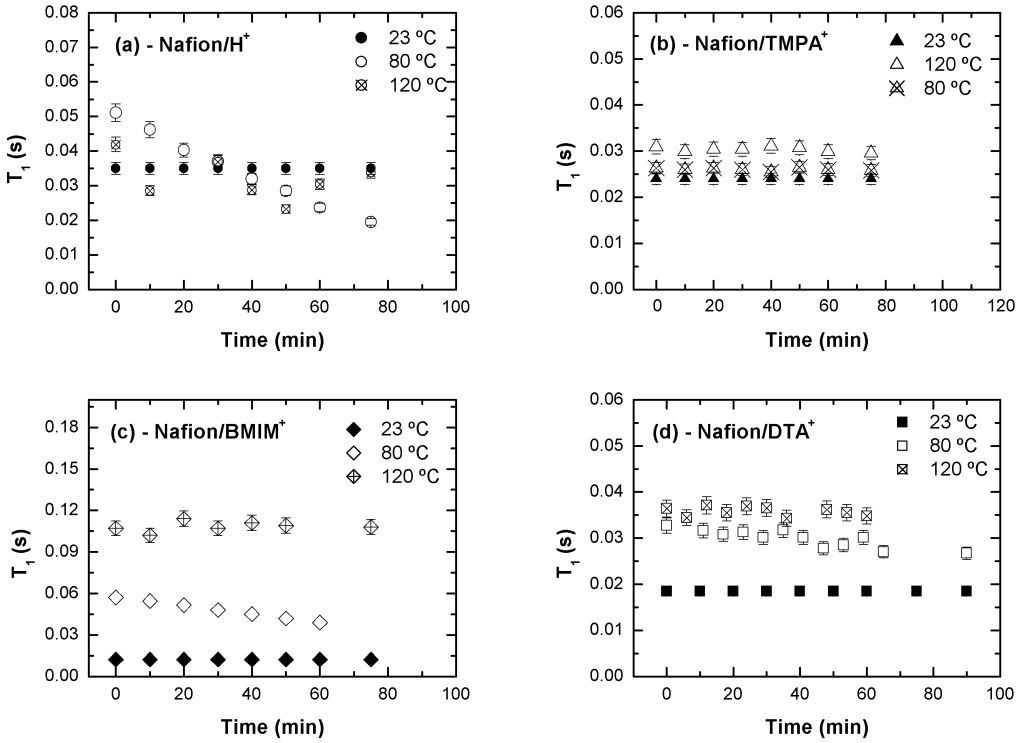

Figure 3.7: Time evolution of the spin-lattice relaxation time for different temperatures: 23 °C, 80 °C and 120 °C for (a) Nafion/H^+, (b) Nafion/$TMPA^+$, (c) Nafion/$BMIM^+$, (d) Nafion/DTA^+ membrane.

ation times decreases with increasing temperature.

Regarding the unmodified Nafion membrane (Fig. 3.7a), a sharp decrease with time is observed at 80 °C in the value of T_1, which is most possibly related with the membrane dehydration at that temperature, previously observed by thermogravimetry analysis (Chaper 2). Membrane dehydration at 80 °C apparently depleted all water contained within the membrane, which is indicated by highly dispersed and "noisy" values obtained in the experiments performed at 120 °C. In the case of Nafion/$TMPA^+$ (Fig. 3.7b) a constant value of T_1 with time was obtained for all the temperatures tested, which may translate the stability of these membranes even at high temperatures. This observation is again in agreement with the previous results obtained through thermogravimetry analysis (Chaper 2), which provides an additional proof of the good stability of Nafion/$TMPA^+$ membrane, in terms of water loss. The results shown in Fig. 3.7d suggest that the Nafion/DTA^+ membrane is somewhat less stable than Nafion/$TMPA^+$. In fact, a slight decrease in T_1 is observed at 80 °C, indicating dehydration of the membrane. At 120 °C the membrane appears to maintain its stability corresponding to constant T_1 values, which is again consistent with previous thermogravimetric results (Chaper 2). The Nafion/$BMIM^+$ membrane can be considered the least stable of the modified membranes studied in this work. Fig. 3.7c shows a steady decrease in T_1 values at 80 °C, indicating water depletion, while at 120 °C the membrane appears to maintain its water content.

The results obtained in this work show that membrane stability to dehydration is linked to the type and degree of cation incorporation, which ultimately determines their water content and water degree of structuring. The Nafion/$TMPA^+$ presents a high cation incorporation degree (95 %) and a reduced but rather stable water content, while Nafion/DTA^+ exhibits also a high cation incorporation degree (68 %)

but a higher water content (Chaper 2). In both cases the water molecules present within the membrane seem to be highly structured, making difficult their loss at higher temperatures, resulting in membranes more stable when compared with the Nafion membrane in the protonated form. In what concerns the Nafion/$BMIM^+$ membrane, it has a low cation incorporation degree (18 %) and relatively high water content. The water present within this membrane appears to be less confined and structured, in comparison with the other modified membranes tested, which is confirmed by its lower stability at higher temperatures.

3.5 Closure

This work shows that proton NMR relaxometry is a technique with a large potential for the characterisation of proton mobility in unmodified Nafion membranes and in Nafion membranes modified with IL cations. Also, it has been shown that this technique makes possible to distinguish between different levels of confinement within the membrane structure.

The results obtained suggest that the molecular dynamics of the modified Nafion/IL cations membranes can be analysed by performing different measurements of the spin-lattice relaxation times (T_1) obtained at different values of frequency. Qualitative results showed that in a Nafion membrane in the protonated form it is not possible to detect slow motions of molecules, while for modified membranes, depending on the frequency range tested, the contribution of the slow motions as well as the fast motions of the molecules present in the membranes could be detected.

The frequency dependence of the spin-lattice relaxation rate (R_1) data obtained for the modified Nafion/IL cation membranes was adjusted to the physical relax-

ation model $(R_1)_{Total} = (R_1)_{BPP} + (R_1)_{RMTD}$ and it was found that the model fits adequately the results. Therefore it was concluded that the approach followed in this work for modifying Nafion membranes with IL cations results in membranes with two different environments: one that is more confined and with a lower proton mobility, described by the RMTD model (low frequencies); and other that is less confined, with a higher proton mobility, described by the BPP model (high frequencies). By using the best fit parameters obtained with the model mentioned above, it was possible to estimate a global diffusion coefficient of the protons present in the membrane. The results obtained suggest that the Nafion membrane incorporated with theTMPA$^+$ cation has a more confined and structured environment, when compared with Nafion/BMIM$^+$ and Nafion/DTA$^+$ membranes, since its estimated diffusion coefficient is one order of magnitude lower, when compared with the values obtained for other two membranes.

NMR relaxometry studies were also applied for assessing the membranes stability at high temperatures. The results obtained are in agreement with those obtained in previous thermogravimetric studies for these membranes. It was concluded that the proton mobility of an unmodified membrane is strongly reduced at high temperatures, while for the modified membranes, especially for Nafion/TMPA$^+$ and Nafion/DTA$^+$ the proton mobility presents small variations with increasing temperature.

Future work will be focused on performing measurements of T_1 for a wider range of frequencies for modelling purposes. Such results could be valuable for determining the dimensions of the confining environments as well as better estimates of both *self*- and *induced*-diffusion coefficients. Moreover, additional experiments with deuterated water could help in the identification and discrimination of individual con-

tributions of ion diffusivities, apparently not possible using this technique with conventional water solutions.

Chapter 4

Methanol and Gas Crossover Through Modified Nafion Membranes by Incorporation of Ionic Liquid Cations

Submitted as: Luísa A. Neves, Isabel M. Coelhoso, João G. Crespo, Methanol and Gas Crossover Through Modified Nafion Membranes by Incorporation of Ionic Liquid Cations, Journal of Membrane Science (2010)

4.1 Summary

Nafion membranes were modified by incorporation of ionic liquid (IL) cations, at controllable degrees, in order to assess the influence of this modification in both the methanol and gas crossover. The effect of using different degrees of incorporated IL cations, as well as the type of IL cation incorporated, in the transport of gases and methanol was studied in detail. The results obtained were compared with those

obtained with an unmodified Nafion membrane. Depending on the IL cation incorporated, a reduction in methanol crossover in the range of 60–600 times was obtained in this work, when compared with a Nafion-112 membrane. This reduction was related both with the type of IL cation incorporated and its incorporation degree which determine the amount of water retained by the membrane and its degree of structuring inside the membrane. Pure H_2, O_2, N_2 and CO_2 permeabilities were also determined, and a lower gas crossover through all of the modified Nafion/IL cation membranes was obtained when compared with those obtained through the unmodified membrane (Nafion-112/H^+). It was concluded that the electric properties, methanol and gas crossover as well the stability at high temperatures of these membranes can be tuned by controlling the degree of incorporation as well as the type of cation incorporated. The best compromise between all these properties has to be found in order to considerer their use in Direct Methanol Fuel Cells (DMFCs).

4.2 Introduction

Direct methanol fuel cells (DMFCs) have been widely studied in the literature over the last years [5, 70, 71] since they can be regarded as a potential energy power source due to their simple design and mode of operation, their ability to operate at relatively low temperatures (up to 150 °C), and their easy fuel storage, when compared with fuel cell systems using H_2 as a fuel. Energy is produced in a DMFC by the catalytic oxidation of liquid methanol at the anode, thereby producing protons, electrons and carbon dioxide. The protons produced are transported by diffusion to the cathode compartment through a polymer exchange membrane (PEM). In this compartment, the protons react with oxygen and electrons to produce water. One

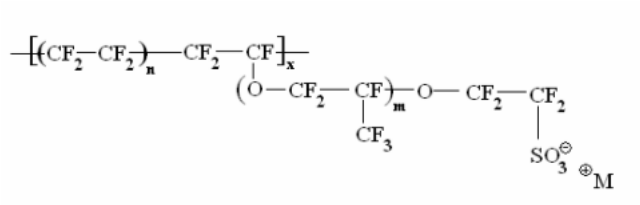

Figure 4.1: Chemical structure of Nafion.

of the key elements that determine the performance and life-time of a DMFC is the polymer exchange membrane. The PEMs used in this type of devices should exhibit a low methanol and gas crossover, an high proton conductivity as well as an high chemical, mechanical and thermal stability at temperatures above 80 °C [7].

The PEM material most studied in DMFCs is Nafion. This polymer consists of a polytetrafluoroethylene (PTFE) backbone with sulphonic acid side-groups arranged in intervals along the chain, as illustrated in Fig. 4.1 [1, 6].

This membrane is widely used in fuel cells studies because it fulfils most of the required properties. Nafion has a high proton conductivity, which depends strongly on its water content, and it also exhibits good mechanical, thermal and chemical stability at temperatures up to 80 °C. However, above this temperature a decrease in its water content is observed lowering the proton conductivity and leading to a loss of the spatial coherence of the membrane. Additionally, when used in a DMFC system, a relatively high methanol and gas crossover is observed [5, 7, 70, 71].

A number of works are available in the literature where Nafion membranes were modified in order to overcome the problem of methanol crossover. Wang et al. [72] modified a Nafion membrane by a direct polymerization of a protonated polyaniline (PANI), in order to obtain a composite membrane. PANI was chosen due to its electrochemical conductivity and stability in corrosive environments. In that work

a reduction of 59 % on the methanol crossover was observed. In the work developed by Li et al. [73] Nafion was modified by an in-situ chemical polymerization of 3-4-ethylenedioxythiophene, and the methanol crossover of the membranes produced was reduced by 30 % to 72 % when compared with unmodified membranes. There is also a number of works that report the development of organic-inorganic composite membranes [74, 75], where reductions in methanol crossover between 50 % and 80 % were obtained. Instead of modifying the Nafion membrane material, other authors prepared less expensive membrane materials as alternatives to Nafion. Examples of such materials are the sulfonated poly(oxa-p-phenylene-3,3-phtalido-p-phenylene-oxa-p-phenilene-oxy-phenylene) (PEEK-WC) membranes, where a reduction of about two orders of magnitude of the methanol crossover was obtained in comparison with Nafion-117 [76], and the sulfonated poly(ether ether ketone) (sPEEK) membranes, where a reduction of 92 % on the methanol crossover was observed [28].

Gas crossover in Nafion membranes is relatively well documented in the literature [77–84]. Despite the fact that crossover of gases, present as reagents and/or reaction products in DMFCs, may be also considered as an important factor influencing the efficiency of a DMFC, strategies to reduce gas crossover have attracted a relatively lower attention when compared to methanol crossover. Strategies for gas crossover reduction were studied for alternative membrane materials with modest results [28, 76, 85, 86]. Drioli et al. [76] studied the permeability of the sulfonated PEEK-WC membranes towards O_2, N_2, CO_2, He and H_2, and obtained lower permeabilities than those obtained with Nafion-117 for the gases O_2, N_2 and CO_2. In the work developed by Silva et al. [28] the permeability of Nafion-112 for N_2, O_2 and CO_2 was determined and compared with a sulfonated poly(ether ether ketone)

membrane with different sulfonation degrees. Depending of the sulfonation degree, permeability reductions in the ranges of 43–57, 20–57 and 12–39 were obtained for N_2, O_2 and CO_2, respectively when compared with a Nafion membrane. Gosalawit et al. [85] tested two types of membranes, the sulfonated PEEK-WC and Krytox-Si-Nafion, and determined the permeability of H_2 and O_2. A reduction in gas crossover was observed for both membranes when comparing with Nafion-117, with a maximum reduction of 91 % for H_2 and 42 % for O_2.

The approach followed in this work was the design of modified Nafion membranes by partially replacing their protons with ionic-liquid (IL) cations, in order to assess the influence of this modification in both the methanol and gas crossover. Ionic Liquids (ILs) are compounds consisting entirely of ionic species comprising an organic cation and an inorganic or organic anion [35], and they present a good electrical conductivity, a high ionic mobility and good thermal and chemical stability [43, 44]. In Chapter 2 the incorporation of IL cations into a Nafion-112 membrane was studied. The IL cations tested were phenyltrimethylammonium ($TMPA^+$), n-dodecyltrimethylammonium (DTA^+), hexadecyltrimethylammonium (CTA^+), 1-n-butyl-3-methylimidazolium ($BMIM^+$), and 1-n-octyl-3-methylimidazolium ($OMIM^+$). After incorporation into Nafion their distribution was characterised by X-ray Photoelectron Spectroscopy (XPS). Additionally, the electrical properties of the modified membranes, with different degrees of cation incorporation, were determined by Electrochemical Impedance Spectroscopy (EIS). The stability of the modified membranes with increasing temperature was determined by thermogravimetric studies, which allowed to establish a plausible relation between the membrane stability at high temperatures with its water content and type of water structuring. The results obtained show that, depending on the incorporated IL cation

in the Nafion structure, the ionic conductivity and consequently the proton mobility of the modified membranes can either decrease or increase. Even though for some of the IL cations incorporated the ionic conductivity of the modified Nafion/IL membranes obtained was compromised, it was observed that all membranes studied remained stable at temperatures up to 200 °C due to their ability to retain water at higher temperatures, which is attributed to water structuring effects within the membrane and water involvement in additional solvation of the incorporated cation.

This work discusses the design of Nafion membranes, modified with different degrees of incorporation of ionic liquid cations, and evaluates the effect of this modification on methanol and gas crossover, comparing it with an unmodified Nafion-112 membrane.

4.3 Experimental

4.3.1 Materials

The membrane used as a reference material was Nafion-112 in the protonated form (equivalent molecular weight of 1100 g mol^{-1} and a thickness of 51 μm), obtained from Dupont (USA).

Different Ionic Liquid (IL) cations were incorporated within the Nafion-112 membrane. The compounds used as source materials for the cations are listed bellow:

- tetramethylammonium chloride, TMA^+Cl^- from Fluka (Germany);
- phenyltrimethylammonium chloride, $TMPA^+Cl^-$ from Fluka (Germany);

- n-dodecyltrimethylammonium chloride, DTA^+Cl^- from TCI Instruments (England);
- hexadecyltrimethylammonium bromide, CTA^+Br^- from Sigma (USA);
- 1-n-butyl-3-methylimidazolium hexafluorophosphate, $BMIM^+PF_6^-$ from Solchemar (Portugal);
- 1-n-octyl-3-methylimidazolium hexafluorophosphate, $OMIM^+PF_6^-$ from Solchemar (Portugal).
- methyl-tricaprylylammonium dicyanamide, $ALIQUAT^+DCA^-$ from Solchemar (Portugal).

The molecular formula, molecular structure, molecular weight and molar volume of the corresponding IL cations are listed in Table 4.1. The IL cations TMA^+, $TMPA^+$, DTA^+, CTA^+ and $ALIQUAT^+$, which are all quaternary amines, were selected in order to study the effect of different alkyl chain lengths, and also to assess the effect of the presence of an aromatic ring in the structure of the cation ($TMPA^+$). ILs with imidazolium type cations with different length of alkyl chain, $BMIM^+$ and $OMIM^+$, were also selected.

4.3.2 Incorporation of Ionic Liquid (IL) cations in Nafion membranes

Each protonated Nafion membrane was immersed in a solution that contains the IL cation for a specific period of time, in order to exchange the protons from the Nafion membrane with the IL cations. The pH and conductivity of the liquid phase were measured, before and after incorporation, using a pH conductivity meter (model

Table 4.1: Characteristics of the ionic liquid cations studied

Ionic liquid cation	Molecular formula	Molecular structure	Molecular weight, $g\,mol^{-1}$	Molar volume, $cm^3 mol^{-1}$ [a]
Tetramethylammonium, TMA^+	$(CH_3)_4N^+$		74	119
Phenyltrimethylammonium, $TMPA^+$	$(CH_3)_3NC_6H_5^+$		136	189
n-Dodecyltrimethylammonium, DTA^+	$C_{12}H_{25}N(CH_3)_3^+$	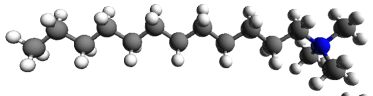	228	350
Hexadecyltrimethylammonium, CTA^+	$C_{19}H_{42}N^+$	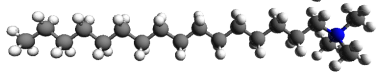	284	434
1-n-Butyl-3-methylimidazolium, $BMIM^+$	$C_8H_{15}N_2^+$	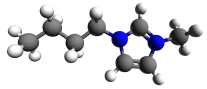	139	182
1-n-Octyl-3-methylimidazolium, $OMIM^+$	$C_{12}H_{23}N_2^+$	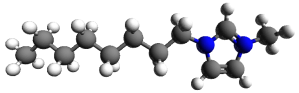	195	266
Methyl-tricaprylylammonium dicyanamide, $ALIQUAT^+$	$C_{25}H_{54}N^+$	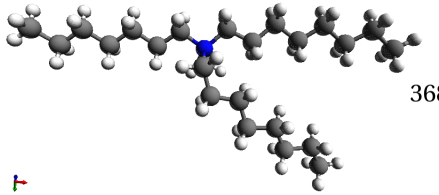	368	560

[a] Estimated parameter by Shroeder's method [45].

720 A, Orion) and a laboratory conductivity meter (model 960, Schott Instruments), respectively, in order to determine the concentration of cations incorporated inside the Nafion membranes (Chapter 2).

4.3.3 Methanol crossover measurements

Methanol crossover measurements of the modified Nafion/IL cation membranes were performed by using a glass diffusion cell with two identical compartments, having a volume of 160 mL each, separated by the membrane. The effective membrane area was determined to be 12.6 cm^2. Both compartments were stirred at 300 rpm, which provided the adequate fluid dynamic conditions to avoid external mass transfer limitations (experimentally validated). One of the compartments contained initially a 15 M aqueous methanol solution and the other compartment contained deionised water. Since the methanol crossover is affected by the feed concentration [5, 87], a methanol concentration of 15 M was used in order to assess the membrane performance at a high concentration level, which is favourable for the fuel cell operation. The evolvement of the methanol concentration in the receiving and donating compartments, due to methanol permeation, was monitored by refractometry. The analytical set-up consisted of an high pressure pump (L-6200A, Merck, Germany), an auto sampler (AS-4000A, Merck, Germany) and a differential refractometer (RI-71, Merck, Germany). A volume of 30 μL of each sample was injected into the refractometer, using water as eluent with a flow rate of 1 mL min^{-1}.

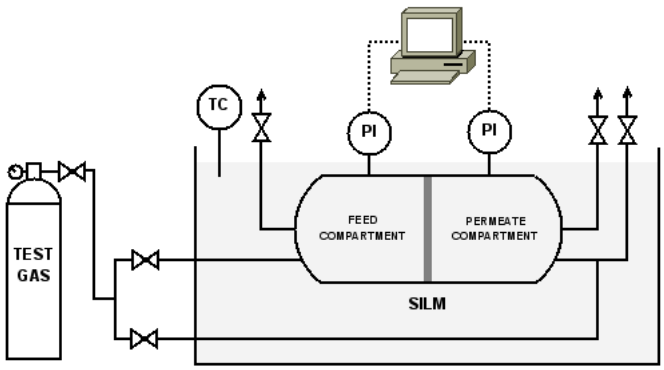

Figure 4.2: Scheme of the experimental set-up for measuring pure gas crossover through the modified Nafion/IL membranes.

4.3.4 Gas crossover measurements

The pure gas crossover of the modified Nafion/IL membranes was measured for H_2, O_2, N_2 and CO_2. These experiments were carried out in the experimental apparatus shown in Fig. 4.2. It is composed by a stainless steel cell with two identical compartments separated by the modified membrane, with an effective membrane area of 15.9 cm^2. Gas crossover was evaluated by pressurizing both compartments (feed and permeate) with a single gas establishing an initial pressure difference of 0.5 bar between both compartments. The pressure evolvement in both compartments was followed by using two pressure transducers (Druck, PDCR 910 models 99166 and 991675, UK). All measurements were performed at a constant temperature of 30 °C, by using a thermostatic bath (Julabo, Model EH, Germany).

The crossover of a pure gas through a membrane may be calculated from the pressure data obtained from both compartments (feed and permeate) shown in Fig. 4.2, according to the following equation [11]:

$$\frac{1}{\beta}\ln\left(\frac{[p_{feed}-p_{perm}]_0}{[p_{feed}-p_{perm}]}\right)=\frac{1}{\beta}\ln\left(\frac{\Delta p_0}{\Delta p}\right)=P\frac{t}{l} \tag{4.1}$$

where p_{feed} and p_{perm} are the pressures in the feed and permeate compartments (Pa), respectively, P is the membrane permeability ($m^2\ s^{-1}$), t is the time (s), and l is the membrane thickness (m). The geometric parameter β (m^{-1}) is characteristic of the geometry of the cell shown in Fig. 4.2, and is given by

$$\beta = A\left(\frac{1}{V_{feed}}+\frac{1}{V_{perm}}\right) \tag{4.2}$$

where A is the membrane area (m^2), and V_{feed} and V_{perm} are the volumes of the feed and permeate compartments (m^3), respectively. The data can be plotted as $1/\beta \cdot \ln\left(\Delta p_0/\Delta p\right)$ versus t/l, and the gas permeability values are obtained from the slope of this representation.

4.4 Results and Discussion

4.4.1 Methanol crossover results

Methanol crossover measurements were performed for modified Nafion/IL as wells as for unmodified Nafion membranes. The methanol crossover, expressed in terms of its diffusivity across the membrane, was determined by using Eq. 4.1, replacing pressure by concentration in each compartment. A crossover of 2.45×10^{-6} cm^2s^{-1} was obtained for the unmodified Nafion-112 membrane in the protonated form, which is within the range of values available in the literature (values in the range of 1.4×10^{-6} cm^2s^{-1} to 3.52×10^{-6} cm^2s^{-1} [70–72, 74, 75, 88–96], therefore validating the experimental method used in the present work.

4.4.1.1 Effect of the incorporation degree of the IL cation

A Nafion-112 membrane was modified by incorporation of the n-dodecyltrimethyl ammonium (DTA^+) cation at different concentrations, in order to study the effect of the incorporation degree on the methanol crossover. To perform these measurements, the protonated membrane was immersed for different periods of time in an aqueous solution of DTA^+Cl^-, as previously described in section 4.3.2. The degree of incorporation of the cation inside the membrane was determined by measuring the pH of the IL aqueous solution before and after incorporation. The procedure followed for incorporating IL cations in Nafion at different concentration degrees has been already described in detail in the previous Chapter 2.

Fig. 4.3 represents the methanol crossover obtained as a function of the DTA^+ cation incorporation degree and as a function of the total volume of incorporated cation per unit membrane volume. This volumetric ratio ($cm^3_{ILcation}$ / $cm^3_{membrane}$) was determined knowing the cation incorporation degree, the DTA^+ cation molar volume (Table 4.1) and the membrane thickness after incorporation. The cation molar volume was estimated by the Schroeder's method [45], which does not account for solvation effects.

It is important to mention that the methanol crossover value obtained for an unmodified Nafion membrane is also represented in Fig. 4.3 and corresponds to 0 % of cation incorporation degree.

When comparing to a Nafion membrane in the protonated form, a significant reduction in the methanol crossover was achieved. It was also noticed that the methanol crossover decreases with an increase in the cation incorporation degree, being observed a sharp decrease up to a cation incorporation degree of approximately

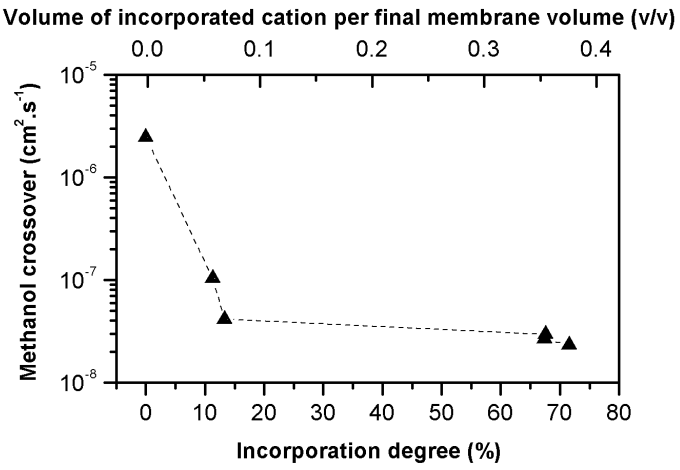

Figure 4.3: Methanol crossover as a function of the DTA^+ cation incorporation degree and of the total volume of incorporated cation per final membrane volume ($cm^3_{ILcation}$ / $cm^3_{membrane}$).

13 %, and a less pronounced variation with further cation incorporation.

During incorporation of the DTA^+ cation into Nafion it is necessary to consider the water exchange between the membrane and the IL aqueous solution. The water molecules inside the Nafion/DTA^+ membrane are deeply involved in solvation processes, namely the solvation of the incorporated DTA^+ cations. Obviously this process is more significant for higher incorporation degrees. The water molecules involved in these solvation processes are in a more confined environment and, due to the strong solvation conditions, they assume a more structured organisation. Therefore, a plausible explanation for a decrease in methanol crossover with an increase in the cation incorporation degree, as shown in Fig. 4.3, is related with water structuring inside the membrane as the cation incorporation degree increases. Such higher confinement and structuring of the water within the membrane material

Table 4.2: Methanol crossover obtained for the different Nafion/IL cation membranes studied

Membranes	Incorporation degree, %	Methanol crossover, cm^2s^{-1}
Nafion/H^+	0	2.45×10^{-6}
Nafion/ TMA^+	95	4.21×10^{-8}
Nafion/ $BMIM^+$	18	5.16×10^{-8}
Nafion/$TMPA^+$	82	3.89×10^{-8}
Nafion/ $OMIM^+$	4	2.59×10^{-8}
Nafion/DTA^+	68	1.56×10^{-8}
Nafion/ CTA^+	65	1.21×10^{-8}
Nafion/ $ALIQUAT^+$	15	4.05×10^{-9}

could lead to an increased viscosity of the hydrophilic domains and, consequently, to a larger diffusional resistance of the modified membrane to methanol transport [90, 97].

4.4.1.2 Effect of the different IL cations incorporated

The effect of incorporating different cations, in the methanol crossover through a Nafion membrane, was evaluated and the resulting cation incorporation degree for each Nafion/IL cation membrane as well as the methanol crossover values obtained are shown in Table 4.2. It is important to mention that, the incorporation degree presented in this Table is the maximum value that was achieved for each membrane.

The analysis of the values presented in Table 4.2 clearly evidences that, when compared with a Nafion membrane in the protonated form, a reduction in the methanol crossover was obtained for all the modified Nafion/IL-cation membranes studied. Since the IL cations studied are quite different in their structure (Table 4.1), as

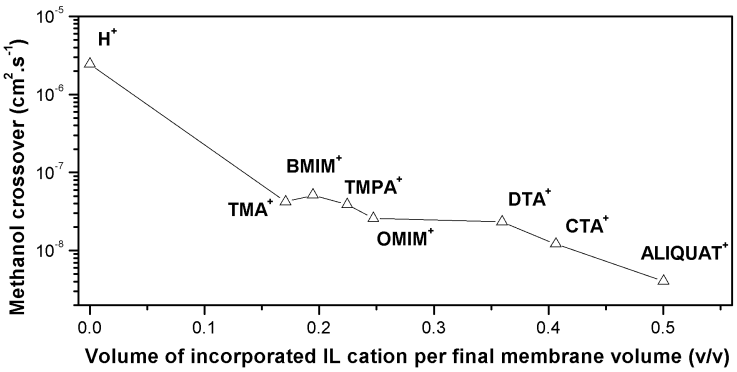

Figure 4.4: Methanol crossover as a function of the volumetric ratio of the incorporated IL cation volume per final membrane volume, in equilibrium ($cm^3_{ILcation}$ / $cm^3_{membrane}$).

well as their maximum incorporation degree (Table 4.2), the volume of the incorporated cation per final membrane volume was calculated. Fig. 4.4 represents the methanol crossover of the different modified Nafion/IL-cation membranes studied as a function of the volumetric ratio of the incorporated IL cation $cm^3_{ILcation}$ / $cm^3_{membrane}$).

It can be observed that the methanol permeability decreases with an increase in the volume of incorporated cation. As stated before, more important than the volume occupied by the bulky IL cation, is the higher water structuring within the Nafion membrane that results from the solvation of the different IL cations incorporated. Thermogravimetric analysis, performed in a previous work, section 2.4.4, Chaper 2, allowed to follow the loss of water by the membrane as the temperature is raised.

Fig. 4.5 illustrates the membrane weight loss as a function of temperature for different Nafion/IL cation membranes. The evolvement of the membrane weight with

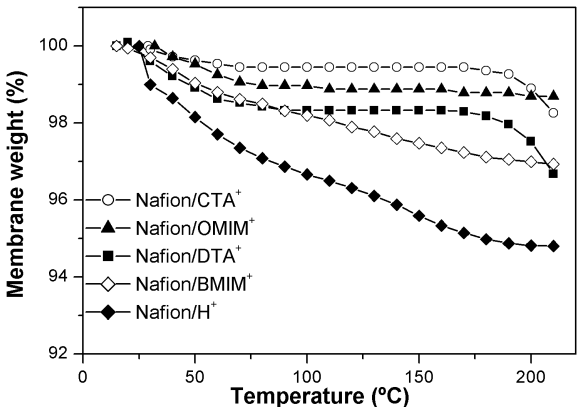

Figure 4.5: Evolvement of each membrane weight with increasing temperature (figure adapted from Chapter 2).

increasing temperature may be associated with the membrane ability to retain water at high temperatures. It is expected that membranes with a higher ability to retain water are the ones where the water molecules are strongly involved in solvation processes. It is observed that the Nafion membrane in the protonated form looses more water, and easily, when compared with all other modified Nafion/IL cation membranes. It is interesting to notice that the sequence in terms of the ability to retain water (Fig. 4.5) agrees very closely with the sequence in terms of the ability to avoid methanol crossover (Fig. 4.4). The explanation for this behaviour has been discussed previously and is certainly related with the degree of water confinement and structuring induced by the solvation of incorporated cations. This effect is expected to be more significant for the largest cations incorporated. Such high degree of water structuring is expected to lead to an augmented diffusional resistance and to a lower methanol crossover. Fig. 4.5 does not include the results for all IL cations studied in this work, such as TMA^+ and $ALIQUAT^+$, but it could be anticipated that

those modified membranes will follow a similar trend.

4.4.1.3 Comparison with the different strategies presented in the literature

As previously mentioned, there are several works in the literature aiming a reduction in the methanol crossover by modifying Nafion membranes or by preparing new membrane materials. Although high methanol feed concentrations are favourable for the fuel cell performance, they can also lead to a high methanol crossover, which is reported to have a long-term negative impact on their performance and lifetime [5, 87]. Actually, most of the works available in the literature are restricted to low methanol concentrations (up to 3 M). Furthermore, thinner membranes such as Nafion-112 (with a thickness of 51 μm), present advantages such as an higher ionic conductivity when compared with a Nafion-117 membrane (which has a thickness of 175 μm), but have the disadvantage of permitting a high methanol crossover, with a negative impact on the fuel cell performance and life-time. In this work, the methanol crossover was determined for a Nafion-112 membrane under high methanol feed concentration conditions (15 M). Table 4.3 compares the methanol crossover reduction obtained in this work with selected examples from the literature. Since these experimental values were obtained under different experimental conditions, operating conditions such as methanol concentration and temperature are also listed in Table 4.3. The reduction in methanol crossover is presented in Table 4.3 as the ratio of the unmodified Nafion methanol permeability to the modified membrane permeability. The analysis of Table 4.3 clearly shows that the reduction in methanol crossover obtained in this work is superior when compared with other approaches in the literature.

One of the most promising results were obtained by Banaszak et al. [90], where

the impact on the methanol crossover was studied by modifying a Nafion-117 membrane with the IL cation $EMIM^+$ (1-ethyl-3-methylimidazolium). Even though the reduction in the methanol crossover obtained in the referred work (11-fold reduction) was inferior to the values obtained in this work (58–605 range of reduction), both results are apparently consistent considering that the $EMIM^+$ cation is smaller than, for example, the $BMIM^+$ and $OMIM^+$ cations.

4.4.2 Gas crossover results

The gas crossover of the modified Nafion/IL cation membranes was measured with pure gases that are typical constituents of the anode side of a fuel cell, such as H_2 and CO_2, and of the cathode side of a fuel cell such as O_2 and N_2. Fig. 4.6 shows the variation of the gas crossover obtained for both modified Nafion/IL membranes and unmodified Nafion-112 membrane, as a function of the Lennard-Jones diameter of each gas [45].

Nafion is described as a complex polymer having distinct regions: a hydrophobic region mainly associated with the polytetrafluoroethylene backbone, which is responsible for the mechanical stability of the membrane, and a hydrophilic region comprised by the sulfonic acid side-groups, which is related to the membrane hydration and proton mobility [6]. Gas transport in such a complex material as Nafion is commonly described as being governed by combined effects of solubility and diffusivity of the transported species through both regions [82, 98].

In a first analysis it is observed that the trend of permeability values is the same as for the Nafion membrane in the protonated form, $P_{CO_2} > P_{H_2} > P_{O_2} > P_{N_2}$ and following a similar behaviour when compared with other polymeric materials. Solubility

Table 4.3: Methanol crossover reduction: comparison with different approaches presented in the literature

Membrane	Experimental conditions	Reduction in methanol crossover	Reference
Nafion/IL cations	15 M aqueous methanol solution; Room temperature	58–605	This work
PANI/Nafion-117	2 M aqueous methanol solution; Room temperature	2	[72]
Poly (3,4–ethylenedioxythiophene)/Nafion	1 M aqueous methanol solution; T = 60 °C	1.4–4	[73]
Silica supported heteropoly acid/Nafion	17 M aqueous methanol solution; Room temperature	1.5–3	[74]
Nafion with functionalized MMT (Organic/inorganic composite membrane)	3 M aqueous methanol solution; Room temperature	2	[75]
Nafion/$EMIM^+$	2.5 M aqueous methanol solution; Room temperature	11	[90]
Surface modification of Nafion by plasma etching, palladium sputtering and a combination of both	2.5 M aqueous methanol solution; Room temperature	1.1–1.6	[94]
Sulfonated PEEK-WC	CH_3OH_{vapour}; Pressure = 120 mbar; T = 25 °C	123	[76]
Sulfonated poly(ether ether ketone) (sPEEK)	5 M aqueous methanol solution; T=25 °C	12	[28]

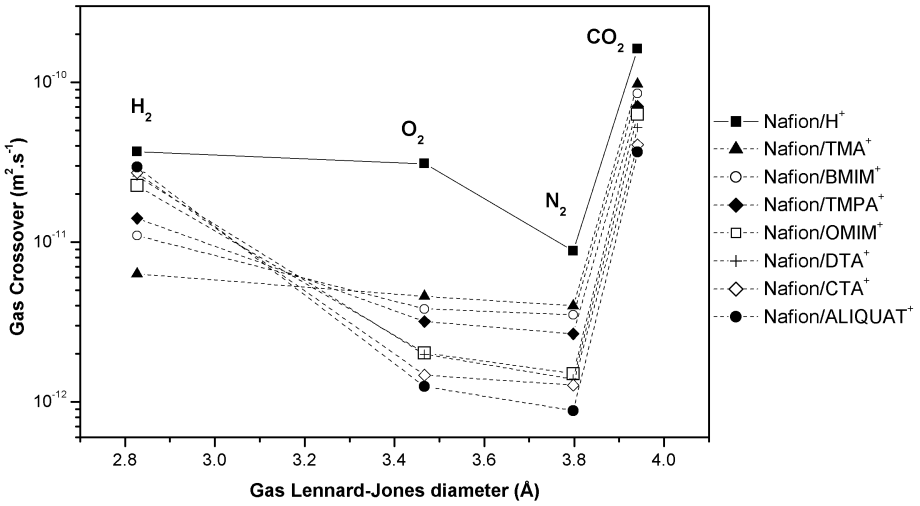

Figure 4.6: Gas crossover obtained for the Nafion/IL membranes as a function of the Lennard-Jones diameter of each gas, at a temperature of 30 °C.

effects dominate for gases of larger molecules (CO_2 and gases/vapours with a higher molecular mass), while permeation of gases of smaller molecules is determined by their diffusivity. These effects explain the high crossover of CO_2, attributed to its high solubility, and the high crossover of H_2, attributed to the high diffusivity of this gas [99].

It is also clearly evidenced in Fig. 4.6 that gas crossover through all of the modified Nafion/IL cation membranes is lower than crossover through the unmodified membrane (Nafion-112/H^+).

The gas crossover values obtained for each gas are represented in Fig. 4.7 as a function of the volume of the incorporated IL cation per final membrane volume. The first point in each subfigure represents the results for the unmodified Nafion membrane. It is observed that, with the exception of hydrogen, gas crossover decreases with an increase in the volume of the incorporated cation.

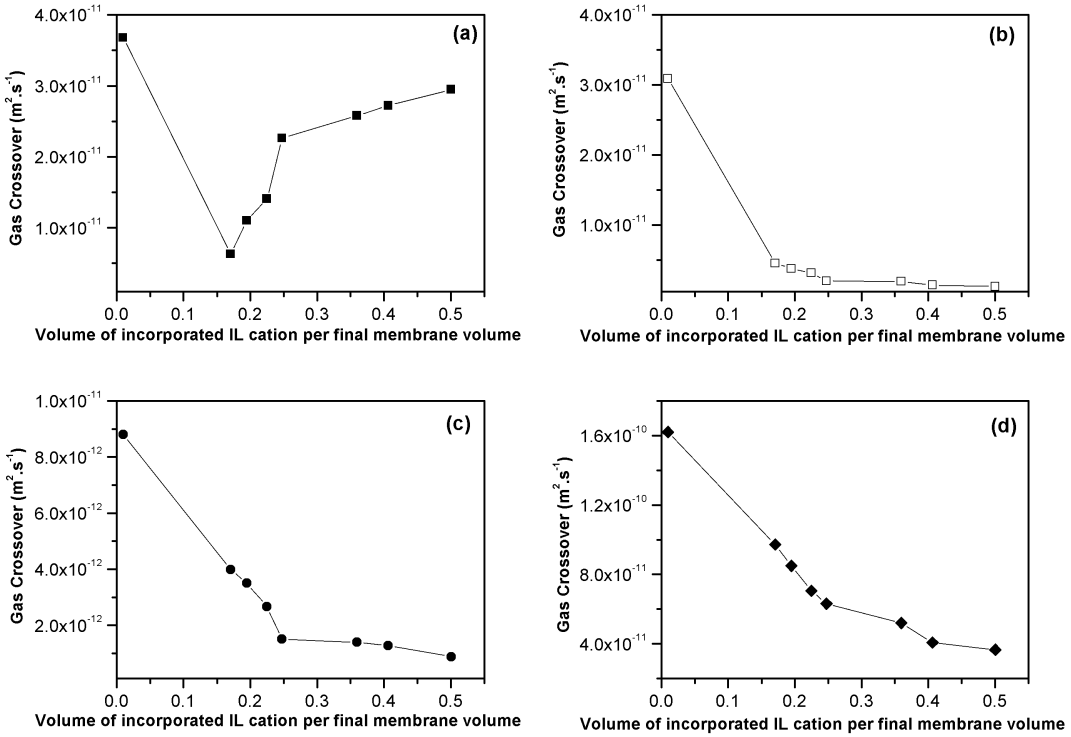

Figure 4.7: Gas crossover of the modified Nafion/IL cation membranes as a function of the volume of incorporated IL cation per final membrane volume, for the gases (a) H_2; (b) O_2; (c) N_2; (d) CO_2.

Table 4.4: Reduction in gas crossover for the modified Nafion/IL cation membranes

Gas	Gas Crossover, $m^2\ s^{-1}$	Reduction in gas crossover
	Nafion-112	$P_{Nafion-112}/P_{Nafion/ILcation}$
H_2	3.68×10^{-11}	2–6
O_2	3.09×10^{-11}	7–25
N_2	8.81×10^{-12}	3–10
CO_2	1.62×10^{-10}	2–5

Also, Table 4.4 summarises the gas crossover reduction values obtained in this work when the H_2, O_2, N_2 and CO_2 crossover of a Nafion unmodified membrane is compared with the crossover of the different Nafion/IL cation membranes studied, at a temperature of 30 °C. The analysis of Table 4.4 indicates that the Nafion/IL cation membranes, show consistently lower gas crossover values.

In the case of the gases O_2, N_2 and CO_2, the results suggest that the change in their crossover behaviour is mainly governed by diffusion mechanisms since gas crossover decreases with an increase of the volume of the cation incorporated in the membrane. As previously discussed, the type and amount of cation incorporated determines the amount and the degree of structuring of the water inside the membrane and, consequently, its viscosity in these confined environments. Still, it is observed that the values of CO_2 crossover are less affected by diffusion than O_2 and N_2, probably due to higher solubility effects.

The high crossover of hydrogen through the unmodified Nafion membrane is attributed to its high diffusivity. The change of its crossover with the type and amount of incorporated cation is difficult to explain supported in these data. Additional studies aiming at measuring the hydrogen solubility in the various membranes will be necessary.

4.5 Closure

It was shown that the simple methodology used in this work for incorporating different IL cations in Nafion membranes at a controllable degree allowed to obtain modified membranes with both reduced methanol and gas crossover in comparison with unmodified Nafion membranes.

These results suggest that the reduced methanol crossover obtained for all the modified Nafion/IL cation membranes is not directly related with the volume occupied by the bulky IL cation, but mainly with the water structuring degree inside the membrane induced by cation incorporation. The higher structuring of water leads to a more viscous micro-environment and therefore to a reduced methanol transport through the membrane. The same explanation may be given for the reduced O_2, N_2 and CO_2 crossover values obtained, in which the results obtained suggest that the transport of gases through these membranes is mainly controlled by diffusion.

In Chapter 2 it has been shown that the ionic conductivity and the thermal stability (up to 200 °C) properties of the modified Nafion membranes could also be tuned according to the type and amount of cation incorporated. In particular, it was observed a drastic improvement of the thermal stability of the modified membranes over Nafion in the protonated form, which typically looses water at temperatures above 80 °C. The promising results obtained in this work in terms of reduction of methanol and gas crossover represent an evidence of their potential use in DMFCs, especially at high temperatures. For such applications, it is therefore necessary to find the best compromise between the resulting electrical properties, the transport of methanol and gases and the stability at high temperatures.

Chapter 5

Gas Permeation Studies using Supported Ionic Liquid Membranes

Submitted as: Luísa A. Neves, João G. Crespo, Isabel M. Coelhoso, Gas Permeation Studies using Supported Ionic Liquid Membranes, Journal of Membrane Science (2010)

5.1 Summary

Room Temperature Ionic Liquids (RTILs) based on the 1-n-alkyl-3-methylimidazolium cation were immobilised in polymeric membranes, in order to study the potential of using supported ionic liquid membranes (SILMs) for CO_2/N_2 and CO_2/CH_4 gas separations. Different aspects were investigated, namely: the evaluation of the SILMs stability using two membrane supports which differ in terms of their hydrophobicity; and the effect of using RTILs with cations of different alkyl chain lenght and also with different anions, on the permeability and selectivity of pure and humidified pure gases as well as gas mixtures. H_2, O_2, N_2, CH_4 and CO_2 gas permeabil-

ities were determined and CO_2/N_2 and CO_2/CH_4 ideal selectivities were calculated and compared with data available in the literature described by the Robeson upper bound correlation. The effect of the presence of water vapour in different gas streams of N_2, CH_4 and CO_2 was also studied. Finally, CO_2/N_2 and CO_2/CH_4 binary mixtures (50 % v/v) were prepared and the selectivity obtained was compared with the ideal selectivity. The results show that the SILMs prepared with the most hydrophobic support are more stable than those based on the hydrophilic support, and have a high affinity for CO_2 when compared with other gases. This behaviour was observed both for pure and gas mixtures, at low pressures. The high selectivity values obtained for CO_2 indicate that these SILMs may be considered for CO_2 separation processes.

5.2 Introduction

The use of supported liquid membranes (SLMs) for gas/vapor separations has been widely studied during the last 16 years [14]. In a SLM, the membrane pores are impregnated with a selected solvent, and transport of the permeating species occurs according to a solution-diffusion mass transfer mechanism. Due to the fact that the diffusion of species in liquids is faster when compared with diffusion in solids, it is expected that the permeability across liquid membranes becomes higher than when using solid membranes. Even though SLMs are considered attractive for gas separations, their application in industry is still limited mainly due to problems in their stability and long-term performance. The stability of the impregnated solvent within the membrane pores may be affected at high temperatures by solvent depletion through evaporation, or due to adverse operating conditions (e.g. the trans-

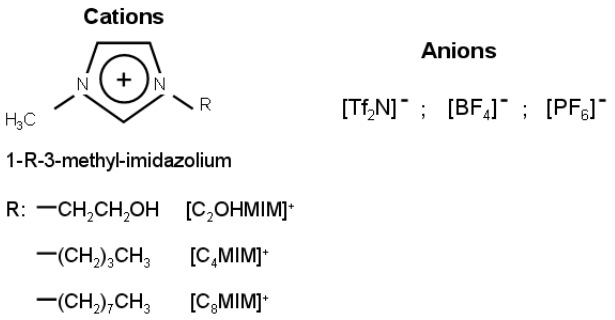

Figure 5.1: Typical cations and anions present in imidazolium type of RTILs.

membrane pressure should not be higher than the breakthrough pressure so that the solvent is not expelled from the membrane pores). One of the most interesting strategies for improving the stability of SLMs seems to be the use of Room Temperature Ionic Liquids (RTILs) as the immobilised phase within the pores, due to the fact that these compounds have a negligible vapour pressure. This feature eliminates the problem of solvent evaporation that typically occurs in SLMs, allowing for obtaining liquid membranes with a high stability [35, 100–104]. RTILs are compounds that typically consist of bulky organic cations, and inorganic anions, and have the special characteristic of being liquids at room temperature. Some of the typical cations and anions present in a RTIL are shown in Fig. 5.1. RTILs exhibit a large variety of properties, such as negligible vapour pressure, thermal stability at high temperatures (above 300 °C), and reduced solubility in various solvents which has additionally made their use as the immobilised phase in Supported Liquid Membranes (SLMs) very attractive [16, 36, 40, 41].

RTILs have received increasing interest in applications involving carbon dioxide separations, due to the large solubility of CO_2 in selected RTILs [19]. Among the large diversity of RTILs, those based in the imidazolium cation typically present a

large solubility for CO_2. Additionally, these RTILs based on the imidazolium cation, may exhibit an even higher solubility for CO_2 by selecting an appropriate RTIL anion, which also plays an important role in the gas solubility due to a weak Lewis acid/base complexation that occurs between CO_2 and the RTIL anion [20]. Additionally, the solubility of CO_2 in RTILs is also expected to increase with an increase in the alkyl chain length of the RTIL cation [105]. In this way, it is possible to design tailor-made membranes with a defined selectivity for a specific application combining different alkyl chain lengths of the RTIL cation and different anions. Among the diverse gas mixtures, the most attractive seem to be the CO_2/N_2 and CO_2/CH_4 separations, associated respectively with the purification of flue gas streams and natural gas processes [17].

There are several works available in the literature where supported ionic liquid membranes were studied for potential applications in gas separations. Scovazzo et al. [106] determined the pure gas permeability of N_2, CH_4 and CO_2 and the corresponding ideal selectivities through a porous hydrophilic polyethersulfone support with different RTILs immobilised. After representing the data obtained in a Robeson-plot the authors concluded that these permeabilities/selectivities of SILMs were competitive or even superior to other membrane materials. The facilitated transport of CO_2 and SO_2 through SILMs was studied by Luis et al. [107]. The permeabilities of air, CO_2 and a mixture of SO_2/air were measured using different SILMs, and ideal selectivities were calculated. It was concluded that SILMs can be very selective to CO_2 and SO_2. Regarding the separation of CO_2/He, Ilconich et al. [108] determined the pure gas permeability of CO_2 and He, and ideal selectivity and membrane stability at different temperatures, up to 125 °C. The ionic liquid 1-n-hexyl-3-methylimidazolium bis(trifluoromethanesulfonyl)imide was immobil-

ised in two different porous polymeric supports and it was observed that membranes prepared with polysulfone supports were stable at high temperatures. Mixed gas permeabilities and selectivities for the CO_2/CH_4 and CO_2/N_2 gas pairs were determined by Scovazzo et al. [109], and it was observed that the selectivity for a gas mixture slightly decreases when compared to the ideal selectivity. The CO_2/CH_4 mixture was also studied by Hanioka et al. [110], where, by using a SLM based on a task specific ionic liquid for CO_2, a highly stable and selective membrane for CO_2 separation (during more than 260 days) was obtained.

Despite the large number of publications concerning supported ionic liquid membranes and the examination of their potential for gas separations, there is still a need for a better understanding of the phenomena taking place. Actually, there is not a clear understanding of the effect of different membrane supports, with diverse chemical nature (typical supports are hydrophilic), on gas permeability and selectivity when using relevant gas mixtures. The effect of the ionic liquid cation structure (namely the length of their side alkyl-chain) and the type of ionic liquid anion are other aspects which have not been investigated. Moreover, in the work developed by Fortunato et al. [101, 102] it was observed that the presence of water influences the stability of SILMs due to formation of water clusters within the ionic liquid. Therefore, another important aspect that needs to be clarified, which is not usually taken into account, is the effect of the water vapour content in the gas stream to be processed, on the selectivity of these SILMs.

This work proposes to investigate the following aspects: 1 - the design of supported ionic liquid membranes by immobilisation of different Room Temperature Ionic Liquids in polymeric membranes; 2 - the evaluation of the stability of the SILMs and the selection of the best membrane support regarding its nature (hydrophobicity); 3

Table 5.1: Polymeric porous membranes used as support of SILMs

Membrane	Material	Pore size, μm	Thickness, μm	Contant angle, °
Vericel (Pall Corporation)	Hydrophilic PVDF	0.20	129	107.2 ± 2.48
Millipore (Millipore Corporation)	Hydrophobic PVDF	0.22	125	121.0 ± 0.63

- the effect of using different alkyl chain lengths of the RTIL cation and different anions on gas permeability; 4 – the effect of the presence of water vapour on the supported ionic liquid membrane performance; 5 – the behaviour of the membranes designed, for separation of selected gas mixtures, CO_2/N_2 and CO_2/CH_4.

5.3 Experimental

5.3.1 Materials

5.3.1.1 Polymeric Porous Membranes

The supported ionic liquid membranes were prepared using two different polymeric porous membranes as supporting material, both made of polyvinylidene fluoride (PVDF), with a similar pore size but with different chemical nature: one being hydrophobic (provided by Millipore Corporation, USA) and the other one being more hydrophilic (provided by Pall Corporation, USA). These membranes are characterized by their high chemical resistance, being previously used in other works as a supporting material for SILMs [35, 100–102]. The pore size, thickness and contact angle of these membranes are summarized in Table 5.1. The membrane contact

angle measurements shown in Table 5.1 were performed with a Krüss drop shape analysis system (DSA 10-MK2, Krüss, USA).

5.3.1.2 Room Temperature Ionic Liquids (RTILs)

The RTILs based in the immidazolium cation studied in the present work were:

- 1-butyl-3-methylimidazolium hexafluorophosphate ($[C_4MIM][PF_6]$);
- 1-octyl-3-methylimidazolium hexafluorophosphate ($[C_8MIM][PF_6]$);
- 1-butyl-3-methylimidazolium tetrafluoroborate ($[C_4MIM][BF_4]$);
- 1-decyl-3-methylimidazolium tetrafluoroborate ($[C_{10}MIM][BF_4]$),
- 1-butyl-3-methylimidazolium bis(trifluoromethanesulfonyl)imide ($[C_4MIM][Tf_2N]$).

All RTILs were supplied by Solchemar (Portugal).

These RTILs were selected to study the effect of using different alkyl chain lengths of the RTIL cation, as well as the effect of different RTIL anions, on the permeability and selectivity to different gases. Their molecular weight, viscosity, density, water solubility in the RTIL and RTIL solubility in water are listed in Table 5.2. The viscosity of each RTIL was measured with a viscosimeter (Haake RS 50, Germany), at a temperature of 30 °C.

5.3.1.3 Gases

The gases used in the experiments were hydrogen (High-Purity Grade (99.999 %), Air Liquide, France), oxygen (High-Purity Grade (99.999 %), Praxair, USA), nitrogen (Industrial Grade (99.99 %), Praxair, USA), methane (Industrial Grade (99.5 %), Praxair, USA) and carbon dioxide (High-Purity Grade (99.998 %), Praxair, USA).

Table 5.2: Properties of the RTILs studied

RTIL	Molecular weight, $g\,mol^{-1}$	Viscosity, mPa s	Density, $kg\,m^{-3}$, 25 °C	Water solubility in the RTIL, mol_{water}/l_{RTIL}, 25 °C [100]	RTIL Solubility in water, mol_{RTIL}/l_{water}, 25 °C [100]
$[C_4MIM][PF_6]$	284	187	1 320 [a]	1.55	0.0676
$[C_8MIM][PF_6]$	340	441	1 190 [a]	0.87	0.0066
$[C_4MIM][BF_4]$	226	71	1 210 [b]	Water miscible	Water miscible
$[C_{10}MIM][BF_4]$	310	231	1 040 [a]	4.70	–
$[C_4MIM][Tf_2N]$	419	58	1 430 [c]	–	–

[a] Fortunato et. al. [100] [b] Data provided by the manufacturer, Solchemar (Portugal) [c] Huddleston et al. [111]

5.3.2 Preparation of supported ionic liquid membranes (SILMs)

The procedure to immobilize the RTIL inside the pores of the polymeric membrane was the following: the membrane was placed inside a desiccator and vacuum was applied for 1 h, in order to remove air from within the pores and, therefore, allowing the RTIL to be introduced easily in the pores of the membrane. Afterwards, still under vacuum, drops of RTIL were spread on the membrane surface using a syringe. After this immobilisation procedure, the membrane surface was cleaned with a paper tissue. The amount of RTIL immobilized in the membrane was determined gravimetrically, by weighing the membrane before and after immobilisation [101].

5.3.3 Stability of supported ionic liquid membranes (SILMs)

The study of the stability of the SILMs was carried out in the experimental set-up shown in Fig. 5.2. The SILMs were placed in a dead-end filtration cell (Amicon 8010), with an effective membrane area of 3.46 cm^2. A pressure up to 2 bar was applied using nitrogen (N_2). To determine their stability, the membranes were weighed using an analytical balance (Sartorius A.G. Göttingen CP225D, Germany) at regular periods of time in order to determine the weight decrease, which is assumed to be related to the loss of RTIL along time. In addition, the flux of N_2 through the membrane was measured using a gas flowmeter (J&W Scientific) connected to the cell permeate outlet, in order to evaluate the stability of SILMs by following the increase of flow with the applied pressure.

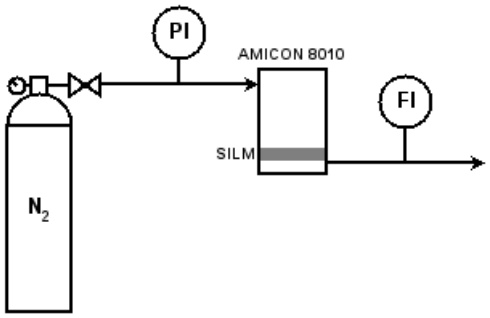

Figure 5.2: Experimental set-up to evaluate the stability of the SILMs.

5.3.4 Gas permeation experiments

5.3.4.1 Single gas permeability

The pure gas permeability of the supported ionic liquid membranes for H_2, N_2, O_2, CH_4 and CO_2 was determined using the experimental apparatus shown in Fig. 5.3a. This rig is composed by a stainless steel cell with two identical compartments separated by the supported liquid membrane. The effective membrane area was 15.9 cm^2. Each individual gas permeability was evaluated by pressurizing both compartments (feed and permeate) with a single gas, and after opening the permeate outlet, a driving force of around 0.7 bar between the feed and the permeate compartments was established. The pressure change in both compartments over time was followed using two pressure transducers (Druck, PDCR 910 models 99166 and 991675, England). All measurements were performed at constant temperature, 30 °C, using a thermostatic bath (Julabo, Model EH, Germany). Also, the membrane weight was measured using an analytical balance (Sartorius A.G. Göttingen CP225D, Germany), before and after the gas permeation experiments, in order to evaluate the stability of these membranes.

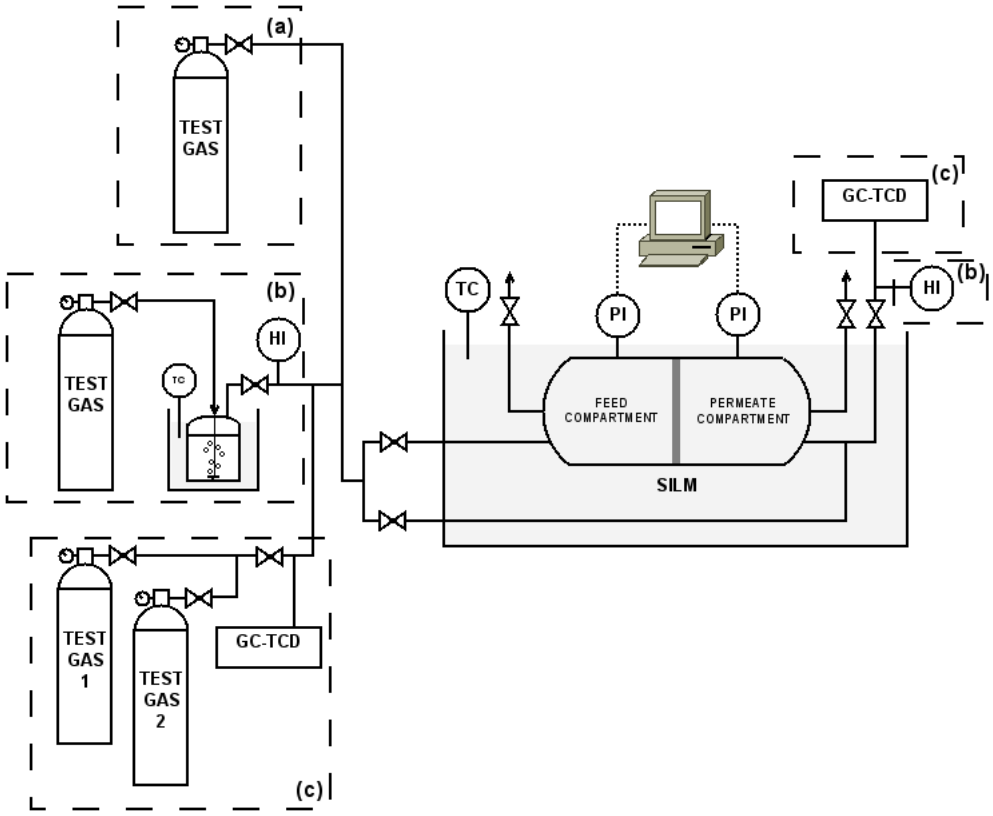

Figure 5.3: Experimental set-up for measuring the permeability of the SILMs (a) for a single gas, (b) for mixed gas/water vapour, and (c) for gas mixtures. TC - Temperature Controller; HI - Humidity Indicator; PI - Pressure Indicator; GC-TCD – Gas Chromatograph - Thermal Conductivity Detector.

5.3.4.2 Humidified gas permeability

In order to evaluate the effect of water vapour content in a gas stream, humidified gas permeability experiments were carried out. Fig. 5.3b shows the mixed gas water vapour permeation set-up designed for these measurements. A gas/water vapour mixture is generated by sparging a selected gas in a reservoir filled with water, which is maintained at a set-point temperature using a thermostatic bath (Haake, model C10, Germany). Then, this gas stream enriched in water vapour enters in both compartments of the permeation cell. The permeation cell is the same as used in the experiments which determined the permeability of SILMs to pure gases, shown in Fig. 5.3a. The gas/water vapour permeability was determined by pressurizing the feed compartment (up to 0.7 bar) with the humidified gas followed by the measurement of the pressure change in both compartments over time, using two pressure transducers. The gas stream humidity before entering in the feed compartment and in the output permeate stream was determined using an humidity indicator (HMI41 Indicator and HMP42 Probe, Vaisala, Finland), which uses an operating principle based on changes in the capacitance of the sensor as its thin polymer film absorbs water molecules in the atmosphere or in an environment with other gases. These measurements were performed at a constant temperature of 30 °C. The effect of the water vapour present in the pure gases (N_2, CH_4 and CO_2) on their permeability and on the selectivity towards CO_2/N_2 and CO_2/CH_4 gas pairs was determined. The membrane stability was evaluated gravimetrically, weighing the membrane before and after each experiment.

5.3.4.3 Gas mixture permeability

Mixed-gas permeation measurements were performed in the experimental set-up shown in Fig. 5.3c, at a constant temperature of 30 °C, for CO_2/N_2 and CO_2/CH_4 binary mixtures using equal partial pressures of both gases. Gas mixture tests were performed by mixing the required gases before entering the feed compartment. Then, the gas mixture was admitted in both compartments of the permeation cell, which was the same as used in the previous experiments. The gas mixture permeability was determined by pressurizing the feed compartment (up to 0.7 bar) with the gas mixture, following the pressure change in both compartments over time using two pressure transducers. Samples from the feed and permeate compartments were collected in the beginning and at the end of the experiment, and their gas composition analysed in a Trace GC Ultra, Thermo Electron Corporation, USA, with a TCD detector and a CarboxenTM 1010 PLOT fused silica capillary column, Supelco, USA.

5.3.5 Calculation methods

The permeability of a pure gas through a membrane is calculated from the pressure data obtained from both compartments (feed and permeate) shown in Fig. 5.3 according to the following equation [11]:

$$\frac{1}{\beta}\ln\left(\frac{\left[p_{feed}-p_{perm}\right]_0}{\left[p_{feed}-p_{perm}\right]}\right)=\frac{1}{\beta}\ln\left(\frac{\Delta p_0}{\Delta p}\right)=P\frac{t}{l} \tag{5.1}$$

where p_{feed} and p_{perm} are the pressures in the feed and permeate compartments (Pa), respectively, P is the membrane permeability ($m^2\ s^{-1}$), t is the time (s), and l is the membrane thickness (m). The geometric parameter β (m^{-1}) is characteristic of the geometry of the cell shown in Fig. 5.3, and is given by

$$\beta = A\left(\frac{1}{V_{feed}} + \frac{1}{V_{perm}}\right) \tag{5.2}$$

where A is the membrane area (m^2), and V_{feed} and V_{perm} are the volumes of the feed and permeate compartments (m^3), respectively. The data can be plotted as $1/\beta \cdot \ln\left(\Delta p_0/\Delta p\right)$ versus t/l, and the gas permeability values are obtained from the slope of this representation.

The ideal selectivity ($\alpha_{A/B}$) can be determined by dividing the permeabilities of two different pure gases (A and B). The selectivity can also be expressed by the solubility (S) and diffusion (D) contribution of each gas:

$$\alpha_{A/B} = \frac{P_A}{P_B} = \frac{S_A D_A}{S_B D_B} \tag{5.3}$$

In the gas mixture experiments, the selectivity ($\alpha_{A/B}$) is given by the equation:

$$\alpha_{A/B} = \frac{y_A/x_A}{y_B/x_B} \tag{5.4}$$

where y_A and y_B are mole fractions of gases A and B in the permeate compartment, respectively, and x_A and x_B are mole fractions of gases A and B in the feed compartment, respectively.

5.4 Results and Discussion

5.4.1 Stability of SILMs

In order to assess the stability of the SILMs developed and to proceed to the selection of the best membrane support, different RTILs were immobilised within two distinct polymeric membranes – hydrophilic PVDF and hydrophobic PVDF. The

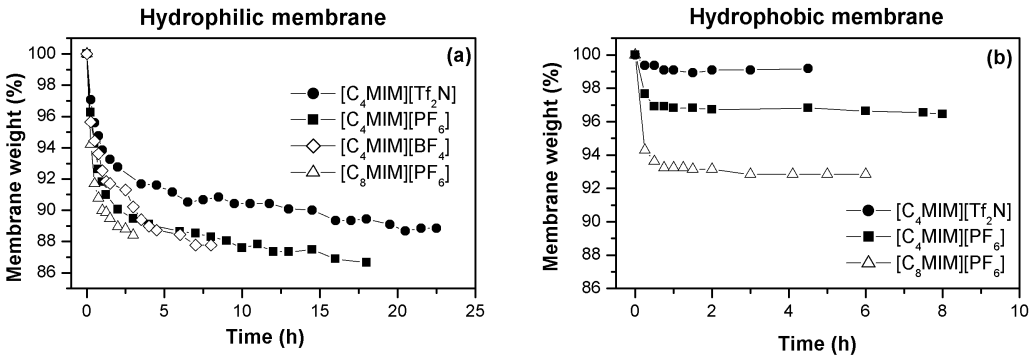

Figure 5.4: Relative membrane weight in (a) hydrophilic, and (b) hydrophobic membranes immobilized with different RTILs as a function of time. Applied pressure difference: 1 bar.

membrane weight as a function of time is represented in Fig. 5.4a and Fig. 5.4b, for the different RTILs immobilized in the hydrophilic and hydrophobic membranes, respectively, for a N_2 applied pressure of 1 bar. It is assumed that the membrane weight loss is only due to the loss of the RTIL immobilised within the membrane material.

In Fig. 5.4a and 5.4b a different behaviour is observed regarding the membrane weight as a function of time for situations where the RTILs are immobilised either in a hydrophilic or in a hydrophobic support. For the hydrophilic support it is observed a sharp initial decrease of weight, followed by a less pronounced weight loss, never reaching a stable value, at least for the time periods studied and for the applied pressure difference of 1 bar. Regarding the hydrophobic support, an initial decrease of weight is observed, which may be mainly associated to a removal of excess of RTIL at the surface of the membrane, followed by a stabilisation in the amount of RTIL within the membrane pores. Also, the hydrophilic membrane looses more

RTIL (11–13 %) than the hydrophobic one (1.5-7 %), at 1 bar of applied pressure.

During these experiments, the flux of N_2 was also measured (results not shown) and, with the exception of the hydrophilic membrane immobilised with the ionic liquid [C_8MIM][PF_6], the N_2 flux was very low (less than 0.01 mL/min). Since this ionic liquid is the most hydrophobic one, the high value of membrane weight loss and N_2 flux observed may be due to a possible weak interaction between the hydrophilic membrane support and the hydrophobic ionic liquid resulting in the fact that the membrane pores may not be completely filled with the RTIL.

The results shown in Fig. 5.4a and Fig. 5.4b also suggest that the membranes immobilized with the ionic liquid [C_4MIM][Tf_2N] seem to be more stable, since they present a lower value of weight loss and achieve a stable weight more rapidly. In order to further explore these observations, Fig. 5.5a and Fig. 5.5b represent the membrane weight loss as a function of time for different applied pressures (up to 2 bar) for, respectively, the hydrophilic and hydrophobic membranes immobilized with [C_4MIM][Tf_2N].

In Fig. 5.5 a decrease in the membrane weight is observed for the hydrophilic support for all the applied pressure differences. However at 2 bar this decrease is even more drastic indicating a possible SILM failure due to the loss of RTIL. Regarding the hydrophobic support, even though in the first hour a slight decrease in the membrane weight is observed, it reaches afterwards a stable value for pressures differences up to 1.5 bar. However, at 2 bar a severe decrease in the membrane weight was observed. This pressure value may have exceeded the breakthrough pressure associated to the surface tension of the RTIL within the membrane pores.

Even though the differences regarding the nature of support, in terms of their hydrophobicity, are not very large, as can be observed in the contact angles val-

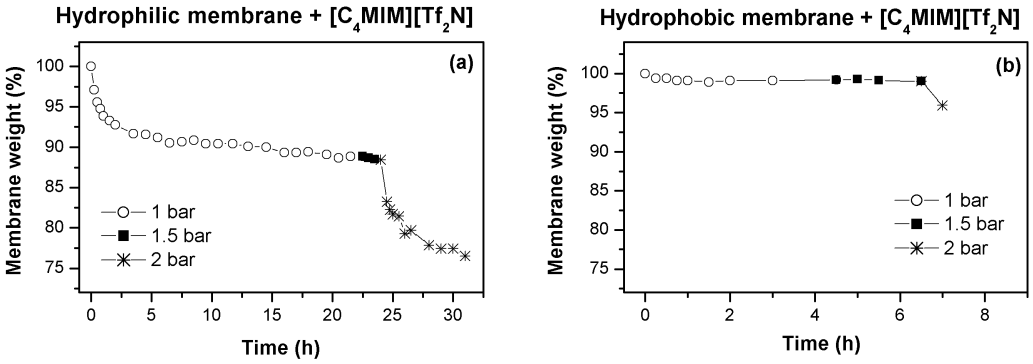

Figure 5.5: Relative membrane weight in (a) hydrophilic, and (b) hydrophobic membranes immobilized with $[C_4MIM][Tf_2N]$ as a function of time, for different applied pressures.

ues present in Table 5.1, all results indicate that the SILMs based on the more hydrophobic support are more stable than those based on the hydrophilic support. Therefore, the subsequent experiments presented in this paper concern only the hydrophobic support.

5.4.2 Single gas permeation results

The effect of using distinct RTIL cations of different alkyl chain length, and distinct anions, on the membrane permeability and selectivity was studied for the pure gases H_2, O_2, N_2, CH_4 and CO_2. In the gas permeation experiments, a maximum weight loss between 0.01 % and 0.05 % was obtained for all membranes tested. These low values indicate that these membranes retained the RTIL immobilised and that they may be considered stable at the tested pressure difference (0.7 bar).

As previously mentioned, all the permeability values were calculated according to Equation 5.1, taking into account the pressure data from the feed and permeate

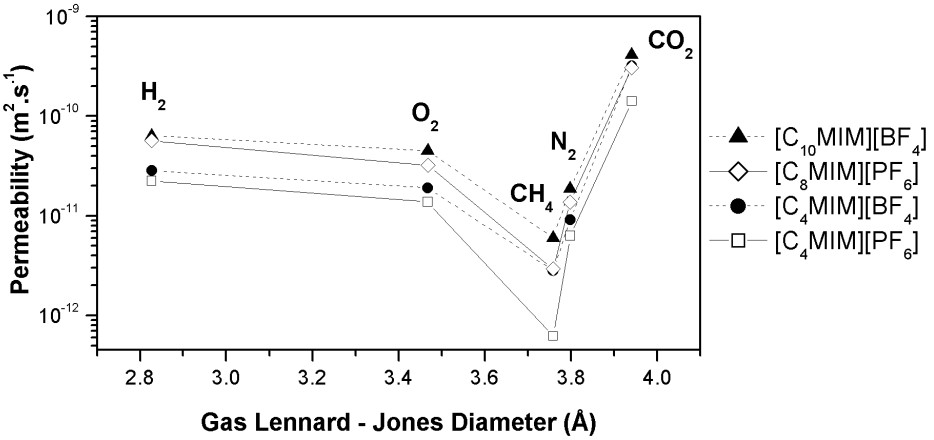

Figure 5.6: Permeability of the SILMs as a function of the gas Lennard-Jones diameter.

compartments, the thickness of the membrane and the geometry of the cell used.

5.4.2.1 Effect of the RTIL cation

The permeability of the SILMs prepared with the hydrophobic support and four different RTILs was measured for the different gases. The RTILs studied were $[C_4MIM][PF_6]$, $[C_8MIM][PF_6]$, $[C_4MIM][BF_4]$ and $[C_{10}MIM][BF_4]$. These RTILs were selected in order to study which is the effect on the gas permeability of using ionic liquids having the same anion (in this case $[BF_4]$- and $[PF_6]^-$) but different alkyl chain lengths of the imidazolium cation. The permeability obtained for the different SILMs is represented in Fig. 5.6 as a function of the Lennard-Jones diameter of each gas [45, 112].

In polymeric membranes, the high permeability values observed for H_2, which is a small molecule, are normally attributed to its high diffusivity, while the high per-

meability towards CO_2 is normally attributed to its high solubility due to a stronger interaction with the polymer matrix. Regarding the low permeability of N_2 it may be attributed to its relatively low diffusivity and low solubility [99]. The same trend of permeability values was observed for the SILMs tested: P_{CO_2}>P_{H_2}> P_{O_2}>P_{N_2} >P_{CH_4}.

The variation of the permeability for the different gases studied, with the number of carbons of the imidazolium cation, for the anions $[BF_4]^-$ and $[PF_6]^-$, is represented in Fig. 5.7.

An increase in the permeability values with an increase in the alkyl chain length of the RTIL cation is observed for all gases studied (H_2, O_2, N_2, CH_4 and CO_2) and for both RTIL anions ($[BF_4]^-$ and $[PF_6]^-$).

The relation $P = D \times S$, where P is the gas permeability, and S and D are, respectively, the solubility and diffusivity of the gases in the RTIL, enables the determination of one of them if the other may be estimated. Morgan et al. [113] developed a correlation for the diffusivity of gases in imidazolium ionic liquids at 30 °C which is shown in Equation 5.5,

$$D_{12} = 2.66 \times 10^{-3} \frac{1}{\mu_2^{0.66\pm0.03} \overline{V_1}^{1.04\pm0.08}} \tag{5.5}$$

where D_{12} is the diffusivity of gases in RTILs ($cm^2\ s^{-1}$), μ_2 is the RTIL viscosity (mPa s) at 30 °C, and $\overline{V_1}$ is the gas molar volume ($cm^3\ mol^{-1}$). Assuming that gas transport occurs only through the RTIL, an estimation of the gas solubility can be obtained with the values of the gas permeability obtained experimentally (P) and estimating D by Equation 5.5. Table 5.3 shows for each pure gas, the effect of the alkyl chain length of the RTIL cation, on the experimental permeabilities measured. The permeability ratios for the pairs C_8MIM^+/C_4MIM^+ and $C_{10}MIM^+/C_4MIM^+$, with

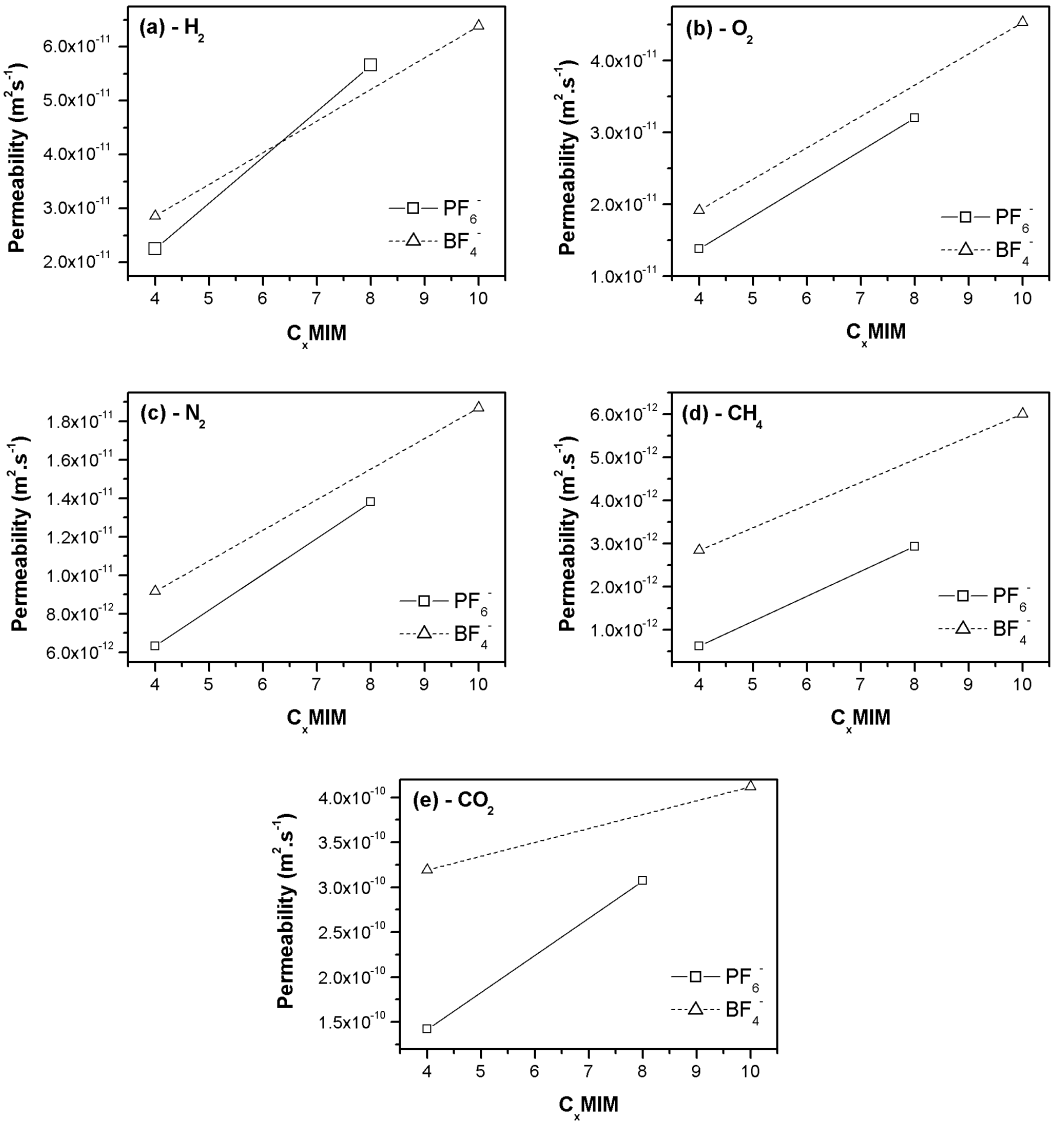

Figure 5.7: Gas permeability of the SILMs prepared with the hydrophobic support and the RTILs $[C_4MIM][PF_6]$, $[C_8MIM][PF_6]$, $[C_4MIM][BF_4]$, $[C_{10}MIM][BF_4]$, as a function of the number of carbons of the imidazolium cation (a) H_2; (b) O_2; (c) N_2; (d) CH_4; and (e) CO_2.

Table 5.3: Permeability, diffusivity and solubility ratios for the pairs C_8MIM^+/C_4MIM^+ and $C_{10}MIM^+/C_4MIM^+$ with the respective anions $[PF_6]^-$ and $[BF_4]^-$

	Gas				
	H_2	O_2	CH_4	N_2	CO_2
	Permeability ratio				
C_8MIM^+/C_4MIM^+ $[PF_6]^-$	2.5	2.3	4.7	2.3	2.2
$C_{10}MIM^+/C_4MIM^+$ $[BF_4]^-$	2.2	2.4	2.1	2.0	1.3
	Diffusivity ratio				
C_8MIM^+/C_4MIM^+ $[PF_6]^-$	0.6	0.6	0.6	0.6	0.6
$C_{10}MIM^+/C_4MIM^+$ $[BF_4]^-$	0.5	0.5	0.5	0.5	0.5
	Solubility ratio				
C_8MIM^+/C_4MIM^+ $[PF_6]^-$	4.4	4.1	8.3	3.9	3.8
$C_{10}MIM^+/C_4MIM^+$ $[BF_4]^-$	4.9	5.2	4.6	4.4	3

the respective anions $[PF_6]^-$ and $[BF_4]^-$, are shown. Additionally, Table 5.3 shows also a similar analysis for the diffusivity ratios (calculated with equation 5.5) and for the solubility ratios, determined by dividing the experimental permeability values by the calculated diffusivities.

It is observed, from the analysis of Table 5.3, that gas permeability increases approximately by a factor of 2 with an increase in the cation alkyl chain length, for both anions ($[PF_6]^-$ and $[BF_4]^-$). An exception appears to be the CH_4 permeability obtained for the anion $[PF_6]^-$. Additionally, when estimating the diffusivities by Equation 5.5, a decrease by a factor close to 2 was obtained, due to higher viscosity of the corresponding RTILs. Therefore the resulting estimated solubility has to increase by a factor of 4, in order to explain the experimentally determined permeability values. These results are extremely interesting because they show that, even though the gas

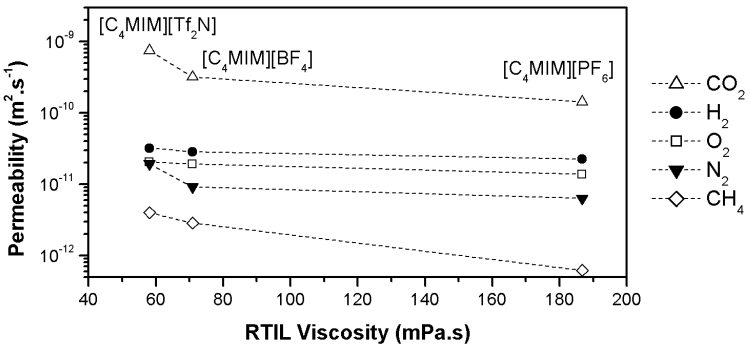

Figure 5.8: Permeability of the SILMs prepared with the hydrophobic support and the RTILs $[C_4MIM][Tf_2N]$, $[C_4MIM][BF_4]$, $[C_4MIM][PF_6]$, as a function of the RTIL viscosity.

diffusivity decreases for the more viscous RTILs, a comparatively higher increase in solubility leads to an overall increase in permeability. Therefore, solubility effects seem to play a more important role in the transport of gases, for RTILs with different cation alkyl chain lengths. Additionally, it is interesting to notice that this solubility effect seems to be identical for all gases studied.

5.4.2.2 Effect of the RTIL anion

The effect of using RTILs based on the $[C_4MIM]^+$ cation, but with different anions ($[Tf_2N]^-$, $[BF_4]^-$ and $[PF_6]^-$) was also evaluated. The permeability of SILMs is represented as a function of the RTIL viscosity as shown in Fig. 5.8. For all gases studied, the permeability is always higher for the RTIL that contains the $[Tf_2N]^-$ anion, which leads to the lowest RTIL viscosity.

Following the same approach used before (Table 5.3), in Table 5.4 it is shown the impact of the RTIL anion on each gas permeability, diffusivity and solubility. More

Table 5.4: Permeability, diffusivity and solubility ratios for the pair $[Tf_2N]^-/[BF_4]^-$

	Gas				
	H_2	O_2	CH_4	N_2	CO_2
	Permeability ratio				
C_4MIM^+ $[Tf_2N]^-/BF_4^-$	1.1	1.1	1.4	2.1	2.3
	Diffusivity ratio				
C_4MIM^+ $[Tf_2N]^-/BF_4^-$	1.1	1.1	1.1	1.1	1.1
	Solubility ratio				
C_4MIM^+ $[Tf_2N]^-/BF_4^-$	1	1	1.2	1.9	2.1

specifically, the ratios obtained for the pair $[Tf_2N]^-/[BF_4]^-$ are shown in this table.

It is observed that the solubility ratio for the non-interacting gases (H_2 and O_2) is very close to 1 and, therefore, for these gases the slight change observed in their permeability can be totally attributed to a decrease of their diffusivity. For more strongly interacting gases, such as N_2 and CO_2, their solubility is more affected, and the resulting permeability ratio clearly exhibits this dependence. It is interesting to notice, in contrast with the analysis of the effect of the RTIL cation alkyl length, how different anions impact differently on the solubility of the various gases, with the corresponding effect on their permeability.

It is also noticed that for the three RTILs tested, the gas permeability decreases in the order as observed in Fig. 5.6: P_{CO_2}>P_{H_2}> P_{O_2}>P_{N_2} >P_{CH_4}. The fact that, for all SILMs studied, the permeability of CO_2 is more than one order of magnitude higher than that of N_2 and CH_4, opens the possibility of using these membranes for CO_2 separations.

Table 5.5: Ideal Selectivities (CO_2/N_2 and CO_2/CH_4) obtained for the tested SILMs

Membrane support	RTIL	CO_2/N_2	CO_2/CH_4
Hydrophobic	$[C_4MIM][PF_6]$	23 ± 0.5	228 ± 1.5
	$[C_4MIM][BF_4]$	35 ± 0.2	113 ± 1.6
	$[C_4MIM][Tf_2N]$	39 ± 0.1	187 ± 1.7
	$[C_8MIM][PF_6]$	23 ± 0.5	105 ± 1.5
	$[C_{10}MIM][BF_4]$	22 ± 0.1	69 ± 1.3

5.4.2.3 Ideal Selectivities

Table 5.5 shows the CO_2/N_2 and CO_2/CH_4 ideal selectivities for the membranes tested. The ideal selectivity was calculated taking into account the ratio of the permeabilities of pure gases (Equation 5.3). It was observed that the selectivity of SILMs towards CO_2 was very high when compared to that of N_2 and CH_4.

In order to compare the ideal selectivities obtained in this study with data available in the literature, the (CO_2/N_2 and CO_2/CH_4) selectivity as a function of the CO_2 permeability is represented in Fig. 5.9.

In Fig. 5.9a it is also represented the present upper bound correlation for CO_2/N_2 separation and in Fig. 5.9b it is represented the present as well as the prior upper bound correlations for CO_2/CH_4 separation. These upper bound correlations were obtained by Robeson et al. [12] from data available in the literature. Therefore, data points above this line may be considered as an improvement over the results published so far. Regarding the CO_2/N_2 separation (Fig. 5.9a), it is observed that the results obtained in this work are generally bellow those available in the literature. However, for one specific SILM – the hydrophobic support immobilised with $[C_4MIM][Tf_2N]$ – the result obtained is close to those of other SILMs from the liter-

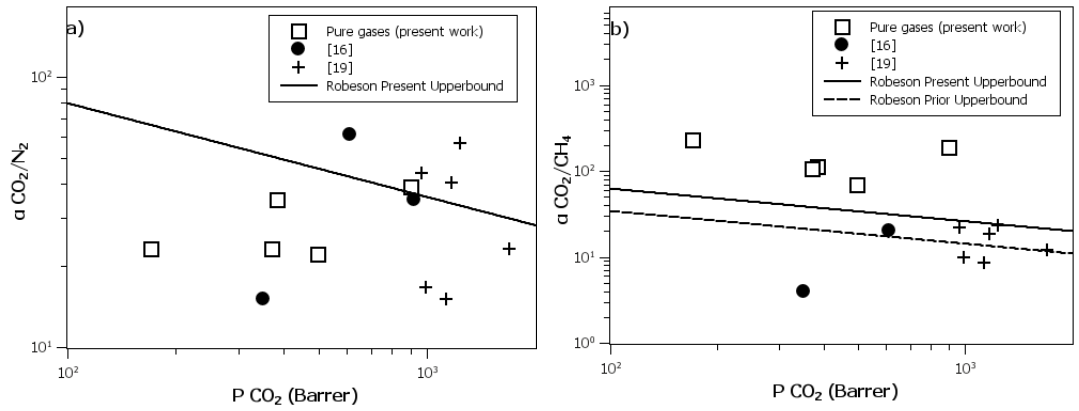

Figure 5.9: (a) CO_2/N_2 selectivity as a function of CO_2 permeability, and (b) CO_2/CH_4 selectivity as a function of CO_2 permeability (1 Barrer = 10^{-10} cm^3 (STP)cm cm^{-2} s^{-1} cmHg^{-1}).

ature [106, 109] and close to the Robeson upper bound correlation. Regarding the CO_2/CH_4 separation, all results obtained in this work are clearly above the upper bound.

5.4.3 Gas streams containing water vapour

It is known that the performance of supported ionic liquid membranes is affected by the presence of water [101, 102]. Therefore, the effect of water vapour in gas streams of CO_2, N_2 and CH_4 was determined and compared with the permeability obtained with pure gases. The RTILs selected were [C_4MIM][PF_6], [C_4MIM][Tf_2N], and [C_8MIM][PF_6], because the hydrophobic membranes immobilized with these RTILs exhibit higher values of ideal selectivity for CO_2/N_2 and CO_2/CH_4 (see Table 5.5). Although the hydrophobic support immobilised with [C_4MIM][BF_4] also presents high values of ideal selectivity, this RTIL was not include in this study because it is completely miscible in water.

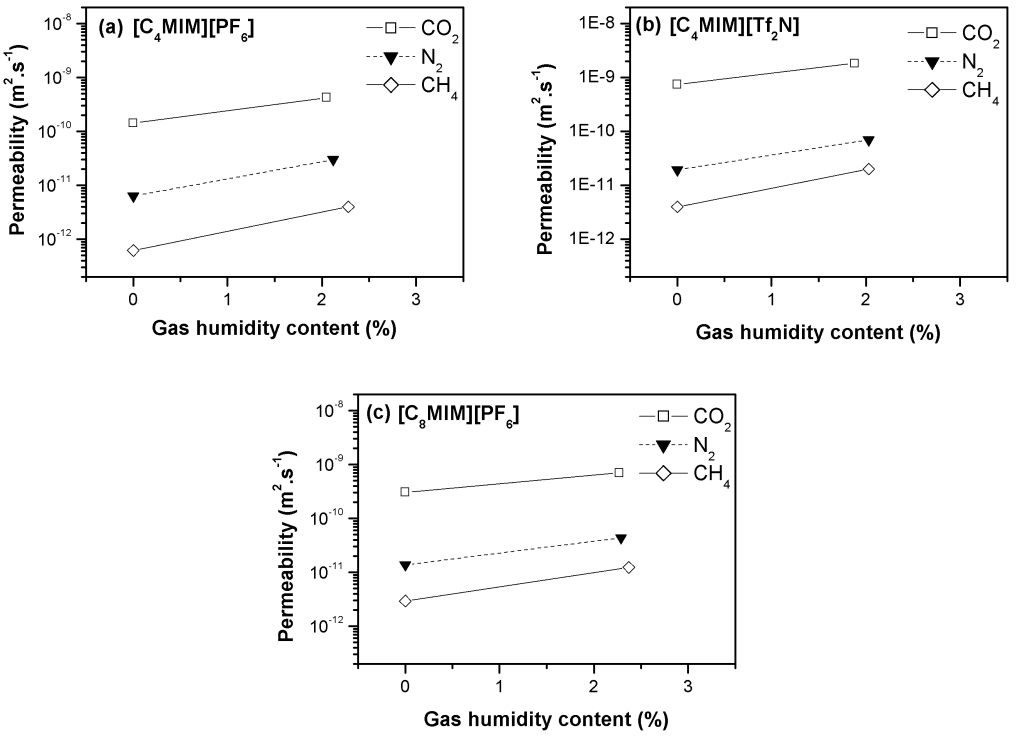

Figure 5.10: CO_2, N_2 and CH_4 gas permeability as a function of the gas humidity content for the hydrophobic support immobilized with (a) $[C_4MIM][PF_6]$, (b) $[C_4MIM][Tf_2N]$, and (c) $[C_8MIM][PF_6]$.

The CO_2, N_2 and CH_4 gas permeabilities as a function of the gas humidity content (w/w) for the hydrophobic support immobilized with $[C_4MIM][PF_6]$, $[C_4MIM][Tf_2N]$, and $[C_8MIM][PF_6]$ are shown in Fig. 5.10, where 0 % gas humidity content corresponds to the pure gas permeability measured, while values close to 2 % correspond to the gas humidity content (mass of water vapour/ mass of dry gas) obtained at 30 °C, using the experimental procedure previously described in section 5.3.4.2.

For all SILMs and gases tested (CO_2, N_2 and CH_4) an increase in the permeability

with an increase in the gas humidity content is observed. Considering that the same supporting membrane is used, and the only variable is the water vapour content of the gas stream, these results indicate that the observed increase in gas permeability should be only associated to an increase in the water content of the ionic liquid. The formation of water micro-domains inside the ionic liquid provides a new environment for the transport of gases which is less selective than the "dry" RTIL environment used previously. On the other hand, the various gases will diffuse more rapidly through these less selective aqueous micro-domains than through the RTILs environment, which are much more viscous.

It can also be observed that, for each RTIL, the permeability of CH_4 is more affected by the presence of water vapour (permeability values increase between 4.2 to 6.4 times), when comparing with the permeabilities towards N_2 (which values increase between 3.2 to 4.8 times) and CO_2 (which values increase between 2.3 to 3 times). These results suggest that the water vapour content has a more important effect on the permeability of gases more affected by diffusion (CH_4), in contrast with gases whose permeability is essentially controlled by solubility (CO_2).

The results obtained seem also to indicate that gas permeability increases more for the most hydrophilic RTILs [114] ([C_4MIM][PF_6]>[C_4MIM][Tf_2N]>[C_8MIM][PF_6]). To better understand this effect, the increase in the permeability values (ratio between the humidified gas permeability, P_H, and the pure gas permeability, P_0) for the different SILMs studied is shown in Table 5.6. This behaviour may be expected because more hydrophilic RTILs can absorb higher amounts of water, at faster rates, leading to larger water clusters, which will allow higher diffusivities of the gases.

A comparison between the CO_2/N_2 and CO_2/CH_4 ideal selectivities obtained with both dry and humidified gases is shown in Table 5.7. It can be observed that

Table 5.6: Ratio (P_H/P_0) between the humidified gas permeability, P_H, and the pure gas permeability, P_0, for the different SILMs

Membrane support	RTIL	CH_4	N_2	CO_2
Hydrophobic	$[C_4MIM][PF_6]$	6.4 ± 0.02	4.8 ± 0.04	3.0 ± 0.02
	$[C_4MIM][Tf_2N]$	5.0 ± 0.02	3.7 ± 0.01	2.5 ± 0.01
	$[C_8MIM][PF_6]$	4.2 ± 0.01	3.2 ± 0.08	2.3 ± 0.01

Table 5.7: CO_2/N_2 and CO_2/CH_4 ideal selectivities obtained with dry and humidified gases

RTIL	CO_2/N_2		CO_2/CH_4	
	Dry	Humidified	Dry	Humidified
$[C_4MIM][PF_6]$	23 ± 0.5	14 ± 0.4	228 ± 1.5	107 ± 2
$[C_4MIM][Tf_2N]$	39 ± 0.1	26 ± 0.3	187 ± 1.7	92 ± 3
$[C_8MIM][PF_6]$	23 ± 0.5	16 ± 0.5	105 ± 1.5	57 ± 1.2

for all the SILMs the selectivity CO_2/N_2 and CO_2/CH_4 decreases for the humidified gases. As previously discussed, this decrease in selectivity can be attributed to the formation of water clusters, which constitute a less selective microenvironment for the transport of gases. The CO_2/N_2 selectivity for the humidified gases is lower due to the fact that the permeability of N_2 is more affected than that of CO_2 when the gas stream is enriched with water vapour, and therefore the ratio of permeabilities (selectivity) decreases. The same behaviour is observed for the CO_2/CH_4 selectivity. It is also possible to observe that this variation in selectivity is more significant for the less hydrophobic ionic liquids, in this case the RTIL $[C_4MIM][PF_6]$.

This study shows that, even though SILMs are selective for CO_2, it is important to take into consideration the water content in the gas stream to be processed, and strategies for its prior removal if necessary. It has been shown that the water content

increases gas permeability but at the same time decreases selectivity. Therefore, in a long-term operation, it will affect the membrane stability due to water absorption by the RTIL, unless specific actions for water removal are taken.

5.4.4 Gas mixture permeation results

Gas mixture permeation experiments were carried out in order to measure gas permeabilities and determine the selectivities CO_2/N_2 and CO_2/CH_4 in gas mixtures, and also to compare these results with the experiments performed with pure gases. The RTILs studied were $[C_4MIM][PF_6]$, $[C_4MIM][BF_4]$, $[C_4MIM][Tf_2N]$, and $[C_8MIM][PF_6]$ because, as previously mentioned, the membranes immobilized with these RTILs exhibit higher values of CO_2/N_2 and CO_2/CH_4 ideal selectivities (please see Table 5.5).

A comparison between the CO_2/N_2 and CO_2/CH_4 selectivities obtained with pure gases (the so called ideal selectivities), with those obtained with mixed gases is shown in Table 5.8. It can be observed that, for all the SILMs, the selectivity towards CO_2/N_2 and CO_2/CH_4 obtained with gas mixtures is lower than that obtained with pure gases. Even though a decrease in the mixed-gas selectivity is observed when compared with the ideal selectivity, this variation is not significant. These results, necessary for process design, agree with observations reported by other authors [115], confirming that at low transmembrane pressure mixed-gas and ideal selectivities do not differ significantly.

The CO_2/N_2 and CO_2/CH_4 mixed-gas selectivity obtained as a function of the CO_2 permeability is shown in Fig. 5.11. For comparison purposes, ideal selectivities obtained in this work, as well as data available in the literature, are also included in

Table 5.8: CO_2/N_2 and CO_2/CH_4 ideal and mixed-gas selectivities obtained for the tested SILMs

RTIL	CO_2/N_2		CO_2/CH_4	
	Ideal	Mixed-gas	Ideal	Mixed-gas
$[C_4MIM][PF_6]$	23 ± 0.5	20 ± 1.6	228 ± 1.5	200 ± 1.5
$[C_4MIM][BF_4]$	35 ± 0.2	32 ± 0.1	113 ± 1.6	102 ± 0.6
$[C_4MIM][Tf_2N]$	39 ± 0.1	30 ± 0.5	187 ± 1.7	161 ± 0.5
$[C_8MIM][PF_6]$	23 ± 0.5	21 ± 0.5	105 ± 1.5	98 ± 0.5

the same figure. It is important to mention that both the pure and mixed-gas CO_2 permeabilities were obtained experimentally using two different analytical methods, one by the pressure decay method and the other using GC-TCD analysis, respectively, as explained in section 5.3.4. Even though two different methods were used, similar CO_2 permeability values were obtained.

A small decrease in the selectivity of mixed-gases compared to pure-gases, shown in Fig. 5.11, results also from a small decrease in CO_2 permeability when a gas-mixture is used. Even though the mixed-gas selectivities are slightly lower than the ideal selectivities for the SILMs tested, the analysis of Fig. 5.11 is similar to that of Fig. 5.9. For the CO_2/N_2 separation (Fig. 5.11a), the results obtained in this work are still located below the present Robeson upperbound. Regarding the CO_2/CH_4 separation (Fig. 5.11b), all the results obtained in this work are clearly above the upper bound, even when using gas mixtures, which represents a clear improvement.

For both separations (CO_2/N_2 and CO_2/CH_4) the SILM membrane that exhibited the best performance was the one with $[C_4MIM][Tf_2N]$ immobilised in the hydrophobic support. This RTIL is the one with a lower viscosity and also with the highest affinity for CO_2, when comparing with $[C_4MIM][PF_6]$ and $[C_4MIM][BF_4]$

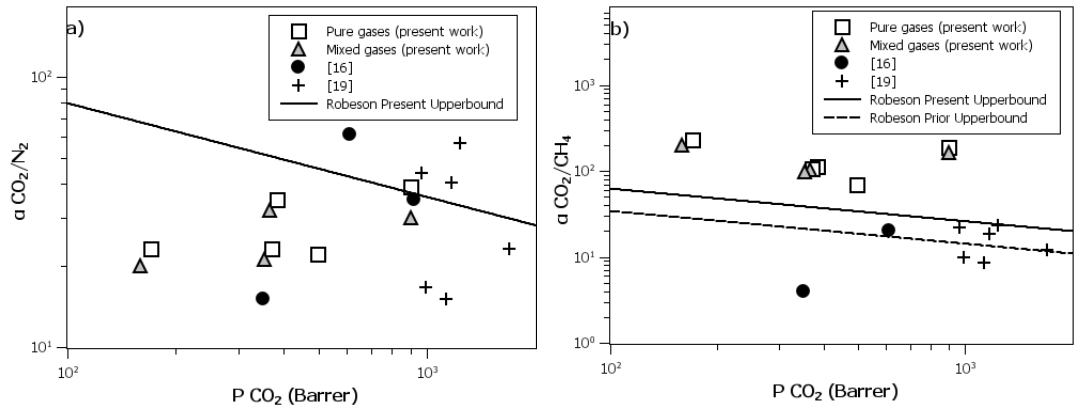

Figure 5.11: (a) CO_2/N_2 selectivity as a function of CO_2 permeability, and (b) CO_2/CH_4 selectivity as a function of CO_2 permeability (1 Barrer = 10^{-10} cm^3 (STP)cm cm^{-2} s^{-1} cmHg^{-1}).

[116]. Further improvement of SILMs for CO_2 separation shall involve the use of ionic liquids that present low viscosities in order to facilitate gas diffusion and high solubility for CO_2.

5.5 Closure

It has been shown that the supported ionic liquid membranes prepared with room temperature ionic liquids (RTILs) based on the 1-n-alkyl-3-methylimidazolium cation are stable, especially those based in the most hydrophobic support, possibly due to a better chemical affinity between the RTILs and the supporting membrane.

The effect of using different alkyl chain lengths of the RTIL cation, as well as different anions, on the pure gas permeability was studied. An increase in the gas permeability with an increase in the alkyl chain length of the RTIL cation was observed for all gases studied. The results obtained may be explained by solubility effects that

become more relevant as the alkyl chain length of the RTIL cation increases. The effect of using different RTIL anions on the permeability of gases was also evaluated and a decrease in permeability was observed with an increase of the RTIL viscosity. In this case, diffusivity effects seem to dominate for non-interacting gases (H_2 and O_2) while solubility effects dominate when more interacting gases (N_2 and CO_2) are used.

The pure gas permeation results have also show that the SILMs used in this work are extremely selective to CO_2 when compared with N_2 and CH_4. Moreover, small differences were observed in the gas mixtures permeabilities and selectivities for CO_2/N_2 and CO_2/CH_4 when compared with ideal ones at the low pressures tested, which may indicate a potential application of using SILMs for selective removal/recovery of CO_2 from gas stream. All results suggest that SILMs are selective for CO_2 separations, especially for CO_2/CH_4 separations where the results obtained in this work are above the ones reported (Robeson upper bound correlation). Still, an important parameter that it is necessary to take into account is the presence of water vapour in the gas stream. The results shown in this work indicate that the presence of water vapour in a gas stream increases the SILMs gas permeability but decreased their CO_2/N_2 and CO_2/CH_4 selectivity significantly, when comparing with a dry gas stream. This decrease in selectivity is due to the formation of water clusters inside the membrane, being this effect more significant for the less hydrophobic RTILs.

Chapter 6

Conclusions and Future Work

Similarly to the thesis structure, its achievements and conclusions may be divided in two different sections: the study of the incorporation of ionic liquid cations in Nafion membranes and their characterisation; and the study of the immobilisation of ionic liquids in porous membranes and gas permeation studies.

6.1 Study of the incorporation of ionic liquid cations in Nafion membranes and their characterisation

In this thesis a new approach for modifying Nafion membranes with ionic liquid cations was developed, as well as the procedure followed to determine their properties, identified as most important for an a-priori characterisation of the modified Nafion membranes.

The method developed for incorporating ionic liquid cations in Nafion membranes at a controllable degree allowed obtaining tailor-made membranes, and an effort in this thesis was made for understanding the physicochemical properties

of these modified membranes with different degrees of incorporated cation. The quantification of the incorporation degree with time was made possible by performing measurements of the pH and of the conductivity of the solution that contains the ionic liquid cation before and after contacting with the Nafion membrane. In the different studies performed, the starting membrane was always a Nafion-112 membrane in the protonated form. At equilibrium, the incorporation degree obtained was also found to be dependent from the type of IL cation studied and whether an aqueous solution was necessary to be prepared for its incorporation in the membrane according to the source of IL cation (solid or liquid at room temperature).

A validation on whether the IL cations were indeed incorporated inside the Nafion membrane was made by XPS (X-ray photoelectron spectroscopy). This technique was used as "ex-situ" to follow the incorporation of the IL cation, and the results obtained were in agreement with the ones obtained with the measurements of pH and conductivity. Additionally, when the modified Nafion membranes were in equilibrium, the distribution of the IL cations in the membrane surface layer (between 2.5 nm and 9.3 nm) was evaluated using XPS, and the results suggested a uniform cation distribution inside the membrane.

Electrical Impedance Spectroscopy (EIS) measurements were performed to evaluate the evolvement of the electric properties of the modified membranes with the cation incorporation degree. EIS was used as an "in-situ" monitoring technique to study the incorporation of the IL cations inside Nafion. The membrane resistance and capacitance for each modified Nafion membrane was determined by using mathematical models of equivalent electrical circuits, and it was found that these electrical parameters were strongly dependent from the type and incorporation degree of the IL cation incorporated. In a first analysis, the membrane resist-

ance increases with an increase in the concentration of the IL inside the membrane structure, and when comparing different membranes in equilibrium, the membrane resistance seemed to be dependent of the size of the IL cation incorporated. For some membranes such as Nafion/DTA^+ and Nafion/CTA^+ it was possible to estimate a proton mobility value, and it was observed that the proton mobility decreases with an increase in the alkyl chain length of the IL cation incorporated. However, for the other membranes studied, Nafion/$TMPA^+$, Nafion/$BMIM^+$ and Nafion/$OMIM^+$, the membrane resistance and consequently the proton mobility was not possible to determine by EIS. In this case, the results were compared with a similar system Nafion-112/HCl and an indication that the Nafion/$TMPA^+$ membrane apparently shows a higher ionic conductivity was obtained.

However, the discussion towards the results obtained regarding the modified Nafion/IL cation membranes electric properties should not be only restricted to the size of the IL cations incorporated. One important parameter, or perhaps the most important one, when studying these modified Nafion/IL cation membranes is the presence of water and its degree of structuring. All the membranes, with the exception of Nafion/$TMPA^+$, have a high water content after IL cation incorporation. The rate of water loss with increasing temperatures, up to 210 °C, was determined by thermogravimetric analysis, and for all the modified Nafion membranes higher ability for water retention was obtained when compared with an unmodified Nafion membrane. The ease with which the membranes loose their water content was directly related with their water degree of structuring. The modified Nafion membranes seems to have a higher degree of water structuring, possibly due to the fact that the water present is deeply involved in solvation of the IL cation, resulting in more stable membranes. In fact, the stability of modified Nafion/IL cation mem-

branes when compared with an unmodified Nafion membrane at high temperatures was also confirmed by a different characterisation technique - proton NMR relaxometry. The Nafion/$TMPA^+$ membrane apparently was again the most attractive membrane, due to its stability at high temperatures. Even though the ionic conductivity of this membrane is higher and it is much more stable at high temperatures than all the membranes studied, it was necessary to determine whether the proton mobility is affected by this modification.

Different molecular motions inside the modified membranes were assessed through proton NMR relaxometry studies, as well as indications of the proton mobility within the membrane structure. Nafion/IL cation membranes may have two distinct environments, regarding their levels of confinement which includes not only different sizes of cavities but also different degrees of structuring of the protons associated either with the IL cations and water. Unlike what was observed with the EIS measurements, where it was not possible to estimate a proton mobility value for all the membranes studied, using NMR relaxometry studies, a diffusion coefficient of all the protons present in the membrane for all the membranes was possible to be estimated. The proton mobility values obtained by EIS can not be directly compared with the self-diffusion coefficient obtained by NMR relaxometry. In one case, the proton mobility given by EIS measurements is obtained for an electric potential difference of 0.01 V (Table 2.3), and in the case of NMR studies it is obtained a self-diffusion coefficient of all the protons in the absence of an electric field (Table 3.3). Assuming that an electric charge of 1 volt is applied to the modified membrane, and comparing the results shown in both tables (2.3 and 3.3), and considering that, by NMR measurements a global diffusion coefficient is obtained, the values determined by both characterisation techniques are in the same order of magnitude.

By doing this exercise, and considering the diffusion coefficient value obtained by NMR for the Nafion/$TMPA^+$ membrane, it is observed that even though its stability at high temperatures is very attractive, the water within the membrane must be highly structured in such a way that the proton mobility is reduced by one order of magnitude when compared with the other membranes studied.

The modification of Nafion membranes by incorporation of IL cations introduces in the membrane certain characteristics that may make their potential use in fuel cells very attractive. On the one hand membranes with a high stability at high temperatures are obtained, and this stability is a result of a higher water degree of structuring; and on the other hand, by changing the type of IL cation as well as the degree of incorporation it is possible to obtain membranes with an proton mobility that may be sufficient for fuel cells applications. A possible application for these membranes may be in direct methanol fuel cells. The methanol crossover obtained for these modified membranes was reduced between 60 to 600 times, when compared with a Nafion membrane in the protonated form. Additionally, the transport of typical gases that may be present in a methanol fuel cell or in a hydrogen fuel cell is clearly reduced in these modified membranes. This reduction in both the methanol and gas crossover is also directly related with the water structuring inside the membrane after the introduction of the IL cations.

The first part of this thesis shows that it is possible to design Nafion membranes incorporated with IL cations, at controllable degrees. The introduction of the IL cations has implications in its water content and respective water structuring. This modification in the water structuring will have direct influence in the electric properties, proton mobility, methanol crossover, gas crossover and the increase in stability at high temperatures of these modified membranes. However, the work de-

veloped in this thesis was not sufficient to clearly answer to the question if these modified Nafion/IL cation membranes can be used in fuel cells applications. In order to accomplish this objective it is necessary to find the best compromise between the stability at high temperatures, the reduction in the methanol or other gases transport and possible reductions in the proton mobility, and testing these membranes in a "real fuel cell" at high temperatures to evaluate their "real" potential.

6.2 Study of the immobilisation of ionic liquids in porous membranes and gas permeation studies

The work developed in the second part of this thesis allowed to evaluate the potential of using SILMs for gas separations, more specifically for CO_2/N_2 and for CO_2/CH_4 separations.

The importance of the nature of the support used in the preparation and stability of supported ionic liquid membranes (SILMs) was determined, and one of the main observations was that the more hydrophobic support leads to more stable membranes.

Supported liquid membranes prepared with room temperature ionic liquids (RTILs) based on the 1-n-alkyl-3-methylimidazolium cation proved to be very selective to CO_2, in comparison with other gases, such as N_2 and CH_4. In particular, the results for CO_2/CH_4 separations obtained in this work are clearly above the ones obtained in the literature, either using pure gas or gas mixtures. In this thesis, more than determining the gas permeability values, an effort was made for understanding how different alkyl chain lengths of the RTIL cation or different anions used may

influence the permeability behaviour. Since the estimated solubility results indicated that the gas solubility is more affected by the different RTIL anions used, than with different alkyl chain length of the RTIL cation, one possible indication is to select RTILs anions with a high selectivity for CO_2. The diffusivity in also an important contribution for the permeability of the gases so, it is necessary to select RTILs which present a low viscosity.

An important factor that was also considered in this study was the influence of the humidified gas streams on the permeability and selectivity of SILMs. The results show that the gas permeability increases but the selectivity was clearly affected. Therefore, in a long-term operation, it may affect the membrane integrity due to water absorption by the RTIL, unless specific actions for water removal are taken.

Future research should focus on the study of the stability, permeability and selectivity of these SILMs at experimental conditions more close to the ones used in gas separation processes, namely pressure, temperature and gas composition.

6.3 Suggestions for Future Research

The results of this study can be improved and extended in several ways. The following recommendations for future work can be proposed.

Firstly, the Proton NMR relaxometry technique used for the work developed in this thesis can be further explored. Different measurements of T_1 (spin-lattice relaxation time) at different values of frequency should be performed for modelling purposes; especially measurements at low frequencies in order to try to estimate different sizes of cavities inside the membrane. Therefore, Proton NMR relaxometry can be used as tool for determining different clusters size, and in this way to understand

how the incorporation of IL cations influences the membrane microstructure, either with different concentration and/or different types of IL cation structure. It would be also interesting to repeat all the measurements performed with the NMR relaxometry, but in a presence of an electric field, to be able to estimate proton mobility values more comparable with the ones obtained with EIS. Moreover, additional experiments with deuterated water could help in the identification and discrimination of individual contributions of the protons associated with the IL cation or associated with the water present in the membrane and in this way, the diffusion coefficient or proton mobility determined could be ascribed to a specific group of protons. Molecular Dynamics studies could additionally help in obtaining a deeper insight on the microscopic phenomena taking place within the membrane material.

In order to evaluate the water degree of structuring inside the membrane and to confirm all the assumptions made in this thesis, Fourier Transform Infrared Spectroscopy (FTIR) may be used as a characterisation technique. In the literature [117–119] there are several references about the use of this characterisation technique to study the state of water inside Nafion membranes. Therefore, this technique may have the potential to be used in the characterisation of possible different states of water, induced by different concentrations of IL cation as well as different types of IL cations incorporated in the membrane.

Extended research is still needed in order to deepen our understanding of the phenomena taking place, in order to direct efforts for effective membrane design. Further work using methodologies for measurement of membrane properties at high temperatures is necessary aiming the assessment of the modified membranes potential application as polymer electrolyte membranes. The ionic conductivity, thermal stability, methanol and gas crossover of the modified membranes should

be determined at high temperatures, followed by experimental work of these membranes in fuel-cell operation for optimization purposes.

In what concerns the study of supported ionic liquid membranes for gas separations, several suggestions for improvement may be given: 1) testing the efficiency of SILMs in different operating conditions regarding specific separations: high pressures, high temperatures (up to 200 °C) and different compositions of binary gas mixtures, ranging from pure CO_2 to either pure N_2 or pure CH_4, depending on the separation envisaged; 2) testing gases with different humidity contents and perform long-term experiments.

Bibliography

[1] J S Lee, N D h Quan, J M Hwang, S D Lee, H Kim, H Lee, and H S Kim. Polymer Electrolyte Membranes for Fuel Cells. *Journal of Industrial and Engineering Chemistry*, 12(2):175–183, 2006.

[2] S Sridhar, B Smitha, and T M Aminabhavi. Separation of Carbon Dioxide from Natural Gas Mixtures through Polymeric Membranes-A Review. *Separation and Purification Reviews*, 36(2):113–174, 2007.

[3] C E Powell and G G Qiao. Polymeric CO_2/N_2 gas separation membranes for the capture of carbon dioxide from power plant flue gases. *Journal of Membrane Science*, 279(1-2):1–49, 2006.

[4] E Serrano, G Rus, and J García-Martínez. Nanotechnology for sustainable energy. *Renewable and Sustainable Energy Reviews*, 13(9):2373–2384, 2009.

[5] A.S. Aricò, S. Srinivasan, and V. Antonucci. DMFCs: From Fundamental Aspects to Technology Development. *Fuel Cells*, 1:133–161, 2001.

[6] K. A. Mauritz and R. B. Moore. State of Understanding of Nafion. *Chemical Reviews*, 104:4535–4585, 2004.

[7] S.S. Kocha, J.D. Yang, and J.S. Yi. Characterisation of gas crossover and its implications in PEM fuel cells. *American Institute of Chemical Engineerings (AIChE Journal)*, 52:1916–1925, 2006.

[8] R.W. Baker and K. Lokhandwala. Natural gas processing with membranes: an overview. *Industrial & Engineering Chemistry Research*, 47(7):2109–2121, 2008.

[9] J.D. Figueroa, T. Fout, S. Plasynski, H. McIlvried, and R.D. Srivastava. Advances in CO_2 capture technology – The US Department of Energy's Carbon Sequestration Program. *International Journal of Greenhouse Gas Control*, 2(1):9–20, 2008.

[10] Naturalgas.org- processing natural gas. www.naturalgas.org/naturalgas/processing_ng.asp.

[11] E.L. Cussler. *Diffusion. Mass Transfer in Fluid Systems.* Cambridge, third edition, 2009.

[12] L. M Robeson. The upper bound revisited. *Journal of Membrane Science*, 320:390–400, 2008.

[13] IM Coelhoso, TF Moura, J. Crespo, and MJT Carrondo. Transport mechanisms in liquid membranes with ion exchange carriers. *Journal of Membrane Science*, 108(3):231–244, 1995.

[14] F.F. Krull, C. Fritzmann, and T. Melin. Liquid membranes for gas /vapor separations. *Journal of Membrane Science*, 325:509–519, 2008.

[15] T Schäfer, C Rodrigues, C A M Afonso, and J G Crespo. Selective recovery of

solutes from ionic liquids by pervaporation-a novel approach for purification and green processing. *Chemical Communications*, pages 1622–1623, 2001.

[16] T. Welton. Room-Temperature Ionic Liquids. Solvents for synthesis and catalysis. *Chemical Reviews*, 99:2071–2084, 1999.

[17] J.E. Bara, T.K. Carlisle, C.J. Gabriel, D. Camper, A. Finotello, D.L. Gin, and R.D. Noble. Guide to CO_2 separations in imidazolium-based room-temperature ionic liquids. *Industrial & Engineering Chemistry Research*, 48(6):2739–2751, 2009.

[18] T Schäfer, RE Di Paolo, and R Franco. Elucidating interactions of ionic liquids with polymer films using confocal Raman spectroscopy. *Chemical Communications*, pages 2594–2596, 2005.

[19] R.E. Baltus, R.M. Counce, B.H. Culbertson, H. Luo, D.W. DePaoli, S. Dai, and C. Duckworth. Examination of the Potential of Ionic Liquids for Gas Separations. *Separation Science and Technology*, 40:525–541, 2005.

[20] Cesar Cadena, Jennifer L. Anthony, Jindal K. Shah, Timothy I. Morrow, Joan F. Brennecke, and Edward J. Maginn. Why Is CO_2 So Soluble in Imidazolium-Based Ionic Liquids? *Journal of the American Chemical Society*, 126:5300–5308, 2004.

[21] Dmitri Bessarabov and Paul Kozak. Measurement of gas permeability in SPE membranes for use in fuel cells. *Membrane Technology*, 12:6–9, 2007.

[22] D. Briggs and MP Seah. *Practical surface analysis by Auger and X-ray photoelectron spectroscopy*. John Wiley & Sons, 1995.

[23] E. Barsoukov and J.R. Macdonald. *Impedance spectroscopy: theory, experiment, and applications*. Wiley-Interscience, second edition, 2005.

[24] B.H. Stuart. *Polymer analysis*, volume 3 – Analytical techniques in the sciences. Wiley, second edition, 2002.

[25] P.J. Sebastião, C. Cruz, and A.C. Ribeiro. *Nuclear magnetic resonance of liquid crystals*, chapter 5, pages 129–167. World Scientific Co., ronald y. dong edition, 2009.

[26] M. D. Bennet and D. J. Leo. Ionic Liquids as stable solvents for ionic polymer transducers. *Sensors and Actuators A*, 115:79–90, 2004.

[27] B. J. Akle, M. D. Bennet, and D. J. Leo. High-strain ionomeric-ionic liquid electroactive actuators. *Sensors and Actuators A*, 126:173–181, 2006.

[28] VS Silva, B. Ruffmann, S. Vetter, M. Boaventura, AM Mendes, LM Madeira, and SP Nunes. Mass transport of direct methanol fuel cell species in sulfonated poly (ether ether ketone) membranes. *Electrochimica Acta*, 51(18):3699–3706, 2006.

[29] T Okada, M Saito, N Arimura, and K Hayamizu. Mechanisms of ion and water transport in perfluorosulfonated ionomer membranes for fuel cells. *Journal of Physical Chemistry B*, 108(41):16064–16070, 2004.

[30] Ana Siu, Jennifer Schmeisser, and Steven Holdcroft. Effect of water on the low temperature conductivity of polymer electrolytes. *Journal of Physical Chemistry B*, 110(12):6072–6080, 2006.

[31] SJ Lue and SJ Shieh. Water States in Perfluorosulfonic Acid Membranes Using Differential Scanning Calorimetry. *Journal of Macromolecular Science Part B-Physics*, 48(1):114–127, 2009.

[32] M Doyle, SK Choi, and G Proulx. High-temperature proton conducting membranes based on perfluorinated ionomer membrane-ionic liquid composites. *Journal of the Electrochemical Society*, 147(1):34–37, 2000.

[33] Dean A. Tigelaar, James R. Waldecker, Katherine M. Peplowski, and James D. Kinder. Study of the incorporation of protic ionic liquids into hydrophilic and hydrophobic rigid-rod elastomeric polymers. *Polymer*, 47(12):4269–4275, 2006.

[34] Christian Schmidt, Tobias Glueck, and Gudrun Schmidt-Naake. Modification of Nafion Membranes by Impregnation with Ionic Liquids. *Chemical Engineering & Technology*, 31(1):13–22, 2008.

[35] R. Fortunato, L.C. Branco, C.A.M. Afonso, J. Benavente, and J.G. Crespo. Electrical impedance spectroscopy characterisation of supported ionic liquid membranes. *Journal of Membrane Science*, 270(1-2):42–49, 2006.

[36] Jairton Dupont, Roberto F. de Souza, and Paulo A. Z. Suarez. Ionic Liquid (Molten Salt) Phase Organometallic Catalysis. *Chemical Reviews*, 102(10):3667–3692, 2002.

[37] VI Parvulescu and C Hardacre. Catalysis in ionic liquids. *Chemical Reviews*, 107:2615–2665, 2007.

[38] RA Sheldon, RM Lau, MJ Sorgedrager, and F Rantwijk. Biocatalysis in ionic liquids. *Green Chemistry*, 4:147–151, 2002.

[39] F van Rantwijk and RA Sheldon. Biocatalysis in ionic liquids. *Chemical Reviews*, 107:1757–2785, 2007.

[40] Y Hu and C Xu. Effect of the structures of ionic liquids on their physical-chemical properties and the phase behaviour of the mixtures involving ionic liquids. *Chemical Reviews*, 2006.

[41] J Ranke, S Stolte, R Störmann, and J Arning. Design of Sustainable Chemical Products - The Example of Ionic Liquids. *Chemical Reviews*, 107:2183–2206, 2007.

[42] RF de Souza, JC Padilha, and RS Gonçalves. Room temperature dialkylimidazolium ionic liquid-based fuel cells. *Electrochemistry communications*, 5(8):728–731, 2003.

[43] P.A.Z. Suarez, V.M. Selbach, J.E.L. Dullius, S. Einloft, C.M.S. Piatnicki, D.S. Azambuja, R.F. de Souza, and J. Dupont. Enlarged electrochemical window in dialkyl-imidazolium cation based room-temperature air and water-stable molten salts. *Electrochimica Acta*, 42(16):2533–2535, 1997.

[44] P. Bonhote, A.P. Dias, N. Papageorgiou, K. Kalyanasundaram, and M. Gratzel. Hydrophobic, Highly Conductive Ambient-Temperature Molten Salts. *Inorganic Chemistry*, 35(5):1168–1178, 1996.

[45] RC Reid, J.M. Prausnitz, and B.E. Poling. *The properties of gases and liquids*. McGraw-Hill New York, 1988.

[46] J.F. Moulder, W.F. Stickle, P.E. Sobol, and K.D. Bomben. *Handbook of x-ray photoelectron spectroscopy: a reference book of standard spectra for identification and interpretation of*. Perkin-Elmer, 1992.

[47] J. Lukas and B. Jezek. Inelastic mean free paths of photoelectrons from polymer surfaces determined by the XPS method. *Collection of Czechoslovak chemical communications*, 48(10):2909–2913, 1983.

[48] M.I. Vázquez, R. de Lara, and J. Benavente. Modification in the transport of nacl and $MgCl_2$ solutions across a ceramic microporous membrane due to chemical and thermal treatment. *Separation and Purification Technology*, 43(3):221–225, 2005.

[49] Bernard Boukamp. Equivalent Circuit Program, 1997.

[50] D. Susac, M. Kono, K. C. Wong, and K. A. R. Mitchell. XPS study of interfaces in a two-layer light-emitting diode made from PPV and Nafion with ionically exchanged $Ru(bpy)^{+}_{32}$. *Applied Surface Science*, 174(1):43–50, 2001.

[51] J. T. F. Keurentjes, J. G. Harbrecht, D. Brinkman, J. H. Hanemaaijer, M. A. Cohen Stuart, and K. van't Riet. Hydrophobicity measurements of microfiltration and ultrafiltration membranes. *Journal of Membrane Science*, 47(3):333–344, 1989.

[52] MJ Ariza, E. Rodríguez-Castellón, M. Muñoz, and J. Benavente. Surface chemical and electrokinetic characterizations of membranes containing different carriers by x-ray photoelectron spectroscopy and streaming potential measurements: study of the effect of pH. *Surface and Interface Analysis*, 34(1):637–641, 2002.

[53] CD Wagner, AV Naumkin, A Kraut-Vass, and JW Allison. NIST X-ray photoelectron spectroscopy database: NIST standard reference database 20, v.2.0. *National Institute of Standard and Technology (NIST)*, 2003.

[54] K. Asaka. Dielectric properties of cellulose acetate reverse osmosis membranes in aqueous salt solutions. *Journal of Membrane Science*, 50(1):71–84, 1990.

[55] B. Malmgren-Hansen, TS Sørensen, JB Jensen, and M. Hennenberg. Electric impedance of cellulose acetate membranes and a composite membrane at different salt concentrations. *Journal of Colloid and Interface Science*, 130(2):359–385, 1989.

[56] J Benavente. *Electrical Characterization of Membranes*, pages 177–207. Wiley-VCH, 2009.

[57] Vito Di Noto, Rocco Gliubizzi, Enrico Negro, Michele Vittadello, and Giuseppe Pace. Hybrid inorganic–organic proton conducting membranes based on Nafion and 5wt.% of MxOy (M=Ti, Zr, Hf, Ta and W)Part I. Synthesis, properties and vibrational studies. *Electrochimica Acta*, 53(4):1618–1627, 2007.

[58] Se-Jong Shin, Aliaksandr I. Balabanovich, Ho Kim, Janghwan Jeong, Joohan Song, and Hee-Tak Kim. Deterioration of Nafion 115 membrane in direct methanol fuel cells. *Journal of Power Sources*, 191(2):312–319, 2009.

[59] Savitha Thayumanasundaram, Matteo Piga, Sandra Lavina, Enrico Negro, Malathi Jeyapandian, Lida Ghassemzadeh, Klaus Müller, and Vito Di Noto. Hybrid inorganic–organic proton conducting membranes based on

Nafion, SiO_2 and triethylammonium trifluoromethanesulfonate ionic liquid. *Electrochimica Acta*, 2009.

[60] R.Y. Dong. *Nuclear magnetic resonance of liquid crystals*. Springer New York, 1997.

[61] PJ Sebastião, D. Sousa, AC Ribeiro, M. Vilfan, G. Lahajnar, J. Seliger, and S. Žumer. Field-cycling NMR relaxometry of a liquid crystal above TNI in mesoscopic confinement. *Physical Review E*, 72(6):61702(1)–61702(11), 2005.

[62] M. Vilfan, T. Apih, PJ Sebastião, G. Lahajnar, and S. Žumer. Liquid crystal 8CB in random porous glass: NMR relaxometry study of molecular diffusion and director fluctuations. *Physical Review E*, 76(5):51708(1)–51708(15), 2007.

[63] J.C. Perrin, S. Lyonnard, A. Guillermo, and P. Levitz. Water Dynamics in Ionomer Membranes by Field-Cycling NMR Relaxometry. *Fuel Cells*, 6(1):5–9.

[64] J.C. Perrin, S. Lyonnard, A. Guillermo, and P. Levitz. Water dynamics in ionomer membranes by field-cycling NMR relaxometry. *Magnetic Resonance Imaging*, 25(4):501–504, 2007.

[65] JC Perrin, S. Lyonnard, A. Guillermo, and P. Levitz. Water dynamics in ionomer membranes by field-cycling NMR relaxometry. *Journal of Physical Chemistry B*, 110(11):5439–5444, 2006.

[66] D.M. Sousa, G.D. Marques, J.M. Cascais, and P.J. Sebastião. Desktop fast field cycling nuclear magnetic resonance spectrometer. *Review of Scientific Instruments*, submitted, 2009.

[67] R. Kimmich and E. Anoardo. Field-cycling NMR relaxometry. *Progress in Nuclear Magnetic Resonance Spectroscopy*, 44(3-4):257–320, 2004.

[68] F. Noack. NMR field-cycling spectroscopy: principles and applications. *Progress in Nuclear Magnetic Resonance Spectroscopy*, 18(3):171–276, 1986.

[69] Software developed for fitting, available in: http://lince.ist.utl.pt.

[70] N.W. DeLuca and Y.A. Elabd. Polymer electrolyte membranes for the direct methanol fuel cell: A review. *Journal of Polymer Science-B-Polymer Physics*, 44(16):2201–2225, 2006.

[71] V. Neburchilov, J. Martin, H. Wang, and J. Zhang. A review of polymer electrolyte membranes for direct methanol fuel cells. *Journal of Power Sources*, 169(2):221–238, 2007.

[72] C.H. Wang, C.C. Chen, H.C. Hsu, H.Y. Du, C.P. Chen, J.Y. Hwang, LC Chen, H.C. Shih, J. Stejskal, and KH Chen. Low methanol-permeable polyaniline/Nafion composite membrane for direct methanol fuel cells. *Journal of Power Sources*, 190(2):279–284, 2009.

[73] L. Li and Y. Zhang. Chemical modification of Nafion membrane with 3, 4-ethylenedioxythiophene for direct methanol fuel cell application. *Journal of Power Sources*, 175(1):256–260, 2008.

[74] H.K. Kim and H. Chang. Organic/inorganic hybrid membranes for direct methanol fuel cells. *Journal of Membrane Science*, 288(1-2):188–194, 2007.

[75] W. Lee, H. Kim, T.K. Kim, and H. Chang. Nafion based organic/inorganic

composite membrane for air-breathing direct methanol fuel cells. *Journal of Membrane Science*, 292(1-2):29–34, 2007.

[76] E. Drioli, A. Regina, M. Casciola, A. Oliveti, F. Trotta, and T. Massari. Sulfonated PEEK-WC membranes for possible fuel cell applications. *Journal of Membrane Science*, 228(2):139–148, 2004.

[77] T. Sakai, H. Takenaka, N. Wakabayashi, Y. Kawami, and E. Torikai. Gas permeation properties of solid polymer electrolyte (SPE) membranes. *Journal of the Electrochemical Society*, 132:1328, 1985.

[78] T. Sakai, H. Takenaka, and E. Torikai. Gas diffusion in the dried and hydrated Nafions. *Journal of the Electrochemical Society*, 133:88–92, 1986.

[79] J.S. Chiou and D.R. Paul. Gas permeation in a dry Nafion membrane. *Industrial & Engineering Chemistry Research*, 27(11):2161–2164, 1988.

[80] K.M. Nouel and P.S. Fedkiw. Nafion®-based composite polymer electrolyte membranes. *Electrochimica Acta*, 43(16-17):2381–2387, 1998.

[81] L. Zhang, C. Ma, and S. Mukerjee. Oxygen permeation studies on alternative proton exchange membranes designed for elevated temperature operation. *Electrochimica Acta*, 48(13):1845–1859, 2003.

[82] X. Cheng, J. Zhang, Y. Tang, C. Song, J. Shen, D. Song, and J. Zhang. Hydrogen crossover in high-temperature PEM fuel cells. *Journal of Power Sources*, 167(1):25–31, 2007.

[83] S. Kundu, M.W. Fowler, and L.C. Simon. Gas selectivity measurements as a diagnostic tool for fuel cells. *Journal of Power Sources*, 180(2):760–766, 2008.

[84] V.A. Sethuraman, S. Khan, J.S. Jur, A.T. Haug, and J.W. Weidner. Measuring oxygen, carbon monoxide and hydrogen sulfide diffusion coefficient and solubility in Nafion membranes. *Electrochimica Acta*, 54(27):6850–6860, 2009.

[85] R. Gosalawit, S. Chirachanchai, A. Basile, and A. Iulianelli. Thermo and electrochemical characterization of sulfonated PEEK–WC membranes and Krytox-Si-Nafion® composite membranes. *Desalination*, 235(1-3):293–305, 2009.

[86] Q. Li, J.O. Jensen, R.F. Savinell, and N.J. Bjerrum. High temperature proton exchange membranes based on polybenzimidazoles for fuel cells. *Progress in Polymer Science*, 34(5):449–477, 2009.

[87] J. Ling and O. Savadogo. Comparison of methanol crossover among four types of Nafion membranes. *Journal of the Electrochemical Society*, 151:A1604–A1610, 2004.

[88] Z. Wu, G. Sun, W. Jin, H. Hou, and S. Wang. A model for methanol transport through Nafion® membrane in diffusion cell. *Journal of Membrane Science*, 325(1):376–382, 2008.

[89] K. Ramya and KS Dhathathreyan. Methanol crossover studies on heat-treated Nafion (R) membranes. *Journal of Membrane Science*, 311(1-2):121–127, 2008.

[90] R.A. Banaszak, S.A. Arbaugh, E.D. Steffee, and R. Pyati. Investigation of Methanol Permeability and Ionic Conductivity of EMI^+ - Doped Nafion Membranes. *Journal of the Electrochemical Society*, 151(7):1020–1023, 2004.

[91] P. Mukoma, BR Jooste, and HCM Vosloo. A comparison of methanol permeability in Chitosan and Nafion 117 membranes at high to medium methanol concentrations. *Journal of Membrane Science*, 243(1-2):293–299, 2004.

[92] B. Jung, B. Kim, and J.M. Yang. Transport of methanol and protons through partially sulfonated polymer blend membranes for direct methanol fuel cell. *Journal of Membrane Science*, 245(1-2):61–69, 2004.

[93] K. Ramya and KS Dhathathreyan. Direct methanol fuel cells: determination of fuel crossover in a polymer electrolyte membrane. *Journal of Electroanalytical Chemistry*, 542:109–115, 2003.

[94] W.C. Choi, J.D. Kim, and S.I. Woo. Modification of proton conducting membrane for reducing methanol crossover in a direct-methanol fuel cell. *Journal of Power Sources*, 96(2):411–414, 2001.

[95] XM Ren, TE Springer, TA Zawodzinski, and S. Gottesfeld. Methanol transport through nafion membranes-Electro-osmotic drag effects on potential step measurements. *Journal of the Electrochemical Society*, 147(2):466–474, 2000.

[96] V Tricoli, N Carretta, and M Bartolozzi. A comparative investigation of proton and methanol transport in fluorinated ionomeric membranes. *Journal of the Electrochemical Society*, 147:1286–1290, 2000.

[97] W R Bowen and J S Welfoot. Modelling the performance of membrane nanofiltration - critical assessment and model development. *Chemical Engineering Science*, 57(7):1121–1137, 2002.

[98] C.E. Perles. Physicochemical properties related to the development of Nafion® membranes for application in fuel cells. *Polímeros*, 18:281–288, 2008.

[99] M. Mulder. *Basic principles of membrane technology*. Springer, second edition, 1996.

[100] R. Fortunato, C.A.M. Afonso, MAM Reis, and J.G. Crespo. Supported liquid membranes using ionic liquids: study of stability and transport mechanisms. *Journal of Membrane Science*, 242(1-2):197–209, 2004.

[101] R. Fortunato, M.J. González-Muñoz, M. Kubasiewicz, S. Luque, JR Alvarez, C.A.M. Afonso, I.M. Coelhoso, and J.G. Crespo. Liquid membranes using ionic liquids: the influence of water on solute transport. *Journal of Membrane Science*, 249(1-2):153–162, 2005.

[102] R. Fortunato, C.A.M. Afonso, J. Benavente, E. Rodriguez-Castellon, and J.G. Crespo. Stability of supported ionic liquid membranes as studied by X-ray photoelectron spectroscopy. *Journal of Membrane Science*, 256(1-2):216–223, 2005.

[103] S. Schlosser, E. Sabolová, R. Kertész, and L. Kubišová. Factors influencing transport through liquid membranes and membrane based solvent extraction. *Journal of Separation Science*, 24(7):509–518, 2001.

[104] F.J. Hernández-Fernández, A.P. de los Ríos, F. Tomás-Alonso, J.M. Palacios, and G. Víllora. Preparation of supported ionic liquid membranes: Influence of the ionic liquid immobilization method on their operational stability. *Journal of Membrane Science*, 341(1-2):172–177, 2009.

[105] P.J. Carvalho, V.H. Álvarez, J.J.B. Machado, J. Pauly, J.L. Daridon, I.M. Marrucho, M. Aznar, and J.A.P. Coutinho. High pressure phase behavior of carbon dioxide in 1-alkyl-3-methylimidazolium bis (trifluoromethylsulfonyl) imide ionic liquids. *The Journal of Supercritical Fluids*, 48(2):99–107, 2009.

[106] P. Scovazzo, J. Kieft, D.A. Finan, C. Koval, D. DuBois, and R. Noble. Gas separations using non-hexafluorophosphate $[PF_6]^-$ anion supported ionic liquid membranes. *Journal of Membrane Science*, 238(1-2):57–63, 2004.

[107] P Luis, L A Neves, C A M Afonso, I M Coelhoso, J G Crespo, A Garea, and A Irabien. Facilitated transport of CO_2 and SO_2 through Supported Ionic Liquid Membranes (SILMs). *Desalination*, 245(1-3):485–493, 2009.

[108] J. Ilconich, C. Myers, H. Pennline, and D. Luebke. Experimental investigation of the permeability and selectivity of supported ionic liquid membranes for CO_2/He separation at temperatures up to 125 ° C. *Journal of Membrane Science*, 298(1-2):41–47, 2007.

[109] P. Scovazzo, D. Havard, M. McShea, S. Mixon, and D. Morgan. Long-term, continuous mixed-gas dry fed CO_2/CH_4 and CO_2/N_2 separation performance and selectivities for room temperature ionic liquid membranes. *Journal of Membrane Science*, 327(1-2):41–48, 2009.

[110] S. Hanioka, T. Maruyama, T. Sotani, M. Teramoto, H. Matsuyama, K. Nakashima, M. Hanaki, F. Kubota, and M. Goto. CO_2 separation facilitated by task-specific ionic liquids using a supported liquid membrane. *Journal of Membrane Science*, 314(1-2):1–4, 2008.

[111] J.G. Huddleston, A.E. Visser, W.M. Reichert, H.D. Willauer, G.A. Broker, and R.D. Rogers. Characterization and comparison of hydrophilic and hydrophobic room temperature ionic liquids incorporating the imidazolium cation. *Green Chemistry*, 3(4):156–164, 2001.

[112] R.W. Baker. *Membrane technology and applications*. Wiley, second edition, 2004.

[113] D. Morgan, L. Ferguson, and P. Scovazzo. Diffusivities of gases in room-temperature ionic liquids: data and correlations obtained using a lag-time technique. *Industrial & Engineering Chemistry Research*, 44(13):4815–4823, 2005.

[114] M.G. Freire, L.M. Santos, A.M. Fernandes, J.A.P. Coutinho, and I.M. Marrucho. An overview of the mutual solubilities of water–imidazolium-based ionic liquids systems. *Fluid Phase Equilibria*, 261(1-2):449–454, 2007.

[115] W.J. Koros and R. Mahajan. Pushing the limits on possibilities for large scale gas separation: which strategies? *Journal of Membrane Science*, 175(2):181–196, 2000.

[116] J.L. Anthony, J.L. Anderson, E.J. Maginn, and J.F. Brennecke. Anion effects on gas solubility in ionic liquids. *Journal of Physical Chemistry B*, 109(13):6366–6374, 2005.

[117] M. Laporta, M. Pegoraro, and L. Zanderighi. Perfluorosulfonated membrane (Nafion): FT-IR study of the state of water with increasing humidity. *Physical Chemistry Chemical Physics*, 1(19):4619–4628, 1999.

[118] DT Hallinan and YA Elabd. Diffusion of water in Nafion using time-resolved fourier transform infrared-attenuated total reflectance spectroscopy. *Journal of Physical Chemistry B*, 113(13):4257, 2009.

[119] L. Barbora, S. Acharya, R. Singh, K. Scott, and A. Verma. A novel composite Nafion membrane for direct alcohol fuel cells. *Journal of Membrane Science*, 326(2):721–726, 2009.